Functional effects of nanoplastics on maternal and fetal innate immune cells

Tyler James Joseph

Swansea University
Prifysgol Abertawe

Submitted to Swansea University in fulfilment of the requirements for the Degree of Master of Science by Research

Swansea University

2024

Abstract

Nanoplastics (NPs) have become a common pollutant in the environment and exposure subsequently leads to infiltration into the human body via ingestion, inhalation and topically. Using animal models, NPs have been shown to translocate from the pregnant animal into the placenta and fetal organs, leading to fetal growth restriction and hepatic toxicity. However, little research has been conducted on the effect of NPs on immune function in the mother and fetus during human pregnancy. Focusing on innate immunity, this project aims to study the uptake of NPs in maternal and fetal mononuclear phagocytes and determine if NP uptake disrupts inflammatory cytokine production. Using 40 nm carboxylated polystyrene beads at $7.6x10^{10}$, $3.8x10^{11}$ and $7.6x10^{11}$ particles/ml, NP uptake was confirmed using flow cytometry and monocytes were shown to be the main cell type in whole blood for NP uptake. This was further confirmed by confocal microscopy. NP uptake in monocytes was unaffected by particle number over a 24-hour period. However, monocytes from pregnant compared to non-pregnant women showed greater NP uptake at 2 hours. Contrastingly, placental macrophages continuously took up NPs over a 24-hour period. Pro- and anti-inflammatory cytokine production analysis in monocytes from non-pregnant and pregnant women exposed to different NP concentrations revealed no significant differences between unstimulated and LPS-stimulated TNFα, IL-1β and IL-10 production. Analysis of placental macrophages revealed that NP exposure led to significant increases in TNFα and IL-1β after LPS stimulation. Overall, NPs are taken up by phagocytes in a dose dependent manner, with increased uptake in monocytes from pregnant women compared to non-pregnant women highlighting the need for greater understanding of the effects of NPs on cell function.

Declarations

i. I declare that I am the author of the work and I confirm that I will submit the **final version** of my thesis as an electronic copy. This will be **archived as a record** of the work in the Research Information System (RIS);

ii. I understand that the electronic version will be deposited by the repository administrator in Cronfa, the Swansea University institutional repository. The bibliographic metadata and abstract will be made immediately available. The full-text version of the thesis will be published online unless access is formally restricted;

iii. I understand that I may submit a second redacted version of the thesis to be made available in Cronfa, the institutional repository if the thesis contains third-party copyright content, sensitive or confidential material I wish to remove. I understand that the author is responsible for any errors or omissions in the content of the thesis;

iv. I declare that the thesis is the result of my own investigations, except where otherwise stated and that other sources are acknowledged by footnotes giving explicit references and that a bibliography is appended. I have taken reasonable care to ensure that the work is original and does not, to the best of my knowledge, break any UK law or infringe any third party's copyright or other Intellectual Property Right;

v. I understand that I retain the right to publish the work in its present version or future versions elsewhere. The rights granted to the Swansea University repository are non-exclusive and royalty free;

vi. I may choose to protect the thesis in Cronfa with a pre-prepared Creative Commons licence added to the metadata record and the document. I authorise the repository administrator to add the licence I may select on this form.

vii. I understand that Swansea University reserves the right to restrict or withdraw access to the electronic version of my work, should there be any cause for Swansea University to do so;

viii. I agree that Swansea University may electronically store, copy or translate the work to any approved medium or format for the purpose of access and future preservation. Swansea University is not under any obligation to reproduce or display the work in the same format or resolution in which it was originally deposited. In addition, I agree that Swansea University may retain a copy for use within the institution;

ix. I understand that the bibliographic metadata and abstract will be available in public access catalogues and searchable via standard web search engines. Swansea University will allow the British Library Electronic Thesis Online Service (EThOS) and the National Library of Wales Theses Collection Wales service, to harvest the bibliographic metadata and make the work available under the declared terms and conditions of their service;

x. If dispute arises between the author and supervisor(s) relating to withholding the thesis, the decision of the supervisor(s) is final.

Signed: 

Date: 21/01/2025

Acknowledgements

I would like to thank everyone who has helped me this past year with completing my research project.

Firstly, I would like to thank Professor Cathy Thornton, Dr Rich Fry, Dr April Rees and Dr Sophie Reed for their time, patience, guidance and support throughout the duration of my research project. Their help was greatly appreciated.

Secondly, I would like to thank Dr Ruth Jones for taking time out of her day to recruit participants for this project. This project would not have been possible without her.

Thirdly, I would like to thank all the fellow students in ILS1 2nd floor for their academic and moral support with any queries I had about my project. I would especially like to thank Dr Megan Chambers, Emma Stanton, Emma Lucas and Molly Raikes as they have been a tremendous help throughout.

Finally, I would like to thank my family, friends and partner for their continuous and unwavering support throughout my academic studies.

Publications

Rees, A., Chambers, M., Richards, O., **Joseph, T. J.**, Fernando, M. G., Yadanar, H., Pocalun, Z. A., Murphy, K., Finall, A., & Thornton, C. (2023). The maternal environment is rich in SARS-related receptors which could be protective for the fetus. *Authorea Preprints*. https://doi.org/10.22541/au.169166181.10996049/v1

Ravelojaona, M., Girouard, J., Chambers, M., **Joseph, T.**, Thornton, C., & Reyes-Moreno, C. (2024). Regulatory role of Leukemia Inhibitory Factor (LIF) and Oncostatin M (OSM) in the maintenance of cell populations involved in intrauterine inflammation at the fetal-maternal interface. *Placenta (Eastbourne)*, *154*, e41-. https://doi.org/10.1016/j.placenta.2024.07.172

Conferences

1. Joseph, T., Rees, A., Fry, R., & Thornton, C. Functional effects of nanoplastics on maternal and fetal innate immune cells. **Swansea University Medical School Conference**, May 2023. Poster presentation. Runner-up award.
2. Joseph, T., Rees, A., Fry, R., & Thornton, C. Functional effects of nanoplastics on maternal and fetal innate immune cells. **British Society of Immunology Annual Congress**, December 2025. Poster presentation.
3. Joseph, T., Rees, A., Fry, R., & Thornton, C. Functional effects of nanoplastics on maternal and fetal innate immune cells. **Swansea University Medical School Conference**, May 2024. Poster presentation.

Contents

List of figures

List of Tables

List of abbreviations

A549	Human lung carcinoma cell line
APC	Allophycocyanin
ATP	Adenosine triphosphate
BACH1	Broad-Complex, Tram track, and Bric-a-brac and Cap'n'collar homology 1
BALF	Bronchoalveolar lavage fluid
BEAS-2B	Bronchial epithelial adult human small airway epithelial cell line
BeWo b30	Human choriocarcinoma cell line
BSA	Bovine serum albumin
CCL	Chemokine ligand
CCR	Chemokine receptor
CD	Cluster of differentiation
CO_2	Carbon dioxide
CX3CR1	Chemokine receptor, CX3C motif
DAPI	4', 6-diamidino-2-phenylindole
DNA	Deoxyribonucleic acid
DRAQ7	Deep red anthraquinone 7
ELISA	Enzyme linked immunosorbent assay
FACS	Fluorescence-activated cell sorting
FBS	Fetal bovine serum
FGF-	Fetal growth factor
FITC	Fluorescein isothiocyanate
FOXO	Forkhead box O
FSC	Forward scatter
GATA	Zinc-finger DNA-binding protein
GDF-	Growth/differentiation factor
GI	Gastrointestinal
H_2SO_4	Sulphuric acid
HaCaT	Human keratinocyte cell line
HBSS	Hanks' Balanced Salt Solution
HEPES	ml 4-(2-hydroxyethyl)-1-piperazineethanesulfonic acid
HK-2	Human adult male kidney cells
HLA-DR	Human leukocyte antigen – DR isotype
HUVEC	Human umbilical vein endothelial cells
HRP	Horseradish peroxidase
IFN-	Interferon
IL-	Interleukin
IUGR	Intrauterine growth restriction
LPS	Lipopolysaccharide
LS	Liquid separation
LSM	Light scanning microscopy
M1	Classically activated macrophage
M2	Alternatively activated macrophage
MACS	Magnetic-activated cell sorting
MCP-	Monocyte chemoattractant protein
MDP	Muramyl dipeptide
MFI	Median fluorescent intensity

MMP	Matrix metalloproteinase
MNC	Mononuclear cell
MNP	Micro-nanoplastic
MP	Microplastic
NEF2	Nucleotide excision repair factor 2
NK	Natural killer
NOD2	Nucleotide-binding oligomerization domain-containing protein 2
NP	Nanoplastic
OXPHOS	Oxidative phosphorylation
PBS	Phosphate buffered saline
PBX1M	Pre-B-cell leukaemia homeobox 1
PE	Phycoerythrin
PET	Polyethylene terephthalate
PM	Particulate matter
pMSC	Pluripotent mesenchymal stem cell
R837	Resiquimod
R848	Resiquimod analog
RBC	Red blood cell
RBL-2H3	Rat basophilic leukaemia cell line
RNA	Ribonucleic acid
ROS	Reactive oxygen species
RPMI	Roswell Park Memorial Institute
SEM	Standard error of mean
SK-BR-3	Human breast cancer cells
SOX	Sex-determining Region Y box
SSC	Side scatter
STAT	Signal transducer and activator of transcription
TEM	Transmission electron microscopy
TL	Toll-like receptor agonist
TLR	Toll-like receptor
TMB	3, 3', 5, 5' tetramethylbenzidine
TNF-	Tumour necrosis factor
TNFRSF12A	Tumor necrosis factor receptor superfamily member 12A
VEGF	Vascular endothelial growth factor
ZO	Zonula occludens

Chapter 1: Introduction

1.1. Overview

Plastic pollution accounts for around 10% of all waste produced globally (Kumar & Samadder, 2017). From this, plastic degrades into particulates known as microplastics (MPs) and nanoplastics (NPs) (Hüffer et al., 2017; Roy, Hakkarainen, Varma & Albertsson, 2011). The human body is exposed to NPs in particular, that can translocate from the respiratory and gastrointestinal (GI) tracts and induce various cytotoxic, genotoxic and metabolic damage. NPs also induce hepatotoxicity in pregnant women, decrease weight of the fetus postpartum and induce damage of the fetal hippocampus (Huang et al., 2022; Jeong et al., 2022; X. Wang et al., 2023). While women undergo several immunological changes during pregnancy, there is little research on how this affects their response to NPs or on analysing the effects of NPs on the functionality of fetal and maternal innate immune cells. The work presented in this thesis investigates the effect of NPs on the functionality of monocytes from pregnant and non-pregnant women and placental macrophages.

1.2. Plastic

1.2.1. Plastic and plastic pollution

Plastic is a polymer, a repeating chain of hydrocarbon monomers with specific functional groups attached to each monomer that are responsible for the differentiation and functionality of plastics. This functional group also allows for the specific characteristics of the plastics. Common plastic structures can be found in figure 1.1. With increasing population, there inevitably will be an increase in waste production, with plastic comprising around 9-11% of all waste produced (Kumar & Samadder, 2017). Plastic debris in the ocean can have detrimental effects. Marine life can be suffocated, lacerated, and trapped leading to infection, starvation and death. MPs and NPs formed by the degradation of plastic can be ingested by marine life and cause issues in homeostasis which disrupt marine food chains (Gallo et al., 2018). Plastic is also disposed of into landfill sites. Analysis of 6 open and closed landfill sites in China found that MP particles due to plastic pollution were anywhere between 1-25 items/litre of soil (He, Chen, Shao, Zhang & Lü, 2019). However, due to plastic pollution varying globally, it is extremely difficult to truly understand the effects of plastic on human health.

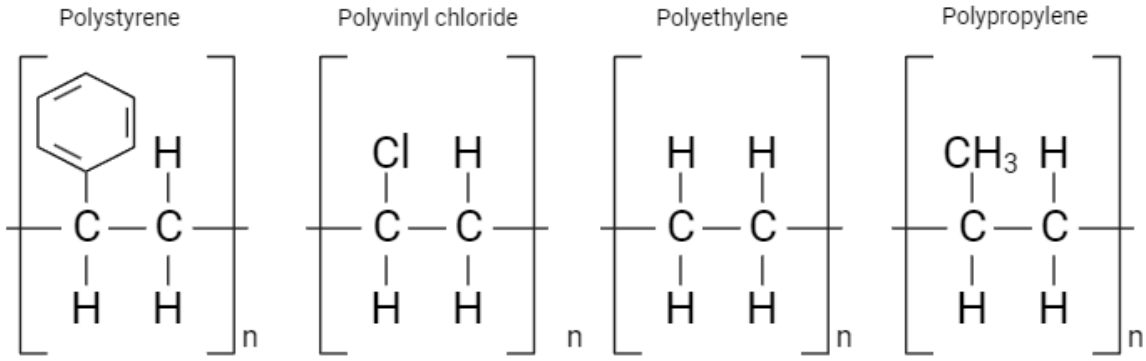

Figure 1.1. Common plastic structures illustrating the varying functional groups. This illustration shows the differing functional groups across plastic structure. Polystyrene contains a benzyl group, polyvinyl chloride a chlorine atom, polyethylene an additional hydrogen atom, and polypropylene a methyl group. n signifies the repetition of monomers to produce the plastic polymer.

1.2.2. Micro and nanoplastics

MPs are defined as plastic particles that are less than 5 mm in diameter, and are usually produced from breakdown of cosmetics, textiles, and larger plastic debris (National Geographic, 2023). NPs, as the name suggests, are plastic particulate matter that are between the sizes of 1 nm and 1 µm (Gigault et al., 2018). In the case of NPs, primary NPs (often referred to as engineered NPs due to their intentional production) are accepted to be between 1 nm and 100 nm in diameter whereas secondary NPs (otherwise known as naturally occurring NPs due to the chemical, mechanical or photocatalytic breakdown of larger plastics) are generally considered to be between 1nm and 1 µm in diameter (El Hadri, Gigault, Maxit, Grassl & Reynaud, 2020; Hüffer et al., 2017; Auta, Emenike & Fauziah, 2017). In the literature, plastic particles are often referred to as NPs despite being larger than 100 nm in diameter, while some studies deem NPs greater than 100 nm as microplastics (MPs) (El Hadri, Gigault, Maxit, Grassl & Reynaud, 2020; Huang et al., 2022). Therefore, for the purpose of this thesis, MPs and NPs collectively will be referred to as micro- and nano-plastics (MNPs) unless otherwise specified. MNPs stem from the breakage of the carbon-carbon bonds in the plastic chain, whether this is due to chemical, mechanical or photocatalytic breakdown (Hüffer et al., 2017; Roy, Hakkarainen, Varma & Albertsson, 2011). While MPs are present in the environment, it has been shown that NPs are also present and, once humans are exposed to them, they are able to penetrate the human body via various exposure routes and translocate to organs and tissues (see sections 1.3.2 – 1.3.7), calling for more research into the effects of NPs in the body and their effects on many cell types and organs including the immune system.

1.2.3. Areas of NP pollution

While MPs in environmental settings have been studied extensively (Zhu, Zhu, Wang & Gu, 2019; Dissanayake et al., 2022; Chai et al., 2023), research has now branched into the identification of NP composition and quantification in water sources. Using fish GI tracts, polypropylene, polystyrene, polyethylene and polysiloxanes were among the most frequent NPs discovered, with polystyrene being discovered in 84% of fish analysed (Garcia-Torné, Abad, Almeida, Llorca & Farré, 2022). Similarly, the aforementioned plastics as well as polyvinyl chloride were reported to be present in soil samples taken from meadows in central France (Wahl et al., 2021). Air-borne NPs have been shown to be a byproduct of essential urban maintenance such as sewer pipe repairs (Morales et al., 2022). From this, NPs do not solely pose a threat to the marine environment, but to urban and rural areas as well. Likewise, NPs have been shown to have multiple modes of transportation (see sections 1.3.2 - 1.3.5) which, effectively, make them an unavoidable part of life.

1.2.4. Morphology

As plastic pollution and the ecological effects of NPs have become common knowledge, the use of NPs have become increasingly common in research. The morphology of NPs can vary, but it is common for primary NPs to be used throughout research and are usually spherical in shape (González-Pleiter et al., 2019). Alternatively, secondary NPs can “peel” away from the surface during mechanical or photocatalytic degradation to produce fragments (Figure 1.2) (El Hadri, Gigault, Maxit, Grassl & Reynaud, 2020). In current literature, secondary NPs are mainly used to study their effects on the microbiome and marine organisms, however, some research is being conducted on the short-term toxicity of secondary NPs on *Streptomyces coelicolor* and its ability to produce antibiotics (González-Pleiter et al., 2019; Liu, Ahmad, Ma, Wang & Tang, 2023). To date, there is little research identifying the effects of secondary NPs once cells of the human body are exposed.

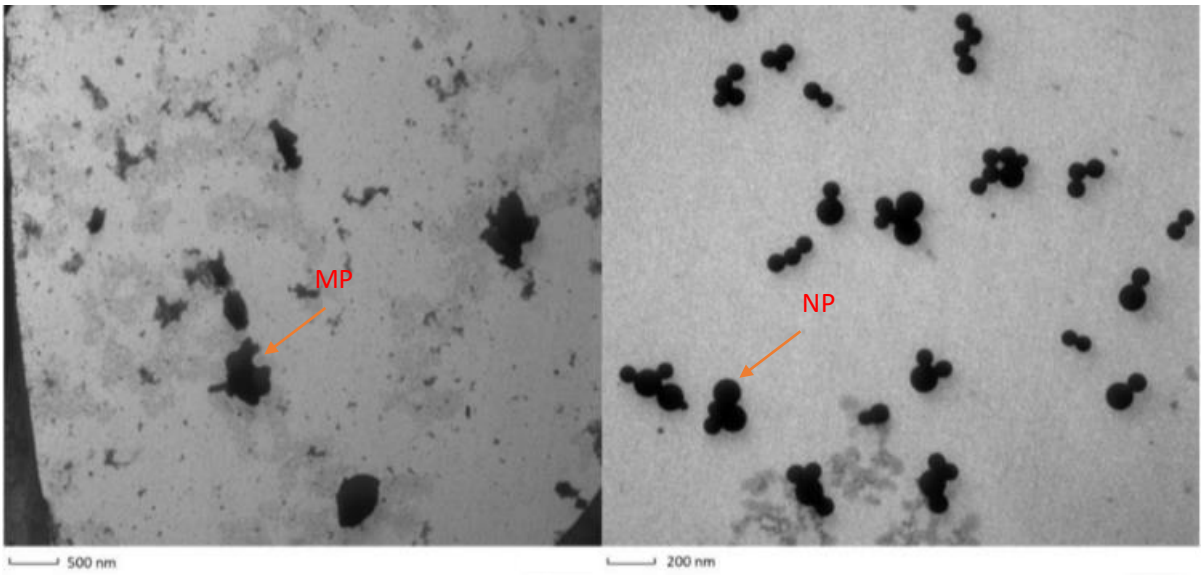

Figure 1.2. Transmission emission microscopy (TEM) images of MP degradation into NP fragments. This image illustrates the heterogeneity of morphology due to natural breakdown of MP in the environment. Image adapted from El Hadri, Gigault, Maxit, Grassl & Reynaud (2020).

1.2.5. Surface chemistry and toxicity

Functional groups such as carboxyl, amidine and amino groups can bind to NPs inducing changes in surface charges which alter the ability to cause cytotoxicity or metabolic and cellular dysfunction (Saavedra, Stoll & Slaveykova, 2019; Halimu et al., 2022). Dissociation or acquisition of protons from the functional groups create a positive or negative charge on the surface of the NP (Saavedra, Stoll & Slaveykova, 2019). The surface charge is described as a zeta potential and can range from anywhere between -50 mV and +50 mV (Saavedra, Stoll & Slaveykova, 2019; Zhu, Fan, Zou, Guo & Fu, 2023). Surface charge must also be considered when considering the effects of NPs. In human alveolar epithelial cells, positively charged polystyrene NP beads from 20 nm to 50 nm have been shown to increase the production of reactive oxygen species (ROS), as well as stimulate matrix metalloproteinase-2 (MMP2) upregulation and E-cadherin downregulation, effectively inhibiting the cell-to-cell adhesion ability of the cells (Halimu et al., 2022). Along with this, the positive charged NPs were found to induce greater dysfunction in alveolar epithelial cells than the negatively charged particles, despite being the same size and type of plastic (Halimu et al., 2022). The same positively charged NPs also induced destabilisation of mitochondria in airway epithelial A549 cells by decreasing mitochondrial membrane potential, with said effects becoming more potent with increasing NP concentrations (Halimu et al., 2022). This emphasises that variations of NP functional groups, surface charges and concentrations induce detrimental effects at epithelial barriers.

1.2.6. Agglomeration

Due to the unique surface chemistry of NPs, they can agglomerate. Homoagglomeration (NP particles binding together), heteroagglomeration (NP particles binding to surrounding biological material) or lack of agglomeration depends on NP size, presence of ions, biological material, zeta potential or simply where the NPs are located. The size of aggregates is inversely proportional to the size of the NPs; in seawater 50 nm NPs were found to form larger agglomerates when compared to their larger counterparts, however, NP diameter had no effect on the *number* of agglomerates (Summers, Henry & Gutierrez, 2018). Homoagglomeration of NPs in natural waters has been suggested to occur randomly and be driven by entropy, but analysis of heteroagglomeration found that calcium ions (Ca^{2+}) induced a faster rate of agglomeration when compared to sodium ions (Na^{+}) even at lower concentrations in water. Likewise, lanthanum ions (La^{3+}) induce a significantly faster agglomeration of NPs than Ca^{2+} (Kim, Herchenova, Chung, Na & Kim, 2022). This is also seen with iron ions (Fe^{3+}) in water inducing a rapid rate of agglomeration with polystyrene NPs (Cai et al., 2018). This suggests that ionic strength of metals in solution are proportional to the rate of agglomeration of NPs. Conversely, NPs have not been seen to agglomerate when in deionised water, indicating the ionic content and strength of a solution is proportional to the number and size of NP agglomerates (Chen, Ma, Shi & Xu, 2023).

1.2.7. Corona formation

Similar to agglomeration, proteins are able to bind to the surface of NPs forming a corona which induces changes in the functionality and motility of the NPs. When proteins are densely bound to NPs, this is referred to as a hard corona, while loosely bound proteins are a soft corona. It was found that protein coronas lead to agglomeration in a fractal like structure (Kihara et al., 2020). NPs with a bovine serum albumin (BSA) corona have enhanced transportation in sand saturated with artificial sea water due to their reduced ability to form agglomerations, emphasising the effect of corona formation on NPs on the transport and deposition in the natural environment (Dong et al., 2020). Following this, there is mixed evidence to conclude that corona formation on NPs is detrimental to cellular and biological stress and may be beneficial to organisms. For example, NPs alone were found to elicit increases in glutathione-S-transferase, catalase and heat shock protein 70 mRNA expression, but NPs with humic acid coronae vastly decreased expression of these, suggesting corona formation may potentially have rescue-like effects on the expression of stress related mRNA production (Fadare et al., 2020).

1.3. NP exposure and internalisation

NP internalisation in humans occurs via 3 main routes of exposure: ingestion, inhalation and topical exposure and equates to approximately 1.6µg/ml of plastic particulates in healthy human blood (Leslie et al., 2022).. With plastic pollution being such a prominent issue over the last few decades, it is inevitable that plastic degradation to NP leads to exposure in humans (Barnes, Galgani, Thompson & Barlaz, 2009).

1.3.1. Atmospheric NP

MNP degradation not only leads to water pollution, but also to air pollution. Atmospheric samples obtained in rural Austria over a 3-month period were used to identify the levels of MNP pollution in an area of dense traffic. Ultrafine MNPs were found to contribute from 1.7% to 4.5% of organic carbon compounds in the atmosphere and 0.67% of all 2.5 µm particulate matter ($PM_{2.5}$), which was consistent across the entire measured time periods (Kirchsteiger, Materić, Happenhofer, Holzinger & Kasper-Giebl, 2023). When analysing $PM_{2.5}$ in these atmospheric samples, polyethylene terephthalate accounted for 50% of the total NPs present, with polyethylene and polypropylene accounting for the remaining 50% (Kirchsteiger, Materić, Happenhofer, Holzinger & Kasper-Giebl, 2023). It is suggested that atmospheric MNP pollution stem from vehicles/traffic, a byproduct of landfills and waste combustion and from industrial emissions (Ortega & Cortés-Arriagada, 2023). This provides evidence that MNPs are present in the surrounding air and suggests that plastic can degrade directly into the air.

1.3.2. Inhalation

Atmospheric NPs inevitably lead to inhalation and deposition within the trachea, bronchioles and alveoli. Aerosolysed polyamide NPs inhaled by rats were found to significantly increase arterial pressure in the alveolar region by 14%, with an increase in neutrophil count in the bronchioalveolar lavage fluid (BALF) of exposed rats, however this increase was found to be physiologically negligible given that no histopathological changes or inflammation were observed in the lung tissue (Cary et al., 2023b). Simulations of NP deposition into lung surfactant found that the surfactant forms a corona around the NPs with the lipid head facing the surface and lipid tails facing outward, reducing hydrophobic properties of the NP and reducing the agglomeration potential with other particulates (L. Li et al., 2022). Interestingly, in the simulation, lung surfactant adsorption onto NP potentially induced dissolving of the NP agglomerates, leading to a dispersion of the plastic in lung surfactant,

and potentially increasing the exposure to lung tissue due to increased surface area of the NPs (L. Li et al., 2022). Polystyrene NPs were found to be endocytosed in lung cells and bronchiole endothelial cells and to accumulate in the mitochondria, with increasing dose and exposure times correlating with NP endocytosis, however, it was found that 53% of 50 nm polystyrene was exocytosed from BEAS-2B cells to the surround culture media after only 1 hr post-exposure, although the mechanisms of this are unclear (Liu et al., 2022). Further analysis of cytokines and chemokines in BALF have found that NPs, specifically polypropylene, increase levels of TNFα, IL-1β, IL-6, and MCP-1, and this is accompanied by an increase in ROS production in lung tissue of exposed mice (Woo et al., 2023). 4 mg/ml of polypropylene nanoparticle exposure to A549 cells was found to induce mitochondrial dysfunction evidenced by reducing the production of ATP and reducing the mitochondrial membrane potential when compared to the vehicle (Woo et al., 2023). Finally, metabolic pathway analysis concluded that polystyrene NPs induce upregulation of biological and molecular pathways in BEAS-2B cells, most notable being upregulation of cellular responses to chemical stimuli, cellular response to stress, anchoring junctions and adherens junctions which indicate that NP toxicity and mechanical stress to epithelial cells induce upregulation of cell-cell maintenance to counteract said damage (Zhang et al., 2022). High (30 μg/cm^2) and low (7.5 μg/cm^2) doses of NPs result in significant up and downregulation of gene expression, with TNFRSF12A, FOXO3, BACH1 and SOX9 being upregulated and FOXO4, GATA2, GATA6, PBX1M, STAT3 and NEF2 being downregulated in BEAS-2B cells when compared to unexposed cells (Zhang et al., 2022).

1.3.3. NPs in food

While atmospheric NP leads to plastic inhalation, plastic degradation in food packaging and passage through food chains potentially lead to human consumption. Studies have shown that bees fed with sucrose syrup inoculated with MP fibres produced wax and honey with traces of MPs, and the wax was found to have significantly more MP than the honey (Alma, de Groot & Buteler, 2023). Despite this, there are very few studies analysing and quantifying the level of NP contamination in food sources, this is due to the unavailability of techniques to readily quantify this contamination. However, recently, the use of asymmetric flow field-flow fractionation with multiple angled light scattering was used to identify NP in fish homogenate, but only in homogenate that was enzymatically digested as acid digestion lead to NP agglomeration rendering them undetectable (Correia & Loeschner, 2018). Despite the lack of literature of NPs in food, direct NP degradation of NP from food packaging has been found. Leachates from common food packages such as paper cups, teabags, instant-noodle packaging and take-away boxes were used to detect various NPs

(polystyrene, polypropylene and polyethylene) (J. Li et al., 2022; Cella et al., 2022). These studies suggest that plastic is present in food due to NP degradation from food packaging contributing to the likelihood of NP ingestion.

1.3.4. Ingestion

Despite the lack of studies identifying and quantifying the presence of NP in food, animal models and cell lines have been used to analyse the cytotoxic, functional, and metabolic effects of NPs within the GI tract. Concentrations between 10 and 100 µg/ml of polystyrene NPs can be endocytosed in Paneth, goblet, endocrine and enterocyte cells (each induced from pluripotent stem cells for this study), inducing a significant increase in IL-8, ROS and NF-κB p65 (Hou et al., 2022). Within these cells, polystyrene NPs were shown to translocate throughout the cell by localising within the lysosomes and to induce DNA damage, as well as an increase in apoptosis (Hou et al., 2022). Aminated polystyrene NPs were found to loosen tight junctions with a significant decrease of tight junction protein levels and increase of paracellular permeability, increasing the likelihood of NPs penetration through intestinal epithelia and deposition in surrounding tissues (Qiao et al., 2021). Along with effects on the cells within the GI tract, NPs also pose a threat to the natural gut flora. Reduced presence of gut bacteria including *Anaerotruncus, Roseburia* and *Butyricicoccus* is associated with the reduction in tight junction protein production as these genera are known to be beneficial to gut epithelial lining upkeep, while other opportunistic/pathogenic bacteria such as *Romboutsia, Achromobacter* and *Parasuttarella* had increased presence in the gut after NP exposure (Qiao et al., 2021). Analysis of zebra fish gut microbiota after NP exposure found an increased abundance of *Fusobacteria* and *Proteobacteria* (associated with gut inflammation), with decreased abundance in *Bacteroidetes* and *Firmicutes* (associated with efficient food breakdown/nutrient supply), further suggesting a disruption in a healthy gut microbiome by NPs (Teng et al., 2022). Finally, NP internalisation in gut epithelial cells occurs in a size-, dose- and time-dependent manner, with endocytosis accounting for approximately half of all cellular uptake and passive uptake accounting for the other half, indicating that prolonged exposure leads to increased, unavoidable damage to cells over time (Hou et al., 2022; Teng et al., 2022).

1.3.5. Skin

With NPs present in many items that come in contact with the skin (clothing, cosmetics, etc.), it is inevitable that NPs will penetrate/diffuse into the skin and induce cytotoxic, genotoxic and

metabolic dysregulation within resident cells. Zebrafish embryonic keratinocytes exposed to polystyrene NPs have underdeveloped or total lack of formation of the surface membrane - fingerprint-like microbridges on the surface membrane (Kantha, Liu, Horng & Lin, 2022). Likewise, HaCaT cells (a human keratinocyte cell line) exposed to polyethylene NP were found to significantly increase the production of IL-6, with a negligible effect on ROS production (Gautam et al., 2022). Dermal fibroblasts exposed to polystyrene NP were analysed, and it was shown that thyroid hormone synthesis and tuberculosis signalling pathways were down- and up-regulated, respectively. This was alongside effects on other pathways relating to biological and metabolic functions with cellular response to toxic substances, antioxidant activity and nonsense-mediated decay of nuclear transcribed mRNA being stand out upregulated pathways (Stojkovic et al., 2023). NP surface chemistry and size have also been shown to induce varying effects on dermal fibroblasts. Aminated and carboxylated polystyrene were not only found to have cytotoxic effects on dermal fibroblasts, but unsurprisingly also led to decreased cell viability, exacerbated by increasing concentrations of NPs (Cheng et al., 2023). While various studies have focussed on the effects of NPs at sites of exposure, NPs retain the ability to translocate and deposit throughout many organs, tissues and cells in the body, inducing indirect adverse effects that might negatively impact health.

1.3.6. NP translocation

Following the idea of NP ingestion, palladium-tagged polystyrene mixed into luminal fluid was injected into the lumen of isolated GI tracts of salmon, the GI tract was clamped shut and placed in a bath serosal fluid (Clark, Khan, Mitrano, Boyle & Thompson, 2022). After a total of 48 hours of exposure, the NP was found to be taken up by the mucosa, serosa and muscularis and was also present in the surrounding serosal fluid (Clark, Khan, Mitrano, Boyle & Thompson, 2022). Ingestion of polystyrene NPs in mice over a 4-week period showed that the plastic was able to translocate from the intestines (with plastic identified in the ileum, jejunum and duodenum) to the liver and kidneys (Meng et al., 2023). Following this, ingested NP was found to cross the placental barrier (with some placental deposition) and translocate throughout the fetus, depositing in the kidneys, liver, heart, lungs and brain of fetal mice (Cary et al., 2023a). This is suggestive that even though the exposure route of NPs is the area most at risk of plastic-induced damage, the NP might translocate to multiple other organs and induce multiple system-wide damage in the body and, in the case of pregnancy, penetrate through the placenta to the fetus and affect fetal development and the pregnancy itself.

1.3.7. NP effect on endothelial dysfunction and disease progression

NPs have been found to have effects on the development of various diseases. Using HUVEC (testis) and HK-2 (kidney) cells in an organ-on-a-chip system, 50nm PS-NPs were endocytosed and increased the PI3K-AKT and MAPK pathways which are known pathways involved in tumour cell survival, tumour formation and metastatic cell growth (M. Xiao et al., 2023). Naked aminated PS-NPs were also shown to increase the aforementioned pathways in SK-BR-3 (breast cancer) cells despite only binding the cell surface membrane (S. Xiao et al., 2024). Using mouse models, PS-NPs were shown to significantly reduce the expression of the ZO-1 protein in the blood brain barrier after 28 days of continuous ingestion (Li et al., 2024). PS-NPs were also found to lead to mitochondrial dysfunction and reduction of ATP production in brain cells of mice, consequently leading to neurodegeneration similar to that observed in Parkinson's disease (Liang et al., 2022). Likewise, aminated PS-NPs induced more vascular endothelial damage than their naked and carboxylated counterparts, as well as lead to dysfunctional coagulation in the vasculature of mouse models (W. Wang et al., 2023). Overall, not only can NPs translocate and disrupt the integrity and functionality of various endothelial cells in the body but could consequently lead to development of neurological and cardiovascular disease and upregulate oncogenic pathways, leading to a range of cancer types.

1.3.8. NP and the placenta

While MNPs have been confirmed to translocate from the mother into the placenta, this translocation appears to have worsened over the last 20 years. Experiments conducted in Hawaii compared 10 placentas from 2006, 2013 and 2021, and found confirmation of MNPs in 60%, 90% and 100% of the placentas respectively, using Raman spectrometry (Weingrill et al., 2023). Some of the most common polluting plastics confirmed in these placentas were polypropylene, polyvinyl chloride, polyester and polyurethane to name a few, with the size and number of MNPs increasing significantly between 2006 and 2021 (Weingrill et al., 2023). Further studies have also confirmed MNPs in the placenta, particles between 2.1 and 18.5 µm were found to deposit intracellularly within syncytiotrophoblasts, residing within the cytoplasm and potentially lysosomes and lipid droplets (Ragusa et al., 2022). Although MNPs were discovered in 100% of placentas in the Hawaiian study in year 2021, there is some discrepancies regarding this as experiments conducted around the same time found that only 13% of healthy placentas analysed contained MNPs, whereas 100% of placentas associated to intrauterine growth restrictions (IUGR), contained MNPs (Amereh et al., 2022; Weingrill et al., 2023). Despite this discrepancy, it was found that MNPs morphology might lead to further induction of IUGR, as placentas associated with IUGR contained pellets, films, fibres

and fragments of MNPs whereas healthy placentas predominantly had fragments and films (Amereh et al., 2022). It was also found that MNP dosage in placentas inversely correlated with fetal head circumference and birth length, suggesting MNPs may alter placental nutrient exchange and lead to dysfunctional fetal development (Amereh et al., 2022). However, these studies do not indicate whether these MNPs were the cause of IUGR and therefore fetal maldevelopments or if increased MNP deposition was the result of placental dysfunction in IUGR.

As mentioned previously (section 1.2.2.), MNPs can be both manufactured and naturally occurring, and experiments have been conducted aiming to identify the toxicity of both pristine (manufactured) and weathered (modified to simulate naturally occurring) MNPs within the placenta. Using choriocarcinoma cell lines (BeWo b30), cell monolayers were exposed to 50 nm to 10 µm weathered or pristine MNPs, however both MNP types at any concentration did not result in cytotoxicity to the cell monolayers or the cells individually, even with increasing concentrations from 0.1 to 100 µg/ml to (Dusza et al., 2022). Regardless of the lack in cytotoxic effect, 50 nm MNPs were observed to transport through the monolayer, using transwell experiments, at an increased rate compared to larger MNPs, likely due to their size allowing for easier movement between the cells of the monolayer (Dusza et al., 2022). Alternatively, PS-NPs were shown to induce apoptosis of trophoblasts by activating Bcl-2 signalling via the mitochondrial pathway which was consistent in both NP-exposed mouse models and patient samples with recurrent miscarriages, as well as induce ROS and decrease mitochondrial membrane potential (Wan et al., 2024). Overall, despite lack of cytotoxic effects in the placenta, NPs could lead to dysregulation of trophoblasts (which, once differentiated into cytotrophoblasts and syncytiotrophoblasts, are integral for nutrient transport to the fetus and pathogenic defence at the placental barrier) potentially leading to miscarriages (Lunghi, Ferretti, Medici, Biondi & Vesce, 2007). Since NPs can potentially disrupt the integrity of the placental barrier and have various coronae (refer to section 1.2.7), it is plausible that NPs translocation inadvertently allow for larger MNPs or pathogens (whether as a corona or by disrupting the placental barrier integrity) to cross the placental barrier, paired with reducing the tolerance of the fetus to the maternal immune system. Likewise, as NPs can cause vascular endothelial injury, it could also be suggested that NP exposure in fetal capillaries could reduce the endothelial integrity and lead to a dysfunction in nutrient transport and gaseous exchange (W. Wang et al., 2023).

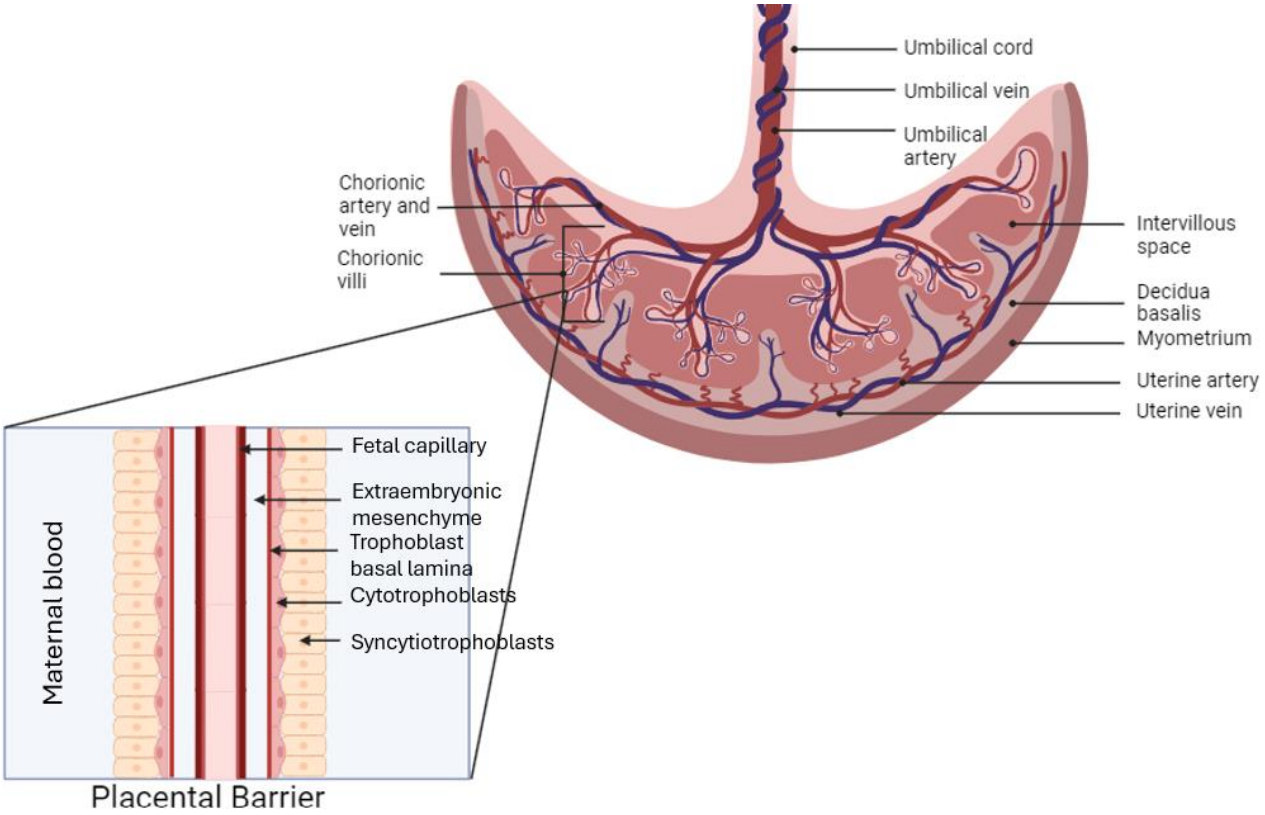

Figure 1.3. Placenta. This diagram shows the anatomy of the placenta, and the cell populations surrounding the fetal capillaries to create the placental barrier. Image adapted from Kulvietis, Zalgeviciene, Didziapetriene & Rotomskis (2011) and Jansen et al. (2020).

1.3.9. NP effect on fetal development and offspring

Research has shown that NP exposure during fetal development leads to adverse effects after birth. Mice offspring were found to have a significantly lower weight 8 weeks postpartum after gestational NP exposure when compared to controls (Huang et al., 2022). Gestational NP exposure also leads to inflammation and oxidative stress in the liver of offspring whilst also dysregulating glycometabolism (Huang et al., 2022; X. Wang et al., 2023). Interestingly, NPs might be able to deposit in the neonatal brain via mother-to-offspring breast feeding, as opposed to being just delivered during pregnancy, leading to abnormalities in the hippocampus suggesting possible behavioural issues (Jeong et al., 2022). However, it is worth noting that hepatic toxicity and behavioural issues have only been identified in female offspring, with little to no effect seen in male offspring, with the mechanisms for this not yet described (X. Wang et al., 2023; Jeong et al., 2022). From these studies, there is evidence to suggest that gestational exposure to NPs has detrimental effects postpartum that might be exacerbated by postpartum exposure, however, little research has been conducted of the effects on the innate immune system, which has a key role in the uptake of and response to particulates, of the mother and fetus during pregnancy.

1.4. Pregnancy

1.4.1. Physiological adaptations in pregnancy

During pregnancy, the fetus is identified as a foreign body by the mother's immune system due to paternal genetic material and the expression of paternal antigens, so immune modulation is required. Briefly, during the first trimester, there is an increase in both pro-inflammatory cytokines (TNF-α and IFN-γ) and T helper 1 (Th1) cells to ensure there is a sufficient immune response against pathogens in tandem with increasing inflammation to ensure successful implantation of the embryo and trophoblast invasion (Wang, Sung, Gilman-Sachs & Kwak-Kim, 2020). As pregnancy continues into the second trimester, the immune system shifts to an anti-inflammatory state as regulatory T cells (Tregs) reduce the activation and proliferation of various immune cells, aided by production of anti-inflammatory cytokines via Th2 cells (Rackaityte & Halkias, 2020; Graham, Longhi & Heneghan, 2021). Finally, in the third trimester, there is an increase in monocytes which have a reduced production of pro-inflammatory cytokines and an increased production of anti-inflammatory, namely IL-10, which is also aided by a further increase in Th2 cell responses (Abu-Raya, Michalski, Sadarangani & Lavoie, 2020; Sharma, Rodrigues, Zaher, Davies & Ghazal, 2022). Further immune, endocrine and metabolic changes during pregnancy are described in table 1.1.

System	Tissue/cell type	Adaptations	Functionality	References
Immune	Natural killer (NK) cells	NK cells allow for enhanced innate immunity. NK cells aid in placental development.	Modulation of NK cells allow for sufficient tissue remodelling during implantation and for placental development.	(Moffett & Colucci, 2014)
	Monocytes	Monocyte numbers are increased during pregnancy and express anti-inflammatory responses.	Reduce maternal inflammation to reduce the induction of an autoimmune attack on the fetus.	(Abu-Raya, Michalski, Sadarangani & Lavoie, 2020)
	Neutrophils	Neutrophil numbers are increased.	For increased phagocytosis and opsonisation of particles and pathogens during pregnancy.	(Gimeno-Molina, Muller, Kropf & Sykes, 2022)
	Macrophages	Proliferation of macrophages at the maternal-fetal interface.	Macrophage differentiation from monocytes for successful development of the placenta and are modulated for sufficient immune responses without attacking the semi-allogeneic fetus.	(Chambers et al., 2021)

	B cells	B cells increase production of immunoglobulin G to facilitate transfer to the fetus.	Prevents autoimmune responses towards the fetus and produces antigens to be transferred to the fetus providing some passive immunity.	(Muzzio, Zenclussen & Jensen, 2013).
	T cells	Regulatory T cells suppress functionality of effector T cells. Cytotoxic T cells are regulated to ensure sufficient immune surveillance and reduce inflammation towards the fetus.	Modulation of T cells maintains immune homeostasis whilst preventing excessive inflammation and providing sufficient protection against pathogens to allow for a successful pregnancy.	(Jenkins, Rees, Jones & Thornton, 2021) (La Rocca, Carbone, Longobardi & Matarese, 2014)
Metabolic	Placenta	Secretion of human chorionic gonadotrophin. Hub of nutrient and gas exchange between maternal and fetal circulations but provides a barrier to reduce pathogenic transfer.	hCG maintains the corpus luteum, blocking the menstruation process and allowing for the corpus luteum to produce progesterone. Gas and nutrient exchange allow for continuous supply of resources to the fetus for optimal growth and development.	(Fowden, Sferruzzi-Perri, Coan, Constancia & Burton, 2009) (Burton & Fowden, 2015)
	Liver	Increase in glycogenolysis and reduction of glycolysis.	For sufficient glucose storage and transportation, to meet energy demands of the mother and fetus.	(Rees et al., 2022)
	Adipose tissue	Maternal adipose tissue reservoirs increase in the first trimester before decreasing in the last trimester. Leptin is produced in moderation.	Adipose tissue catabolism provides energy to meet the metabolic demands of pregnancy, especially in the last trimester. Leptin modulates maternal appetite to ensure sufficient nutrient intake.	(Rees et al., 2022)
Endocrine	Oestrogen Progesterone	Production vastly increases.	Aids immune regulation towards anti-inflammatory responses and reduces functionality of innate immune cells. Catalyses the growth and development of the fetus.	(Magon & Kumar, 2012) (Robinson & Klein, 2012)

Table 1.1. Maternal physiological adaptations during pregnancy. This table describes some of the key immune, metabolic, and endocrine adaptations that occur during pregnancy to ensure a successful pregnancy.

1.4.2. Monocytes

Monocytes are CD14-expressing leukocytes derived from myeloid cells in the bone marrow and are typically found in the peripheral blood once differentiated (Goasguen et al., 2008). Monocytes can be characterised into 3 different subsets: CD14++CD16- (classical), CD14++CD16+ (intermediate) and $CD14^{dim}CD16$++ (non-classical) (Ziegler-Heitbrock et al., 2010; Xing et al., 2017). Monocytes have 3 main functions: phagocytosis, antigen presenting and cytokine production. Monocytes phagocytose pathogens such as bacteria to neutralise them and inhibit any further tissue/cellular damage (Schwarzmaier, Foell, Weinhage, Varga & Däbritz, 2013). Monocytes also produce pro- and anti-inflammatory cytokines for immune modulation and activation (Sconocchia et al., 2005; Schwarzmaier, Foell, Weinhage, Varga & Däbritz, 2013). During infection, monocytes are some of the first cells to respond and migrate to the site of infection (monocyte recruitment), they do this by ligand-receptor interactions (Tsou et al., 2007; Vanbervliet et al., 2002; Tacke et al., 2007). A key example of this is CC chemokine receptor 2 (CCR2) expressed on the monocyte's surface that binds to CC chemokine ligand 2, 7, 8 and 16 (CCL2, CCL7, CCL8 and CCL16 respectively) that is present in blood and produced by cells at sites of infection (Tsou et al., 2007; Tacke et al., 2007; She et al., 2022). The diffusion of CCL2 through blood drives monocyte chemotaxis, as the monocytes will adhere to CCL2 and move towards the site of infection (or from a low CCL2 concentration to a high CCL2 concentration) (Gschwandtner, Derler & Midwood, 2019).

1.4.3. Monocytes in pregnancy

During pregnancy, peripheral blood monocytes undergo phenotypic changes. Progesterone, oestradiol and hydrocortisone are positively correlated with increased CD14 expression, along with increased expression of CD163 (endocytosis) in both resting and activated monocytes (Mendoza-Cabrera et al., 2020). Despite the increase in CD14 expression, there is also an increase in non-classical monocytes ($CD14^{dim}CD16^{+}$) during pregnancy which are phenotypically pro-inflammatory, however this may be explained by the overall increase in peripheral monocytes in pregnancy (Rees et al., 2022; Rees et al., 2024). Similarly, monocytes from pregnant women have increased expression of Fc gamma (Fcγ) receptors which are involved in triggering phagocytosis (Davis, Kaufmann & Moticka, 1998). Increased circulation of leptin in pregnancy may also contribute to the increased phagocytic capabilities as its binding to the leptin receptor (CD295, which is upregulated in pregnancy) and subsequent activation stimulates the proliferation and phagocytic functionality of monocytes (Rees et al., 2024; Señarís et al., 1997; Francisco et al., 2018). Paired with increased phagocytic functionality, monocytes from pregnant women have been shown to have increased

expression CD80, HLA-DR, CD64, CD38 and CD169 (Rees et al., 2024). This indicates that monocytes develop a more phagocytic phenotype during pregnancy, while also increasing signalling for T cell activation and proliferation. While phagocytic ability was increased, production of pro- and anti-inflammatory cytokines was reduced in resting and activated monocytes in the first trimester, with an increase in pro-inflammatory cytokine production at the third trimester. However, cytokine production during pregnancy depends on the stimulating factor used to invoke said responses (Mendoza-Cabrera et al., 2020; Rees et al., 2022). LPS stimulated non-pregnant monocytes where not shown to have significant differences in TNF-α, IL-1β, IL-6 or IL-8, but muramyl dipeptide (MDP) stimulated monocytes significantly decreased the production of IL-6 and TNF-α (Rees et al., 2024). Monocytes during pregnancy increase the production of oxygen free radicals and readily produce IL-12 indicating their enhanced immune reaction should it be required (Rees et al., 2022). The characteristics of monocytes throughout pregnancy indicate that there needs to be a systemic modulation of inflammation to both protect the mother from pathogens/infections, and by extension, the fetus, while also maintaining immune tolerance of the developing fetus.

1.4.4. Placental Macrophages

Like monocytes, placental macrophages are innate immune cells and reside in the placental villi for the duration of pregnancy (Palani et al., 2011). They include fetally-derived Hofbauer cells. Placental macrophages are suggested to be derived from primitive haematopoiesis prior to fetal circulation development, but later in pregnancy stem from the differentiation of fetal monocytes once the fetal circulation has developed (possibly mediated by placental mesenchymal stem cells) (Thomas et al., 2021; Simoni, Jurado, Abrahams, Fikrig & Guller, 2017). Placental macrophages aid in implantation, angiogenesis, and placental homeostasis as well as exhibiting typical phagocyte functions (Abumaree et al., 2013; Joerink, Rindsjö, van Riel, Alm & Papadogiannakis, 2011). While expressing CD14, placental macrophages also express CD68 on lysosomes/phagosomes which are involved in phagocytosis and lysosomal metabolism, with overexpression associated with dysfunction (Okada et al., 2016; Kim et al., 2007). Macrophages can be classified broadly into 2 main subsets: classically activated M1 macrophages (which are phenotypically pro-inflammatory and are stimulated by IFN-γ or LPS) and alternatively activated M2 macrophages (which are phenotypically anti-inflammatory, involved in tissue homeostasis and activation of antibody-mediated immunity and are stimulated by IL-4 and/or IL-13) (Xue et al., 2014; Liu et al., 2022). With regards to M2 macrophages, these can be further categorised into M2a, M2b and M2c macrophages, which are classified depending on their gene expression profiles and by their molecular activations (Martinez, Sica, Mantovani & Locati,

2008). The M1/M2 classification of macrophages is now considered to represent the two ends of the spectrum of macrophage phenotypes, which are mediated by a range of transcription factors and activating molecules, therefore, macrophage classification may be better referred to as gradations within a spectrum rather than a binary (Kang & Kumanogoh, 2020). In early gestation, placental macrophages initially fall into the M1-like category, this is to promote implantation via increased pro-inflammatory response within the uterine tissues allowing for the adherence of the blastocyst to the uterine walls (Swieboda et al., 2020). In turn, in the later stages of pregnancy once the fetus, mother and placenta have reached a symbiosis, the placental macrophages typically develop into an M2-like phenotype and therefore skew towards production of anti-inflammatory cytokines such as IL-4 and IL-10, in an effort to reduce inflammation during infections or tissue damage and reduce the chance of fetal rejection (Swieboda et al., 2020; Joerink, Rindsjö, van Riel, Alm & Papadogiannakis, 2011; Liu et al., 2022).

1.5. Rationale

With previous research exploring the effects of NPs in pregnancy, offspring development postpartum and innate immune cells in the non-pregnant setting, there is a gap in knowledge about how NPs affect the innate immune response during pregnancy. This project will provide an insight into the potential hazards that NPs pose during pregnancy and the development of the fetus.

1.6. Hypothesis

Monocytes and macrophages, as mononuclear phagocytes, will be the primary cell type to take up NPs in a dose dependent manner with differences in the ability of monocytes from pregnant and non-pregnant women to take up NPs. NP internalisation will modulate inflammatory function of the cells.

1.7. Aims

1. To identify the main cell type in peripheral blood that takes up NPs.
2. To explore how varying NP concentrations are taken up by monocytes and placental macrophages at different timepoints over 24 hours and how uptake affects cell viability.
3. To compare NP uptake between monocytes of non-pregnant and pregnant women.

4. To observe changes in and compare production of TNFα, IL-1β and IL-10 in monocytes of non-pregnant and pregnant women as well as placental macrophages in response to NPs.

Chapter 2: Materials and Methods

2.1. Ethical approval

Blood from pregnant women was obtained at full term pregnancy (37+ weeks), prior to a scheduled delivery via caesarean section. Blood from non-pregnant women was donated by healthy women aged between 18 and 40 years of age to function as a control. Donors who received a vaccine and/or had an infection 2 weeks prior to donation were excluded from the study. Donors with any autoimmune conditions were also excluded from the study. Blood was collected in 9 ml BD Vacutainer heparin coated blood collection tubes (Greiner Bio-One). A maximum of 120 ml of healthy donor blood and 35 ml of pregnant blood could be donated. Placenta samples were also obtained during caesarean section. Ethical approval was granted via the Wales Research Ethics Committee 6 (placentas and pregnant blood: REC No. 11/WA/0040, healthy donors: REC No. 13/WA/0190) and Swansea University institutional ethics for healthy donors. Due to handling of blood, hepatitis B vaccinations were obtained prior to handling. All donations were voluntary and full informed and written consent was obtained prior to placenta and blood donations. Participants were able to withdraw consent for the study at any given time should they wish to.

2.2. Nanoplastics

Carboxylate-modified polystyrene at 0.04 µm and with yellow-green fluorescence (505/515) (Invitrogen), were used throughout this research project. NPs were sonicated for 5 mins before use to ensure separation of agglomerates. Initial stock NP concentration was provided by Invitrogen ($1.8x10^{15}$ particles/ml). By diluting in phosphate buffered saline (PBS; Gibco), $7.6x10^{13}$ particles/ml, $3.8x10^{13}$ particles/ml and $7.6x10^{12}$ particles/ml of NPs were produced. These concentrations were further diluted by a hundred-fold in blood or media to create $7.6x10^{11}$ particles/ml, $3.8x10^{11}$ particles/ml and $7.6x10^{10}$ particles/ml, which were used throughout the project. Despite being elevated compared to physiological exposure (refer to section 1.3), higher NP concentrations were used to investigate the impact on the functionality of monocytes and placental macrophages during pregnancy. A titration was performed prior to continuation with the aforementioned concentrations (refer to table 2.1 and section 3.1).

2.3. Identification of leukocytes/thrombocytes that take up NPs

500 µl whole blood from pregnant and non-pregnant women was cultured in individual falcon tubes per NP concentration. The tubes were cultured at 37°C with 5% CO_2 for the allocated time as stated in table 2.1.

		Timepoints			
		T0	T2‡	T6‡	T24
NP concentrations (particles/ml)	0	✓	✓	✓	✓
	$3.8x10^7$				✓
	$7.6x10^7$				✓
	$3.8x10^8$				✓
	$7.6x10^8$				✓
	$3.8x10^9$				✓
	$7.6x10^9$				✓
	$3.8x10^{10}$				✓
	$7.6x10^{10}$		✓	✓	✓
	$3.8x10^{11}$		✓	✓	✓
	$7.6x10^{11}$		✓	✓	✓

Table 2.1. Timepoints and NP concentrations. This table describes NP concentrations used at various timepoints for analysis of leukocytes and thrombocytes. T0, 0 hrs; T2, 2 hrs; T6, 6 hrs; T24, 24 hrs. ‡ denotes that these timepoints were used in later experiments specifically analysing NP uptake in monocytes in whole blood.

At the respective timepoints, 100 µl of blood was removed and pipetted into two FACS tubes (Corning®, Fischer Scientific); due to configuration of cytometer settings, one tube is needed specifically for platelet analysis, and another tube for leukocyte analysis). Following this, 3 ml of lysis buffer (10% lysing solution [BD] in deionised water) was added to each FACS tube and left in the dark at room temperature for 15 mins. The tubes were centrifuged for 7 mins at 515 x *g* and the supernatant was discarded. The cells were washed twice with 3 ml of FACS buffer (0.05% filtered sodium azide [Sigma-Aldrich] and 1% bovine serum albumin [BSA, Sigma-Aldrich] in PBS), centrifuging between washes at the aforementioned settings. Finally, the cells were resuspended in 200 µl of FACS buffer ready for acquisition via the Cytek Aurora™ flow cytometer (Cytek®, 4 Laser 16V-14B-10YG-8R).

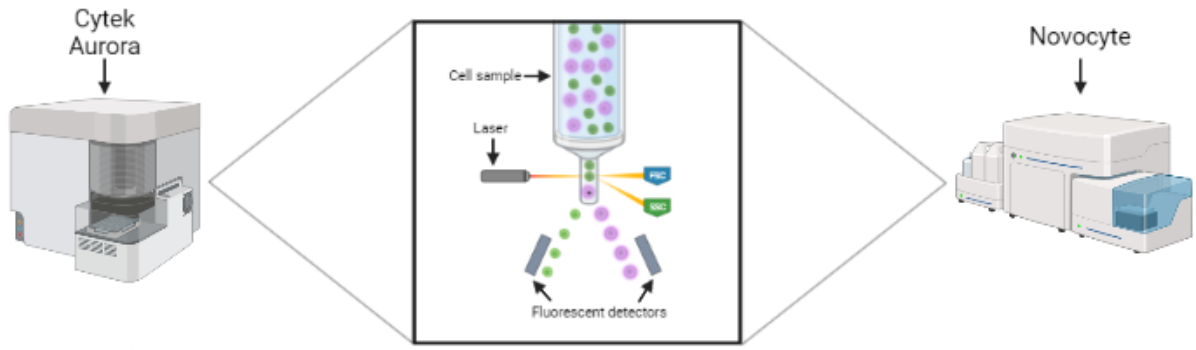

Figure 2.1. NovoCyte and Cytek Aurora flow cytometers. This diagram shows an example of cells within flow cytometers. The machines described show cells being passed through, single file, and subjected to lasers, allowing for light scattering based on size and granularity of said cells. Specific fluorophores bound to these cells are detected by fluorescent detectors.

2.3.1. Gating strategy for leukocyte/thrombocyte analysis

To identify the main cell subset(s) in whole blood that might take up NPs, monocytes, lymphocytes, neutrophils and platelets were identified by their characteristic forward scatter (FSC) and side scatter (SSC), followed by gating for removal of debris. A series of gates were then used to select single cells followed by using FITC expression to determine NP presence with cells and presenting this as a histogram. The median fluorescent intensity (MFI) of this signal was used as a measure of NP uptake analysis.

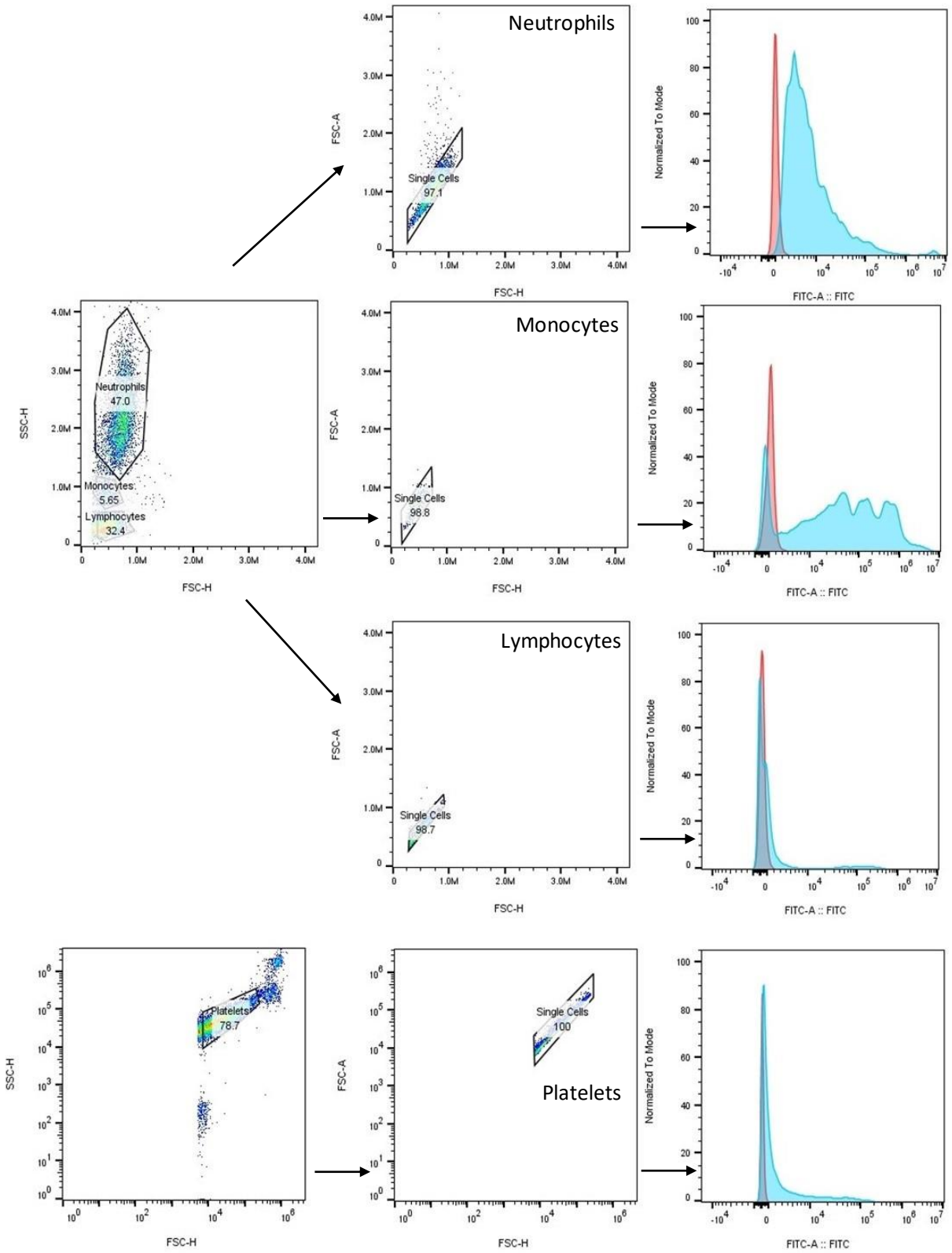

Figure 2.2. Leukocytes and platelets with NPs gating strategy. FSC-H by SSC-H dot plots were used to exclude any debris from the cellular populations. Singlet leukocytes and platelets were isolated via gating on FSC-H by FSC-A dot plots. Histograms were used to identify NP uptake in the populations via their NP MFI. This figure uses leukocytes and platelets cultured with 7.6×10^{11} particles/ml of NPs for 24 hrs compared with the control as an example.

2.4. Monocytes

2.4.1. Monocyte Isolation

Firstly, peripheral blood was diluted with PBS (1:4); 30 ml of the diluted blood was layered over 15 ml of Lymphoprep™ (Stemcell). This was centrifuged at 400 x *g* for 40 mins with no acceleration or brake. The plasma layer was discarded, and the mononuclear cells (MNCs) were extracted.

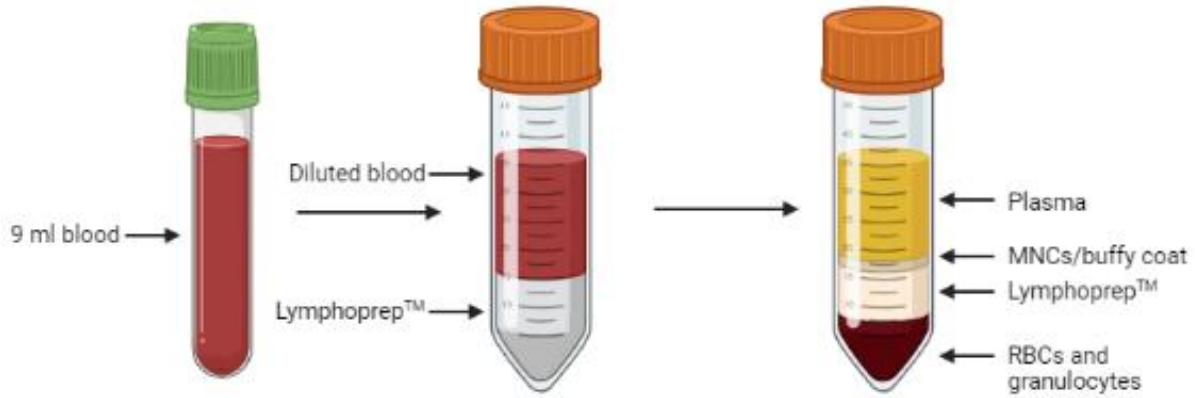

Figure 2.3. MNCs isolation by density gradient centrifugation. 9 ml of blood in heparin tubes was collected from non-pregnant and pregnant donors. The blood was diluted 1:4 with PBS and layered over 15 ml of Lymphoprep™. After centrifugation, the blood separated by density into layers of plasma, MNCs, Lymphoprep™ and red blood cells (RBCs) and granulocytes.

The MNCs were washed twice with RPMI 1640 + GlutaMAX (Gibco) and centrifuged at 515 x *g* for 10 mins. The media was removed and the MNC pellet was resuspended in 1 ml of RPMI 1640 + GlutaMAX. A 2 µl aliquot was diluted 1:30 for pregnant blood and 1:40 for non-pregnant blood with RPMI 1640 + GlutaMAX. 10 µl of these dilutions were mixed with 0.4% trypan blue (NanoEntek) (1:1) and counted on the Countess™ 3 FL Automated Cell Counter (Invitrogen). The cell suspension was centrifuged for 300 x *g* for 10 mins and the supernatant was removed, followed by resuspending the pellet with 80 µl of magnetically activated cell sorting (MACS) buffer (1% fetal bovine serum [FBS, Fisher Scientific] in PBS) per 10^7 cells. 20 µl of CD14 magnetic beads (Miltenyi Biotec) per 10^7 cells were added to the cell suspension and then incubated in the dark at 4°C for 15 mins. The cells were washed with MACS buffer and then centrifuged at 300 x *g* for 10 mins. The supernatant was removed, and the pellet was resuspended in 500 µl of MACS buffer and run on an autoMACS Pro separator (Miltenyi Biotec) twice via positive selection to isolate the monocytes.

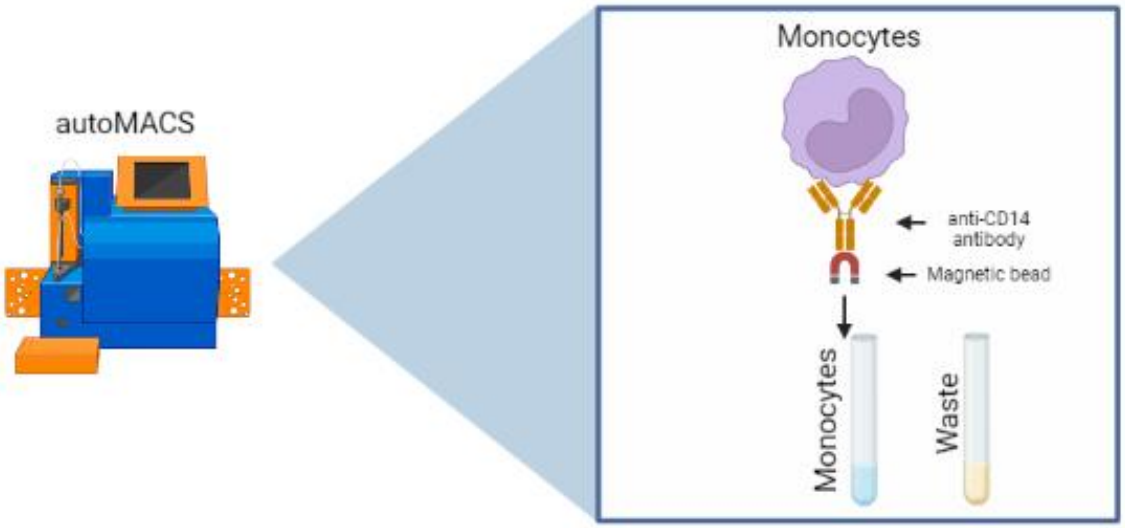

Figure 2.4. Positive selection and isolation of monocytes. Monocytes were selectively bound to anti-CD14 antibodies bound to magnetic beads. Mononuclear cells were then passed through an autoMACS Pro separator. A magnetic field allowed the labelled cells to bind, letting unlabelled cells pass through. The magnetic field was removed allowing for the collection of the attached cells.

Finally, the monocyte suspension was centrifuged at 300 x *g* for 10 mins. The supernatant was removed, and the pellet was resuspended in 500 µl of culture media A (10% Hyclone FBS [Fisher Scientific], RPMI 1640 + GlutaMAX, 0.2% 2-mercaptoethanol [Gibco]). 2 µl of cells were diluted with culture media (1:5) and 10 µl of this dilution was mixed with 0.4% trypan blue (1:1) for a live cell count via the Countess™ 3 FL Automated Cell Counter (Invitrogen).

2.4.2. Monocyte isolation purity

After isolating monocytes, $0.1x10^6$ cells/100 µl of FACS buffer were used to determine purity of the monocyte preparation. 5 µl of anti-human CD14 Pacific Blue (BioLegend, clone: 63D3) was added to one tube, leaving the remaining tube unstained. The cells were left on ice in the dark for 15 minutes. Following this, 3 ml of FACS buffer was added and the cells were centrifuged at 515 x *g* for 7 mins at 4ºC. The supernatant was then tipped off and the cells resuspended in 200 µl of FACS fix (10% CellFix [BD Bioscience] in deionised water) for purity analysis on the NovoCyte ACEA flow cytometer (NovoCyte 3000 System). A sample was accepted for further analysis when cell purity was ≥ 95%.

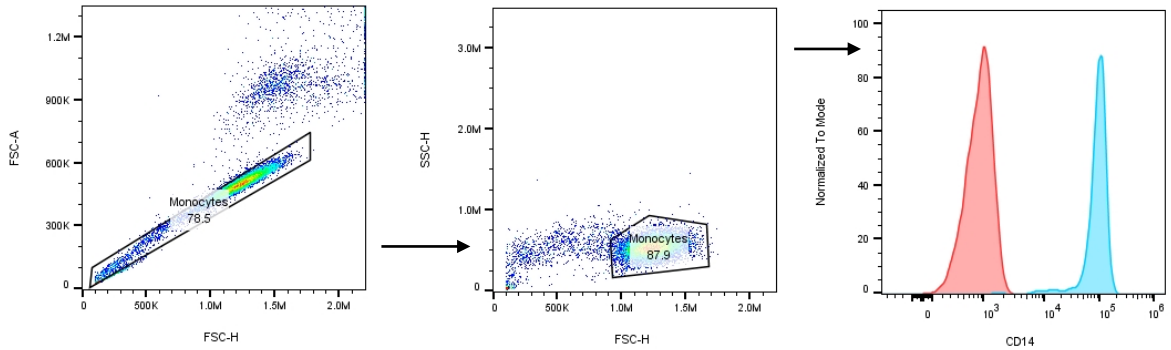

Figure 2.5. Monocyte purity gating strategy. Singlet monocytes were identified using forward scatter height (FSC-H) by forward scatter area (FSC-A) and a gate is drawn. FSC-H by side scatter height (SSC-H) dot plots were then used to exclude any debris from the monocyte population. Histograms were used to compare the unstained to the anti-CD14 stained monocytes and to calculate purity.

2.4.3. Monocyte Culture

Monocytes were cultured at $0.2x10^6$ cells/200 µl of culture media A in a flat bottom 96 well plate (Greiner Bio-One). $7.6x10^{11}$ particles/ml, $3.8x10^{11}$ particles/ml, $7.6x10^{10}$ particles/ml and 0 particles/ml of NPs were added to monocyte cultures with and without lipopolysaccharide (LPS, 10 ng/ml [Invivogen]). Monocytes were cultured at 37°C with 5% CO_2 for 20 hours. Following this, the monocytes were centrifuged at 515 x *g* for 7 mins and the cell free supernatant was extracted and stored at -20°C for later use.

2.4.4. Monocyte subset identification

To identify phenotypes of monocytes present in whole blood, 100 µl of blood was removed and pipetted into two FACS tubes (Corning®, Fischer Scientific). Leaving one tube unstained, 5 µl of anti-human CD14 Pacific Blue (BioLegend, clone: 63D3) and anti-human CD16 APC (Miltenyi Biotec, clone: 3G8) was added to the second tube and placed on ice for 30 mins in the dark. Following this, 3 ml of lysis buffer (10% lysing solution [BD] in deionised water) was added to each FACS tube and left in the dark at room temperature for 15 mins. The tubes were centrifuged for 7 mins at 515 x *g* and the supernatant was discarded. The cells were washed twice with 3 ml of FACS buffer, centrifuging between washes at the aforementioned settings. Finally, the cells were resuspended in 200 µl of FACS buffer ready for acquisition via the Cytek Aurora™ flow cytometer (Cytek®, 4 Laser 16V-14B-10YG-8R).

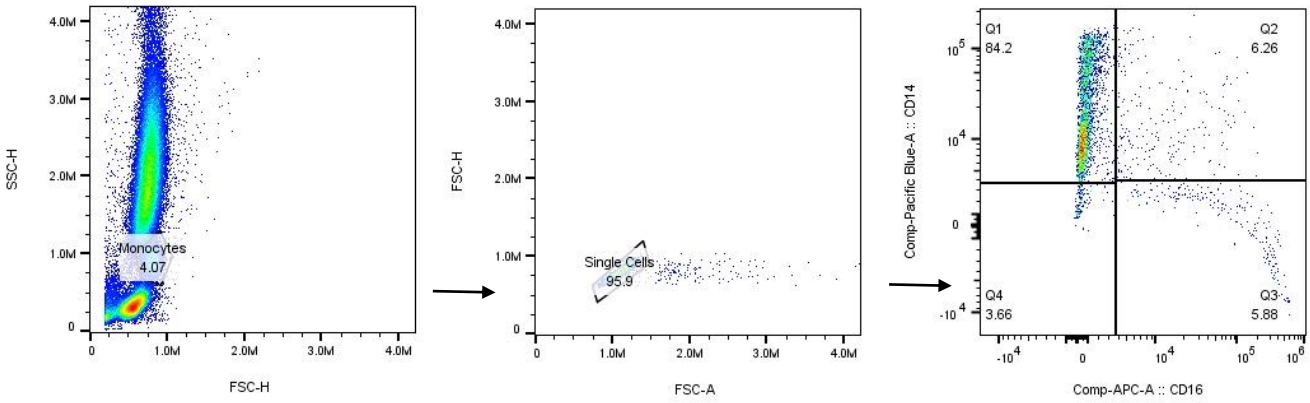

Figure 2.6. Monocyte subsets. FSC-H by SSC-H dot plots were used to exclude any debris from the monocyte population. Singlet monocytes were then isolated via FSC-H by FSC-A dot plots. Subsets of monocytes were then identified by their CD14/CD16 profiles. NP MFIs were then analysed per subset. Q1, classical monocytes; Q2, intermediate monocytes; Q3, non-classical monocytes; Q4, CD14-CD16- cells.

2.5. Placental macrophages

2.5.1. Placental macrophage isolation

Firstly, the placenta was placed into a sterile kidney dish, followed by the maternal decidua being removed with scissors. 120 g of placental tissue was then taken and placed in 0.9% saline (Baxter) and washed thoroughly to remove all maternal blood. 337.5 ml of digestion solution was made in two separate T175 flasks, and comprised the following:

1. 300 ml Hank's balanced salt solution (HBSS) (Life Technologies)
2. 7.5 ml 4-(2-hydroxyethyl)-1-piperazineethanesulfonic acid (HEPES buffer) (Gibco)
3. 30 ml 2.5% trypsin solution 10X (Gibco)
4. 60mg filtered DNase I (Sigma-Aldrich)
5. 300mg filtered $MgSO_4$ (Sigma-Aldrich)

140 ml of digestion solution was removed from each T175 and kept for later use before adding placental tissue to the remaining digestion solution in the T175. The washed placental tissue was divided evenly and added to each flask. The flasks were incubated for 45 mins at 37°C on a plate shaker at 400 rpm. The digestion solution was removed and strained through 100 µm cell strainers (pluriStrainer® 100 µm; pluriSelect) into falcon tubes containing 2 ml of FBS, reaching a total volume of 50 ml. 140 ml of fresh digestion solution was then added to the tissue in the T175 flasks and incubated for a further 30 mins with the same aforementioned specifications. Finally, the remaining digestion solution was removed and strained as before. The falcon tubes were centrifuged at 15 mins at 1000 x *g*. Pellets were resuspended in HBSS and combined into three 50 ml falcons, followed

by topping up to 50 ml with HBSS. 30 ml of the cell suspension was layered over 15 ml of Lymphoprep™ (Stemcell) and then centrifuged at 400 x *g* for 40 mins with no acceleration or brake. The buffy coat layer was isolated into 50 ml falcons (around 15 ml/falcon) and topped up to 50 ml with RPMI 1640 + GlutaMAX. The MNC cell suspension was centrifuged at 700 x *g* for 10 mins, followed by resuspending and combining the cell pellets with RPMI 1640 + GlutaMAX. Cell count was either done neat or 1:5 with RPMI 1640 + GlutaMAX depending on pellet size and 10 µl of the cell suspension 1:1 stain of trypan blue was counted using a cell counter.

The isolated MNCs were then centrifuged at 500 x *g* for 10 mins and after discarding the supernatant the pellet was resuspended in MACS buffer and CD14+ microbeads (80 µl and 20 µl/10^7 cells respectively). The cells were incubated for 30 mins, in the dark at 4^{O}C. Following this, 4 ml of MACS buffer was added to the cell suspension before centrifuging for 10 mins at 500 x *g* and 4^{o}C. The cell pellet was resuspended in 500 µl/10^8 cells of MACS buffer. 3 ml of MACS buffer was allowed to pass through the MACS liquid separation (LS) column (Miltenyi Biotec) that was held in a separator magnet (Miltenyi Biotec). A 30 µm pre-separation filter (Miltenyi Biotec) was placed on top of the LS column and the MNC suspension then applied to the column and allowed to pass into the column. The column was washed 3 times each with 3 ml of MACS buffer. Finally, the pre-separation filter was removed, and 5 ml of MACS buffer was added before swiftly plunging the captured magnetically labelled macrophages out into a 15 ml falcon. This isolation process was repeated, disregarding the pre-separation filter. The macrophage suspension was centrifuged for 10 mins at 500 x *g* at 4^{o}C. The pellet was resuspended in 1 ml of culture media B (10% Hyclone FBS, RPMI 1640 + GlutaMAX, 100 µM 2-mercaptoethanol, 1% pen-strep). 2-10 µl of cells were diluted with culture media (between neat and 1:5 depending on pellet size). 10 µl of these dilutions were mixed with 0.4% trypan blue (1:1) for a live cell count on the Countess™ 3 FL Automated Cell Counter (Invitrogen).

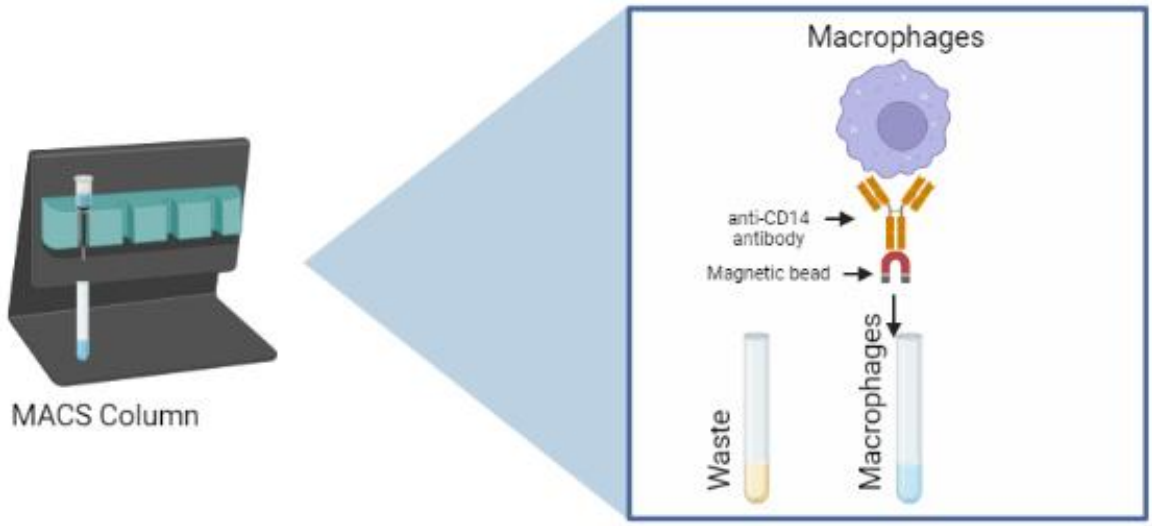

Figure 2.7. Positive selection and isolation of placental macrophages. Placental macrophages were selectively bound to anti-CD14 antibodies bound to magnetic beads. Placental macrophages were passed through a MACS LS column. A magnetic field allowed the labelled cells to bind, letting unlabelled cells pass through. The magnetic field was removed allowing for the collection of the attached cells.

2.5.2. Placental macrophage purity

CD14 staining for macrophages follows the same protocol as section 2.4.2. However, after centrifugation and tipping off supernatant, cells also were stained intracellularly with anti-human CD68 PE antibodies (Miltenyi Biotec, clone: REA886) as CD68 is expressed on lysosomes and indicates macrophages from a monocytic lineage (Okada et al., 2016; Kim et al., 2007). Cells were resuspended in 250 µl FACS buffer and 250 µl Inside Fix (Miltenyi Biotec) then incubated for 20 mins at room temperature. Following this, the cells were centrifuged for 5 mins at 300 x *g*. After discarding the supernatant, the cells were resuspended in 1 ml of FACS buffer and centrifuged again at 300 x *g* for 5 mins. The supernatant was again removed, and the cells resuspended in 100 µl Inside Perm (Miltenyi Biotec) along with 2 µl of CD68 PE antibodies. The macrophages were incubated in the dark for 10 mins at room temperature followed by a further 1 ml Inside Perm which was added before the cells were centrifuged for 300 x *g* for 5 mins. Finally, the supernatant was tipped off and the cells were resuspended in 200 µl of FACS fix before acquisition on the NovoCyte flow cytometer. Purity acceptance followed the same method as monocyte purity (section 2.4.2).

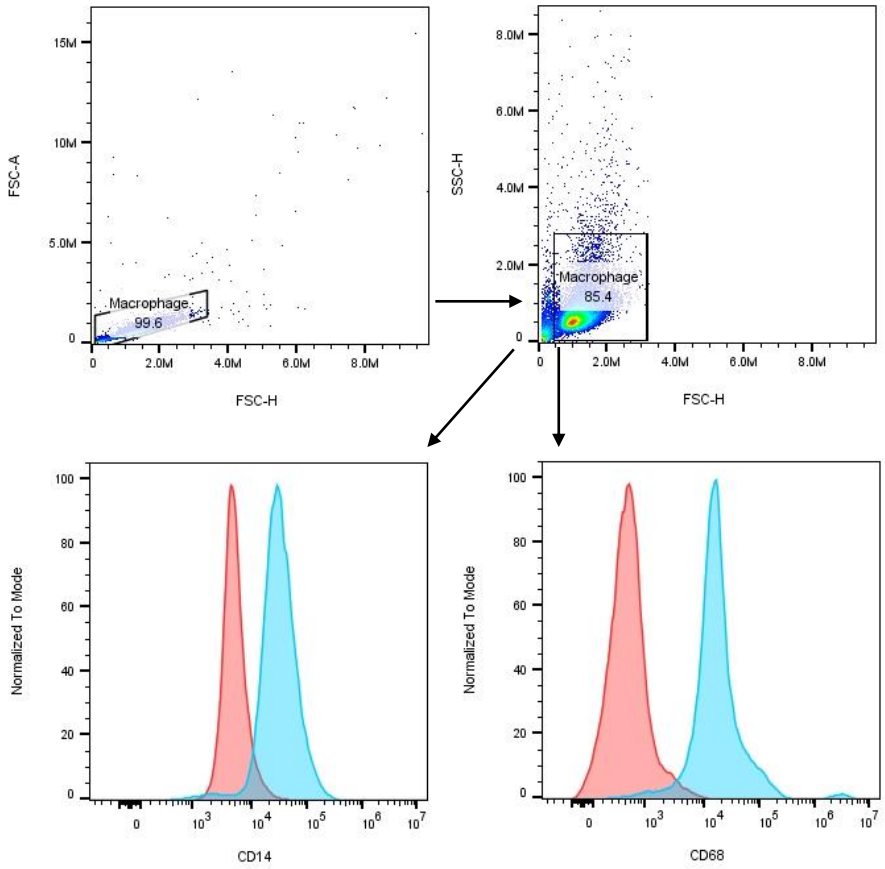

Figure 2.8. Placental macrophage purity gating strategy. Singlet placental macrophages were identified via FSC-H by FSC-A dot plots. FSC-H by SSC-H dot plots were used to exclude any debris. Histograms were used to calculate purity by comparing the unstained to the anti-CD14 stained and anti-CD68 stained monocytes.

2.5.3. NP fluorescence in placental macrophages

Placental macrophages were cultured in tissue culture tubes (VWR) at $0.25x10^6$ cells/500 µl of culture media B. The macrophages were allowed to rest at 37°C with 5% CO_2 for 16 hrs before any experimental conditions were introduced, with the macrophages in individual tissue culture tubes ready for the same conditions mentioned in section 2.4.3. After the 16 hrs, the macrophages were centrifuged at 515 x *g* for 7 mins and the supernatant was discarded. The macrophages were then resuspended in 500 µl of culture media with NP concentrations previously mentioned in section 2.4.3 and cultured at 37°C with 5% CO_2.

At the respective timepoints, the macrophages were centrifuged at 515 x *g* for 7 mins and the supernatant was tipped off. Each tube of macrophages was resuspended thoroughly in 200 µl of FACS buffer and 100 µl of the suspension was added to a new FACS tube. To analyse the effect of NP on the viability of placental macrophages, the use of DRAQ7 (BioLegend) was implemented. DRAQ7

binds to double stranded DNA of dead or permeabilised cells, allowing for the differentiation of live and dead cells within a population (BioLegend, 2024). 5 µl of DRAQ7 (1:15 in FACS buffer) was added to one tube, leaving the other unstained, and left for 15 mins at room temperature in the dark. The macrophages were washed in 3 ml of FACS buffer before centrifuging for 7 mins at 515 x *g*. The supernatant was tipped off and the macrophages were resuspended in 200 µl of FACS fix or FACS buffer until ready for acquisition on the Cytek Aurora flow cytometer.

2.5.4. Gating strategy for placental macrophage selection

Like monocytes, isolated placental macrophages were analysed via flow cytometry (Figure 2.8). Singlets were initially selected followed by the gating out of debris. DRAQ7 expression was used to determine the viability of placental macrophages, represented as a percentage. This was paired with the MFI of the live placental macrophages to analyse the uptake of NPs in placental macrophages and the effects of NPs on macrophage viability.

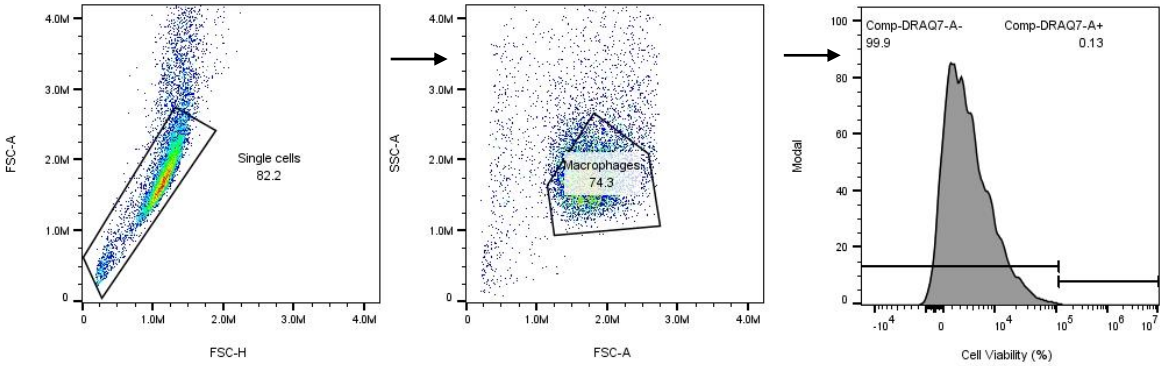

Figure 2.9. Placental macrophage viability with NPs gating strategy. Singlet placental macrophages were isolated via FSC-H by FSC-A dot plots. FSC-H by SSC-H dot plots were used to exclude any debris from the macrophage population. Histograms were used to identify cell viability with NP exposure, paired with FITC MFI for NP uptake. This figure uses the cell viability of monocytes cultured with $7.6x10^{10}$ particles/ml of NPs for 2 hrs as an example.

2.5.5. Placental macrophage culture

Placental macrophages were cultured at $0.2x10^{6}$ cells/200 µl of culture media B and allowed to rest for 16 hrs at 37°C with 5% CO_2 before any experiments. Following this, the plated macrophages were centrifuged at 515 x *g* for 7 mins. The supernatant was discarded, and fresh culture media B was added to the cells along with $7.6x10^{11}$ particles/ml, $3.8x10^{11}$ particles/ml, $7.6x10^{10}$ particles/ml and 0 particles/ml of NPs, with and without LPS (10 ng/ml). The macrophages were then cultured for 24

hrs at 37°C with 5% CO_2. After this time, the macrophages were centrifuged at 515 x *g* for 7 mins, and the cell free supernatant was removed and stored at -20°C for later use.

2.6. Flow cytometry compensation

Compensation was used to account for the overlap of emission wavelengths of the various fluorophores used with both cell types under investigation. This was achieved by using the unmix/compensation tool on SpectroFlo, a program used in conjunction with the Cytek Aurora for flow analysis. As purity of monocytes and macrophages was analysed on the NovoCyte flow cytometer, compensation was achieved using the compensation tool on FlowJo and gating for positive and negative peaks, creating a matrix to distinguish overlaps in fluorophores. This compensation was then applied to purity samples.

2.6.1. Flow cytometry data analysis

High parameter flow cytometry was analysed by exporting the data from SpectroFlo as .fcs files to FlowJo version 10.8.1 (BD Biosciences), followed by imputing the data into GraphPad.

2.7. Confocal Microscopy

While NPs can be taken up by monocytes and macrophages, they may also bind to the surface of the cells. Therefore, confocal microscopy was conducted to confirm NP internalisation.

2.7.1. Monocytes

Monocytes were cultured in an 8-well chamber slide (Millicell® EZ slide; Merck) at $0.1x10^6$ cells/300 µl of monocyte culture media A with 0, $7.6x10^{10}$, $3.8x10^{11}$ and $7.6x10^{11}$ particles/ml of NPs and incubated at 37°C with 5% CO_2 for 20 hrs. Following this, the media was removed from the wells and 300 µl of Formalin 10% (Sigma-Aldrich) was added and left at room temperature for 15 mins. Formalin 10% was removed, and each well was washed twice with 300 µl of PBS. While leaving the cells in PBS to prevent drying, 4', 6-diamidino-2-phenylindole (DAPI) and CellMask Orange stains were prepared (0.01% DAPI [Invitrogen], 0.01% CellMask Orange [Invitrogen] in PBS). DAPI binds to the nuclei of cells for a blue-fluorescence (ex/em 358/461 nm) and CellMask Orange binds to the cell membrane for an orange-fluorescence (ex/em 556/571 nm). The PBS was removed from the wells

and 300 µl of the staining solution was added to each well and left in the dark at room temperature for 15 mins. The staining solution was removed, and the cells were washed twice with 300 µl of PBS. The cells were left in PBS to prevent drying while the chamber compartment was removed. Finally, the remaining PBS was removed and 20 µl of VECTASHIELD (Vector Laboratories) was added. The slide was covered with a coverslip (Ultima) and sealed with clear nail polish (Rimmel London). The cells were kept at 4°C until ready for analysis via the ZEISS LSM 980 with Airyscan.

2.7.2. Placental macrophages

Placental macrophages were cultured in an 8-well chamber slide at $0.1x10^6$ cells/300 µl of culture media B with different NP concentrations and incubated at 37°C with 5% CO_2 for 16 hrs. Following this, the media was removed, and the cells were cultured with 300 µl of macrophage culture media and 0, $7.6x10^{10}$, $3.8x10^{11}$ and $7.6x10^{11}$ particles/ml of NPs for 24 hrs. The methodology proceeding this followed that described in section 2.7.1.

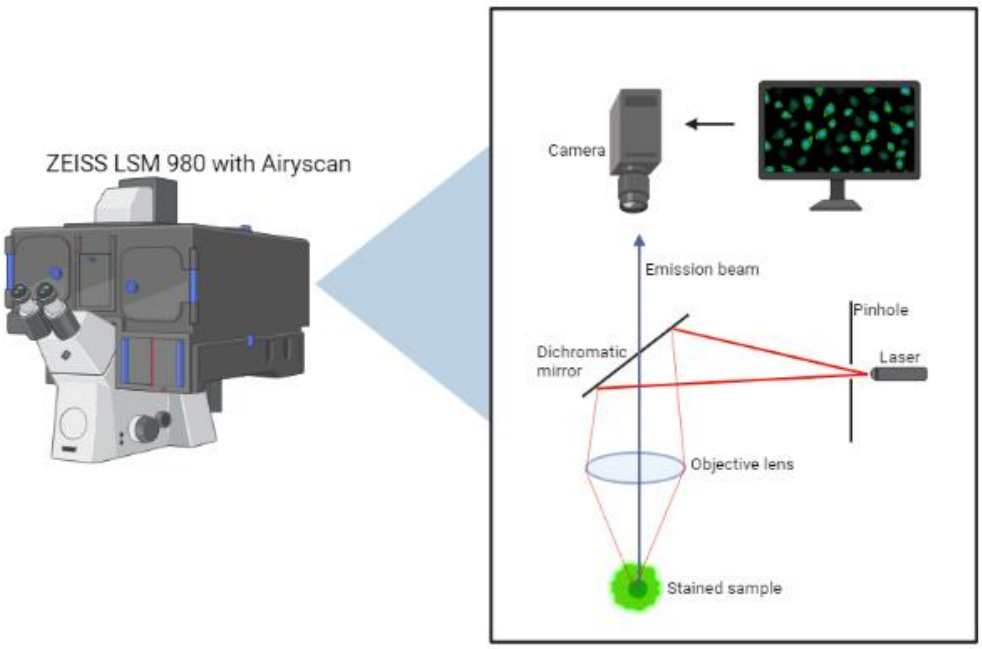

Figure 2.10. Zeiss LSM 980 with Airyscan. This diagram gives a basic description of confocal microscopy. A laser is passed through a pinhole which reaches dichromatic mirrors. The laser beam is then reflected into an objective lens which focuses the laser onto the stained sample. The emission beam is then reflected upwards and picked up by the attached camera allowing for visualisation of the stained sample.

2.7.3. Confocal microscopy compensation

As overlap of excitation/emission spectra of the fluorescent stains may occur, compensation was used to correct this and ensure accurate representation of the fluorescent signals in the stained sample. The fluorescent signals were compensated using the ZEISS ZEN Pro version 3.8 in-built compensation tool.

2.7.4. Confocal microscopy data analysis

Cells were optimised for confocal microscopy via the ZEISS ZEN Pro version 3.8. Images were exported as .jpeg files and edited using ImageJ version 1.54f.

2.8. Cytokine production

Enzyme linked immunosorbent assays (ELISAs) were conducted using DuoSet matched pairs (Biotechne) and following the R&D System guidelines. TNFα, IL-1β and IL-10 were the three cytokines analysed throughout this project and dilutions for all reagents are detailed in table 2.2.

Reagent	Dilutions		
	TNF-α	IL-1β	IL-10
Standard	1:120	1:380	1:75
Capture antibody†	1:120	1:120	1:120
Monocyte unstimulated^	1:50	1:50	Neat
Monocyte LPS^	1:300	1:200	Neat
Placental macrophage unstimulated^	Neat	Neat	Neat
Placental macrophage LPS^	1:30	Neat	1:10
Detection antibody	1:60	1:60	1:60
Streptavidin-HRP	1:40	1:40	1:40

Table 2.2. Reagent dilutions. All reagents/samples used within cytokine production analysis and their respective dilutions per cytokine under investigation. Each reagent used blocking buffer (1% BSA in PBS) as a diluent. † signifies that capture antibody uses PBS as a diluent; ^ denotes cell culture supernatants.

Capture antibodies were diluted in PBS and 50 µl/well were added to a 96 half-area plate (Greiner Bio-One) to be incubated at 4°C overnight. After incubation, the capture antibodies were tipped off and 150 µl/well of blocking buffer (1% bovine serum albumin [BSA, Sigma-Aldrich] in PBS) was added. The plate was incubated for 1 hr on a plate shaker (Titramax 1000; Heidolph) set to 400 rpm.

After this, the plate was washed three times with ELISA wash buffer (0.05% Tween 20 [ThermoFisher Scientific], 1 PBS sachet [Gibco] in 1 L deionised water). Samples and cytokine standards were diluted as optimised in blocking buffer and 50 µl/well was added to the plate. The plate was incubated for 2 hrs on a plate shaker at 400 rpm. The plate was then washed four times with wash buffer. Detection antibodies were diluted in blocking buffer and added to the wells at 50 µl/well and the plate incubated for 2 hours on a plate shaker set to 400 rpm. The plate was aspirated 4 times with wash buffer. Streptavidin-horse radish peroxidase (streptavidin-HRP) was diluted with blocking buffer and added to the plate at 50 µl/well. The plate was incubated for 20 mins on a plate shaker at 400 rpm. The plate was aspirated 6 times with wash buffer before addition of 3, 3', 5, 5' tetramethylbenzidine (TMB, BD Biosciences) which is made in a 1:1 ratio of Substrate A and Substrate B. 50 µl/well of TMB was added and incubated in the dark until a blue colour developed throughout the standard curve. The reaction was stopped by adding 50 µl/well of 1 M sulphuric acid (H_2SO_4). The absorbance was measured on a plate reader (FLUOstar Omega) at a wavelength of 450 nm (Figure 2.10).

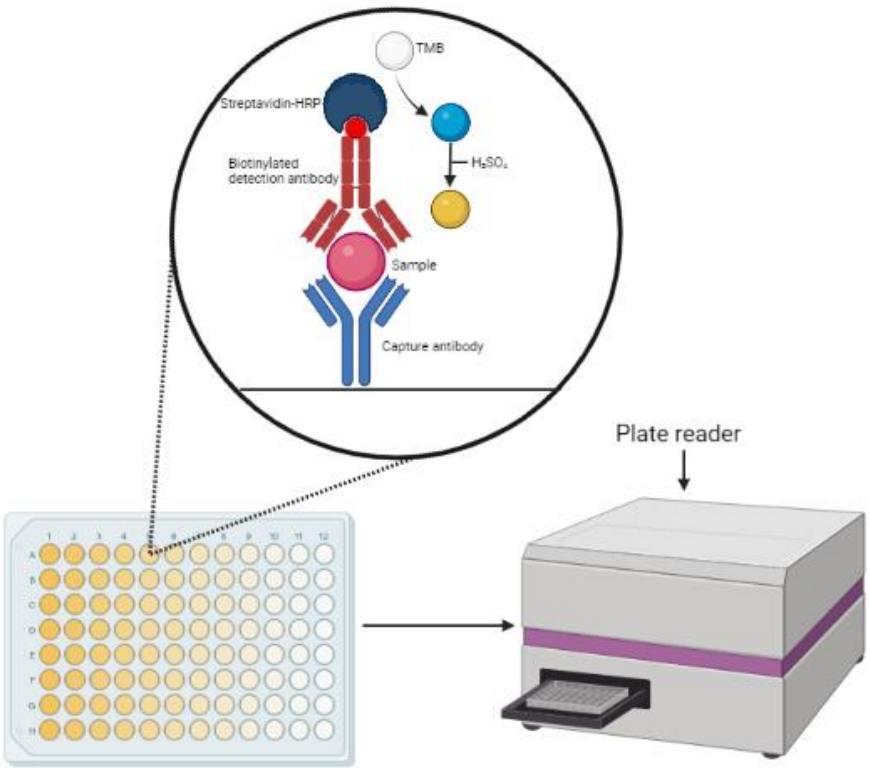

Figure 2.11. Sandwich ELISA experiments for analyte detection. A Greiner 96 half-well plate is coated with a capture antibody. After blocking non-specific binding, the sample with appropriate dilution is then added which binds to the capture antibody. A biotinylated detection antibody is then added creating the "sandwich." Streptavidin-HRP is added followed by TMB which is catalysed by HRP to undergo a colour change. The reaction is then stopped by addition of H_2SO_4. The plate is then analysed in a NovoCyte plate reader for measurement of absorbance.

2.8.1 ELISA data analysis

ELISA data was analysed by exporting as an .xlsx file from Omega MARS version 3.42 R5 to Microsoft Excel version 2304 for analysis before exporting data to GraphPad.

2.9. Statistical analysis

The results for all experiments are represented as mean ± standard error of mean (SEM). GraphPad Prism 9.5.1 was used for statistical analysis. One-way ANOVAs, Two-way ANOVAs with Tukey post hoc tests and Mann-Whitney tests were used as statistical tests throughout the project. Significance was accepted when $p \leq 0.05$.

Chapter 3: NP uptake in peripheral and resident mononuclear phagocytes

3.1. NP uptake optimisation in monocytes and placental macrophages

Initial experiments used blood from non-pregnant donors to identify the candidate cell type and NP concentrations for further work (figure 3.1). Non-pregnant whole blood was cultured at 37°C and 5% CO_2 for 24 hrs with various NP concentrations to identify NP uptake in each cell type within whole blood using the gating strategy shown in figure 2.2. Of all the cell types analysed, monocytes and neutrophils were shown to significantly take up NPs, but this was only seen at $7.6x10^{11}$ particles/ml when compared to the control (figure 3.1C and 3.1D). Further analysis into the differences of NP uptake per cell type showed that monocytes took up significantly more NPs when compared to all other cell types, as displayed in figure 3.2 where all cell types are compared at the same number of NPs.

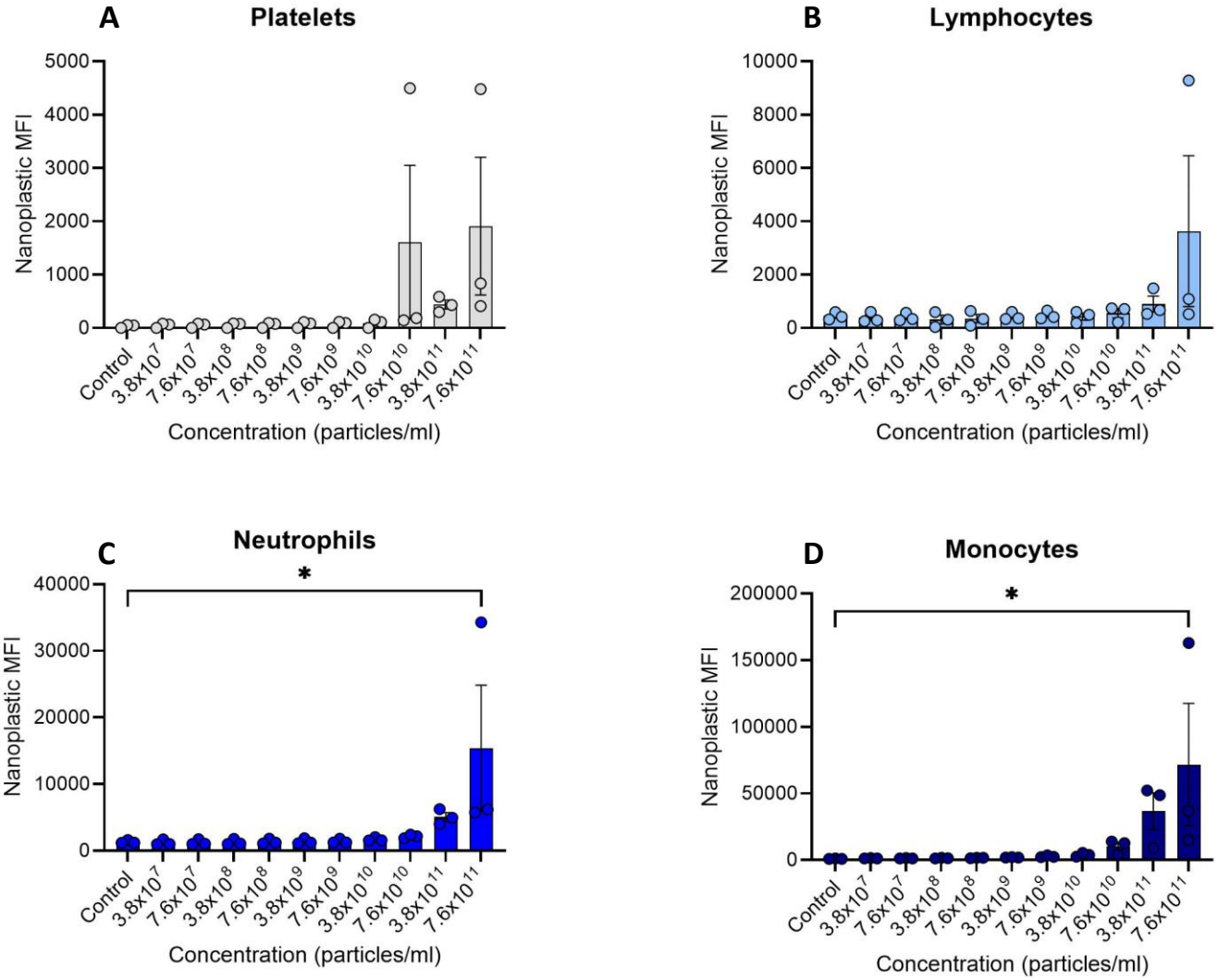

Figure 3.1. NP uptake in whole blood cells. Non-pregnant whole blood collected into heparin-coated tubes was cultured with differing NP concentrations for 24 hrs at 37°C and 5% CO_2 and analysed using the Cytek Aurora™ for cell type identification and subsequent NP MFI. Statistical analysis was conducted via a one-way ANOVA, with significance accepted to be $p < 0.05$. With each cell type, each NP concentration was compared to their respective controls (0 particles/ml); $3.8x10^7$ particles/ml (**A**, **B**, **C** and **D** $p > 0.9999$); $7.6x10^7$ particles/ml (**A**, **B**, **C** and **D** $p > 0.9999$); $3.8x10^8$ particles/ml (**A**, **B**, **C** and **D** $p > 0.9999$); $7.6x10^8$ particles/ml (**A**, **B**, **C** and **D** $p > 0.9999$); $3.8x10^9$ particles/ml (**A**, **B**, **C** and **D** $p > 0.9999$); $7.6x10^9$ particles/ml (**A**, **B**, **C** and **D** $p > 0.9999$); $3.8x10^{10}$ particles/ml (**A**, **B**, **C** and **D** $p > 0.9999$); $7.6x10^{10}$ particles/ml (**A** $p = 0.3556$, **B** $p > 0.9999$, **C** $p > 0.9999$, **D** $p = 0.9997$); $3.8x10^{11}$ particles/ml (**A** $p = 0.9993$, **B** $p > 0.9999$, **C** $p = 0.9451$, **D** $p = 0.4546$);); $7.6x10^{11}$ particles/ml (**A** $p = 0.1944$, **B** $p = 0.1031$, **C** $p = 0.0158$, **D** $p = 0.0178$). Data is presented as mean ± standard error of mean (SEM), * $p < 0.05$, n = 3/group.

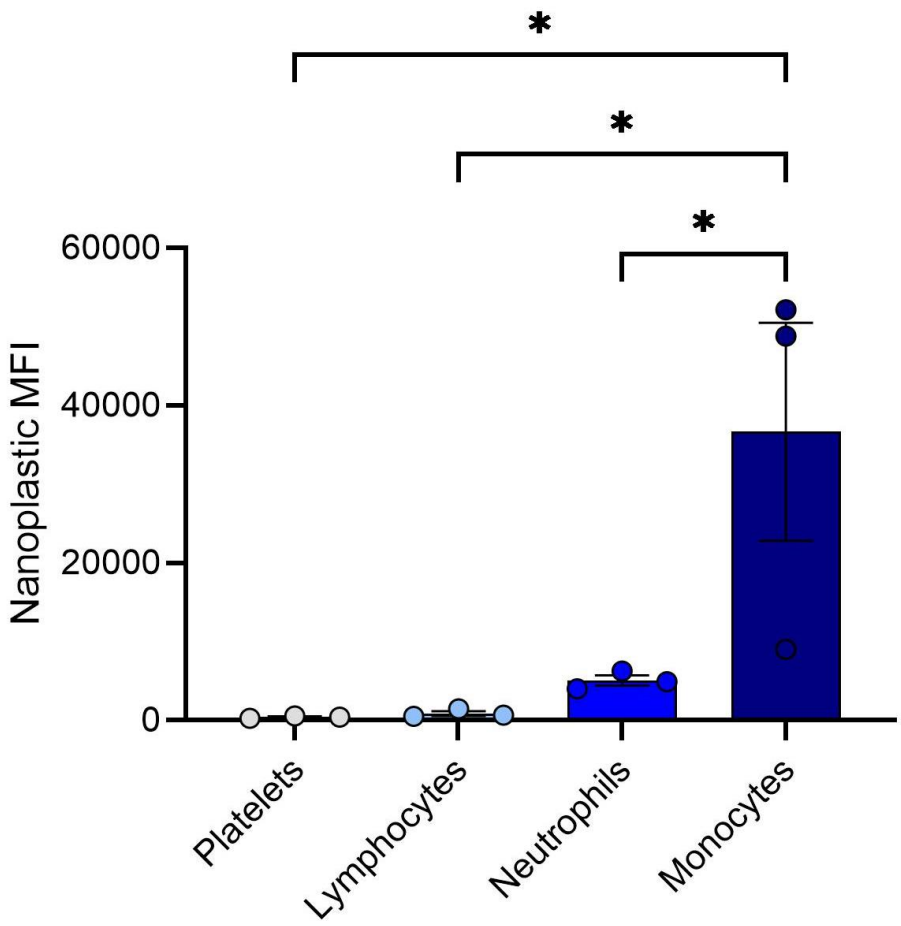

Figure 3.2. Example of NP uptake in monocytes compared to other peripheral blood cells. Non-pregnant whole blood collected into heparin-coated tubes was cultured with different NP concentrations for 24 hrs at 37°C and 5% CO_2 and analysed using the Cytek Aurora™ for cell type identification and subsequent NP MFI. This figure uses $3.8x10^{11}$ particles/ml as an example. Statistical analysis was conducted via a one-way ANOVA, with significance accepted to be $p < 0.05$. NP MFI in monocytes was compared to platelets ($p = 0.0252$), lymphocytes ($p = 0.0269$) and neutrophils ($p = 0.0486$). Data is presented as mean ± SEM, * $p < 0.05$, n = 3/group.

3.2. Optimisation of timepoints and prolonged exposure of NPs with monocytes

Using flow cytometry and non-pregnant monocytes identified in whole blood, a time course was conducted to identify which timepoint would be optimum to be used throughout the experiments. Simultaneously, it would also identify if NP uptake increased in monocytes over time due to prolonged exposure. Whole blood was cultured for 2 hrs, 6 hrs and 24 hrs with 0 particles/ml, $7.6x10^{10}$ particles/ml, $3.8x10^{11}$ particles/ml and $7.6x10^{11}$ particles/ml of NPs. No significance was identified between any concentration at any timepoint (figure 3.3). From then on, non-pregnant and pregnant whole blood was cultured for 2 hrs with NPs.

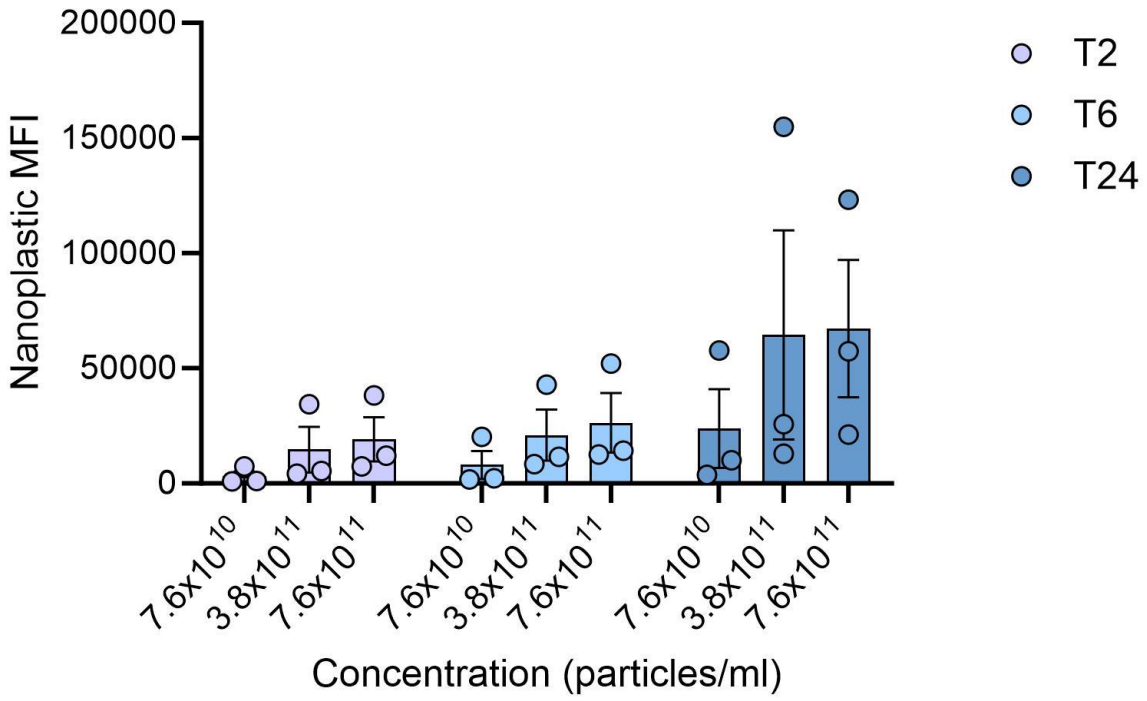

Figure 3.3. NP uptake over time by non-pregnant monocytes. Non-pregnant whole blood collected into heparin-coated tubes was cultured with different NP concentrations for 0, 2, 6 and 24 hrs at 37°C and 5% CO_2 and analysed using the Cytek Aurora™ for monocyte identification and subsequent NP MFI. Statistics were determined by conducting a two-way ANOVA with a Tukey post-hoc test. Significance was accepted if $p < 0.05$. The timepoints for NP MFI measured were 2 hrs (grey, $7.6x10^{10}$ particles/ml vs $3.8x10^{11}$ particles/ml $p > 0.9999$, $3.8x10^{11}$ particles/ml vs $7.6x10^{11}$ particles/ml $p > 0.9999$, $7.6x10^{10}$ particles/ml vs $7.6x10^{11}$ particles/ml $p = 0.9996$), 6 hrs (light blue, $7.6x10^{10}$ particles/ml vs $3.8x10^{11}$ particles/ml $p > 0.9999$, $3.8x10^{11}$ particles/ml vs $7.6x10^{11}$ particles/ml $p > 0.9999$, $7.6x10^{10}$ particles/ml vs $7.6x10^{11}$ particles/ml $p = 0.9991$) and 24 hrs (dark blue, $7.6x10^{10}$ particles/ml vs $3.8x10^{11}$ particles/ml $p = 0.8812$, $3.8x10^{11}$ particles/ml vs $7.6x10^{11}$ particles/ml $p > 0.9999$, $7.6x10^{10}$ particles/ml vs $7.6x10^{11}$ particles/ml $p = 0.8405$). Comparison of NP concentrations across each timepoint were $7.6x10^{10}$ particles/ml (2 hrs vs 6 hrs $p > 0.9999$, 6 hrs vs 24 hrs $p = 0.9997$, 2 hrs vs 24 hrs p =u 0.9978), $3.8x10^{11}$ particles/ml (2 hrs vs 6 hrs $p > 0.9999$, 6 hrs vs 24 hrs $p = 0.8390$, 2 hrs vs 24 hrs $p = 0.7263$) and $7.6x10^{11}$ particles/ml (2 hrs vs 6 hrs $p > 0.9999$, 6 hrs vs 24 hrs $p = 0.8765$, 2 hrs vs 24 hrs $p = 0.7594$). Data is presented as mean ± SEM, n = 3/group.

3.3. Prolonged exposure of NP in placental macrophages

Like monocytes, exposure of placental macrophages to NPs was analysed to identify if placental macrophages could take up NPs and if prolonged exposure correlates with increased uptake. Isolated placental macrophages were cultured with $7.6x10^{10}$ particles/ml, $3.8x10^{11}$ particles/ml and $7.6x10^{11}$ particles/ml of NPs and analysed after 2 hrs, 6hrs and 24 hrs (figure 3.4). Similar to the data presented in figure 3.3, NP uptake did not significantly differ when comparing each concentration across each of the timepoints. However, within each time point, as the concentrations increased, the NP MFI increased significantly between $7.6x10^{10}$ particles/ml and $7.6x10^{11}$ particles/ml and $3.8x10^{11}$ particles/ml and $7.6x10^{11}$ particles/ml. There was no significant difference in NP MFI at any timepoint when comparing $7.6x10^{10}$ particles/ml and $3.8x10^{11}$ particles/ml.

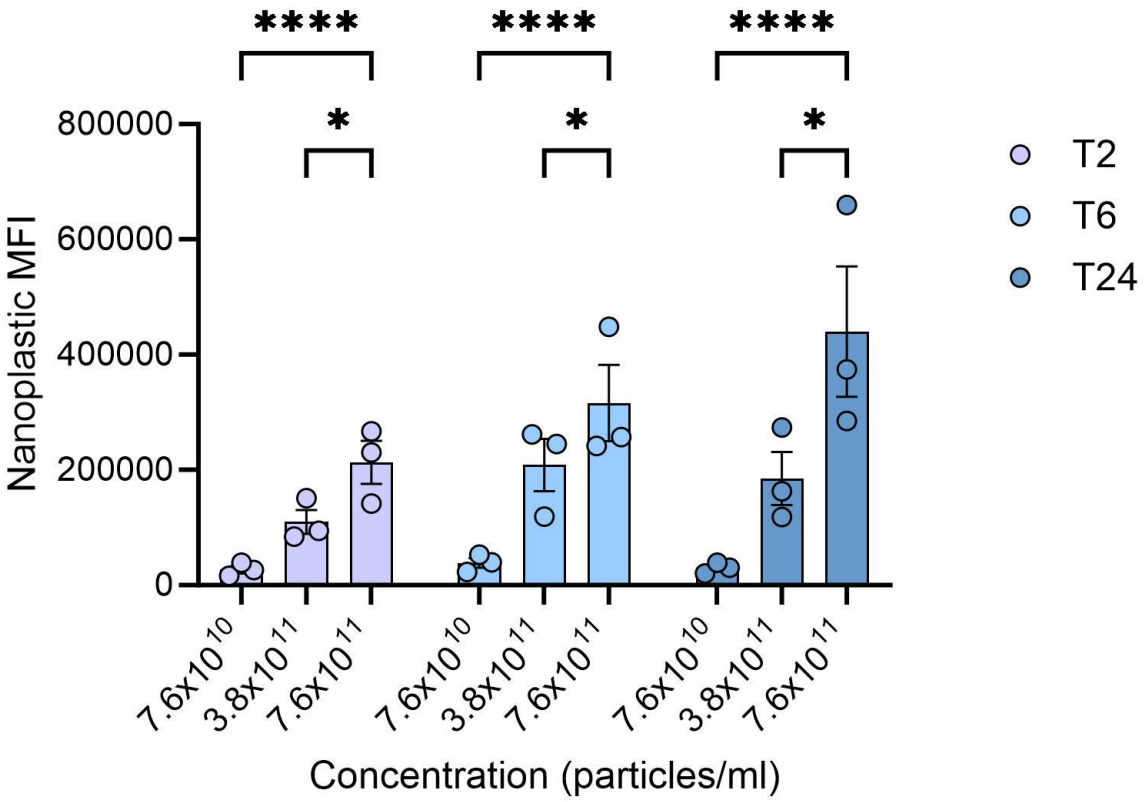

Figure 3.4. NP uptake in placental macrophages over time. Placental macrophages were enzymatically digested from placental tissue and cultured with different NP concentrations for 0, 2, 6 and 24 hrs at 37°C and 5% CO_2 and analysed using the Cytek Aurora™ for subsequent NP MFI per each NP concentration. Statistical analysis was via a two-way ANOVA with Tukey post-hoc tests, with significance accepted to be $p < 0.05$. Timepoints for NP uptake measured were 2 hrs (purple, $7.6x10^{10}$ particles/ml vs $3.8x10^{11}$ particles/ml $p = 0.0883$, $3.8x10^{11}$ particles/ml vs $7.6x10^{11}$ particles/ml $p = 0.0349$, $7.6x10^{10}$ particles/ml vs $7.6x10^{11}$ particles/ml $p < 0.0001$), 6 hrs (light blue, $7.6x10^{10}$ particles/ml vs $3.8x10^{11}$ particles/ml $p = 0.0883$, $3.8x10^{11}$ particles/ml vs $7.6x10^{11}$ particles/ml $p = 0.0349$, $7.6x10^{10}$ particles/ml vs $7.6x10^{11}$ particles/ml $p < 0.0001$) and 24 hrs (dark blue, $7.6x10^{10}$ particles/ml vs $3.8x10^{11}$ particles/ml $p = 0.0883$, $3.8x10^{11}$ particles/ml vs $7.6x10^{11}$ particles/ml $p = 0.0349$, $7.6x10^{10}$ particles/ml vs $7.6x10^{11}$ particles/ml $p < 0.0001$). Comparison of NP concentrations across each timepoint

were $7.6x10^{10}$ particles/ml (2 hrs vs 6 hrs p = 0.7721, 6 hrs vs 24 hrs p = 0.9981, 2 hrs vs 24 hrs p = 0.3564), $3.8x10^{11}$ particles/ml (2 hrs vs 6 hrs p = 0.7721, 6 hrs vs 24 hrs p = 0.9981, 2 hrs vs 24 hrs p = 0.3564) and $7.6x10^{11}$ particles/ml (2 hrs vs 6 hrs p = 0.7721, 6 hrs vs 24 hrs p = 0.9981, 2 hrs vs 24 hrs p = 0.3564). Data is presented as mean ± SEM, * p < 0.05, **** p < 0.0001, n = 3/group.

3.4. NP effect on placental macrophage viability

As well as NP MFI, flow cytometry was used to analyse the effect of increasing NP concentrations and prolonged exposure on cell death of placental macrophages (figure 3.5). From observation, there appears to be a slight decrease in cell viability as the NP concentrations increase within each timepoint especially at 24 hours but was no significant decrease in cell viability across the concentrations and timepoints.

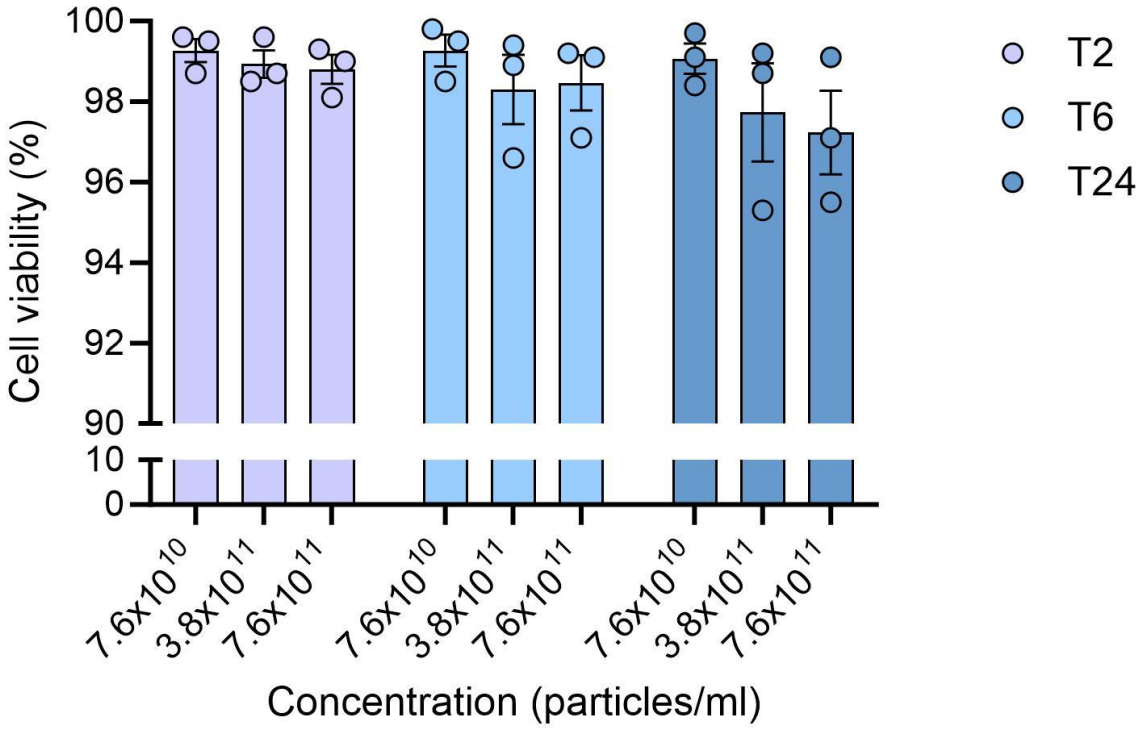

Figure 3.5. NP effect on placental macrophage viability. Placental macrophages were enzymatically digested from placental tissue and cultured with different NP concentrations for 0, 2, 6 and 24 hrs at 37°C and 5% CO_2, followed by staining with DRAQ7 for analysis using the Cytek Aurora™ for the effect of prolonged NP exposure on cell viability. Statistical analysis was via a 2-way ANOVA with Tukey post-hoc tests with significant difference accepted as p < 0.05. The timepoints for NP effect on cell death were 2 hrs (grey, $7.6x10^{10}$ particles/ml vs $3.8x10^{11}$ particles/ml p > 0.9999, $3.8x10^{11}$ particles/ml vs $7.6x10^{11}$ particles/ml p > 0.9999, $7.6x10^{10}$ particles/ml vs $7.6x10^{11}$ particles/ml p = 0.9999), 6 hrs (light blue, $7.6x10^{10}$ particles/ml vs $3.8x10^{11}$ particles/ml p = 0.9863, $3.8x10^{11}$ particles/ml vs $7.6x10^{11}$ particles/ml p > 0.9999, $7.6x10^{10}$ particles/ml vs $7.6x10^{11}$ particles/ml p = 0.9951) and 24 hrs (dark blue, $7.6x10^{10}$ particles/ml vs $3.8x10^{11}$ particles/ml p = 0.9037, $3.8x10^{11}$ particles/ml vs $7.6x10^{11}$ particles/ml p = 0.9998, $7.6x10^{10}$ particles/ml vs $7.6x10^{11}$ particles/ml p = 0.6519).

Comparison of NP concentration effect on cell death across each timepoint were $7.6x10^{10}$ particles/ml (2 hrs vs 6 hrs $p > 0.9999$, 6 hrs vs 24 hrs $p > 0.9999$, 2 hrs vs 24 hrs $p > 0.9999$), $3.8x10^{11}$ particles/ml (2 hrs vs 6 hrs $p = 0.9990$, 6 hrs vs 24 hrs $p = 0.9996$, 2 hrs vs 24 hrs $p = 0.9463$) and $7.6x10^{11}$ particles/ml (2 hrs vs 6 hrs $p > 0.9999$, 6 hrs vs 24 hrs $p = 0.9349$, 2 hrs vs 24 hrs $p = 0.8028$). Data is presented as mean ± SEM, n = 3/group.

3.5. Monocyte uptake of NPs is increased in pregnancy

To determine the differences in NP uptake by monocytes from non-pregnant and pregnant women, each of the NP concentrations were cultured for 2 hrs in whole blood from non-pregnant and pregnant women and analysed via flow cytometry. Monocytes from pregnant monocytes have internalised more NPs after 2 hrs than their non-pregnant counterpart as indicated by significantly great MFI (figure 3.6).

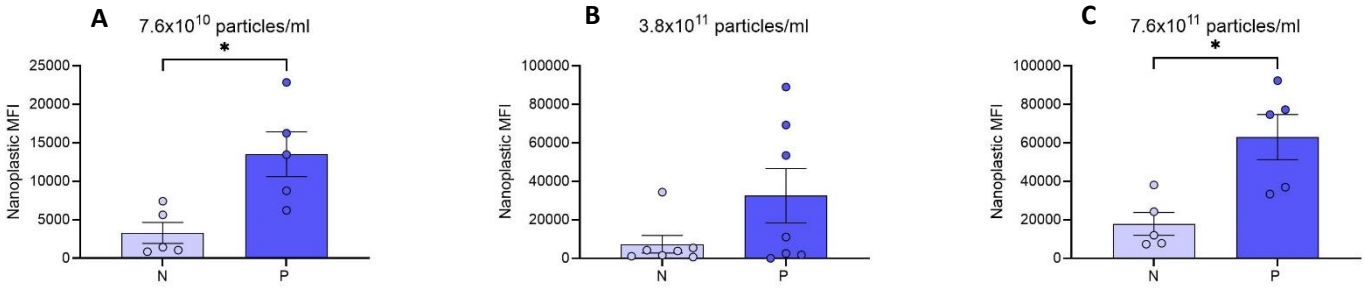

Figure 3.6. NP uptake comparison between non-pregnant and pregnant monocytes in whole blood. Non-pregnant (N, grey) and pregnant (P, blue) whole blood collected into heparin-coated tubes was cultured with different NP concentrations for 0 and 2 hrs at 37°C and 5% CO_2 and analysed using the Cytek Aurora™ for monocyte identification and subsequent NP MFI. Statistical analysis was via a Mann-Whitney test and significance was accepted if $p < 0.05$. The NP concentrations for uptake between monocyte populations measured were **(A)** $7.6x10^{10}$ particles/ml (n= 5/group, $p = 0.0159$), **(B)** $3.8x10^{11}$ particles/ml (n= 7/group, $p = 0.3176$) and **(C)** $7.6x10^{11}$ particles/ml (n= 5/group, $p = 0.0317$). Data is presented as mean ± SEM, * $p < 0.05$.

The possibility that monocyte subsets might show differences in uptake of NPs was then considered. With regards to non-pregnant monocytes (figure 3.7), NP uptake in classical and intermediate monocytes significantly increased when comparing $7.6x10^{11}$ particles/ml to the control ($p = 0.0032$ and $p < 0.0001$, respectively). No significant increases were observed at any NP concentration with non-classical monocytes (figure 3.7). When comparing the non-pregnant monocyte subsets within each concentration, intermediate monocytes significantly took up more NPs when compared to non-classical at $7.6x10^{11}$ particles/ml (figure 3.7, $p = 0.0005$). Excluding this, no significant differences between other subsets at each NP concentration was observed (figure 3.7). In pregnant monocytes, classical and intermediate took up NPs significantly more compared to the control at $3.8x10^{11}$ and

$7.6x10^{11}$ particles/ml (figure 3.8). NP uptake in non-classical monocytes did not significantly differ across any NP concentration when compared to the control (figure 3.8). When comparing pregnant monocyte subsets within each concentration, intermediate monocytes significantly took up more NPs than classical and non-classical at $7.6x10^{11}$ particles/ml ($p = 0.0049$ and $p < 0.0001$, respectively) (figure 3.8).Unlike non-pregnant, pregnant classical monocytes also showed to take up more NPs when compared to non-classical at $7.6x10^{11}$ particles/ml ($p = 0.0019$) and intermediate monocytes took up more compared to non-classical at $3.8x10^{11}$ particles/ml ($p = 0.0015$) (figure 3.8).

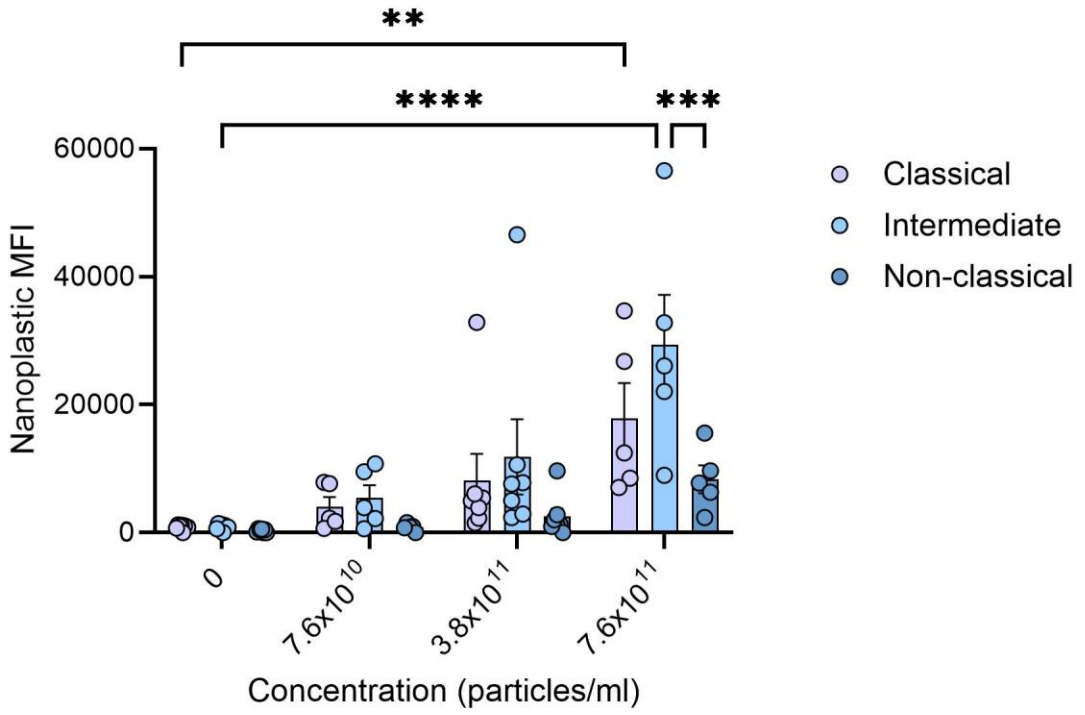

Figure 3.7. NP uptake in non-pregnant monocyte subsets. Non-pregnant whole blood collected into heparin-coated tubes was cultured with different NP concentrations for 0 and 2 hrs at 37°C and 5% CO_2 and analysed using the Cytek Aurora™ with Pacific Blue-CD14 and APC-CD16 anti-human antibodies for monocyte subset identification and subsequent NP MFI. Statistics were determined via conduction of a 2-way ANOVA with Tukey post-hoc tests and significance were accepted if $p < 0.05$. Classical; CD14++CD16-, intermediate; CD14++CD16+ and non-classical; $CD14^{dim}CD16+$. Each subset with NPs was compared to the same subsets' control (Classical; $7.6x10^{10}$ particles/ml $p = 0.9027$, $3.8x10^{11}$ particles/ml $p = 0.3265$, $7.6x10^{11}$ particles/ml $p = 0.0032$, intermediate; $7.6x10^{10}$ particles/ml $p = 0.7660$, $3.8x10^{11}$ particles/ml $p = 0.0587$, $7.6x10^{11}$ particles/ml $p < 0.0001$, non-classical; $7.6x10^{10}$ particles/ml $p = 0.9994$, $7.6x10^{11}$ particles/ml $p = 0.9511$, $7.6x10^{11}$ particles/ml $p = 0.3267$). Within each NP concentration, each monocyte subset was also compared to each other ($7.6x10^{10}$ particles/ml; classical vs intermediate $p = 0.9629$, classical vs non-classical $p = 0.8134$ and intermediate vs non-classical $p = 0.6579$, $3.8x10^{11}$ particles/ml; classical vs intermediate $p = 0.6816$, classical vs non-classical $p = 0.4195$, intermediate vs non-classical $p = 0.0973$, $7.6x10^{11}$ particles/ml; classical vs intermediate $p = 0.0823$, classical vs non-classical $p = 0.1695$, intermediate vs non-classical $p = 0.0005$). Data is presented as mean ± SEM, n = 5-12/group, * $p < 0.05$, ** $p < 0.01$, *** $p < 0.001$, **** $p < 0.0001$.

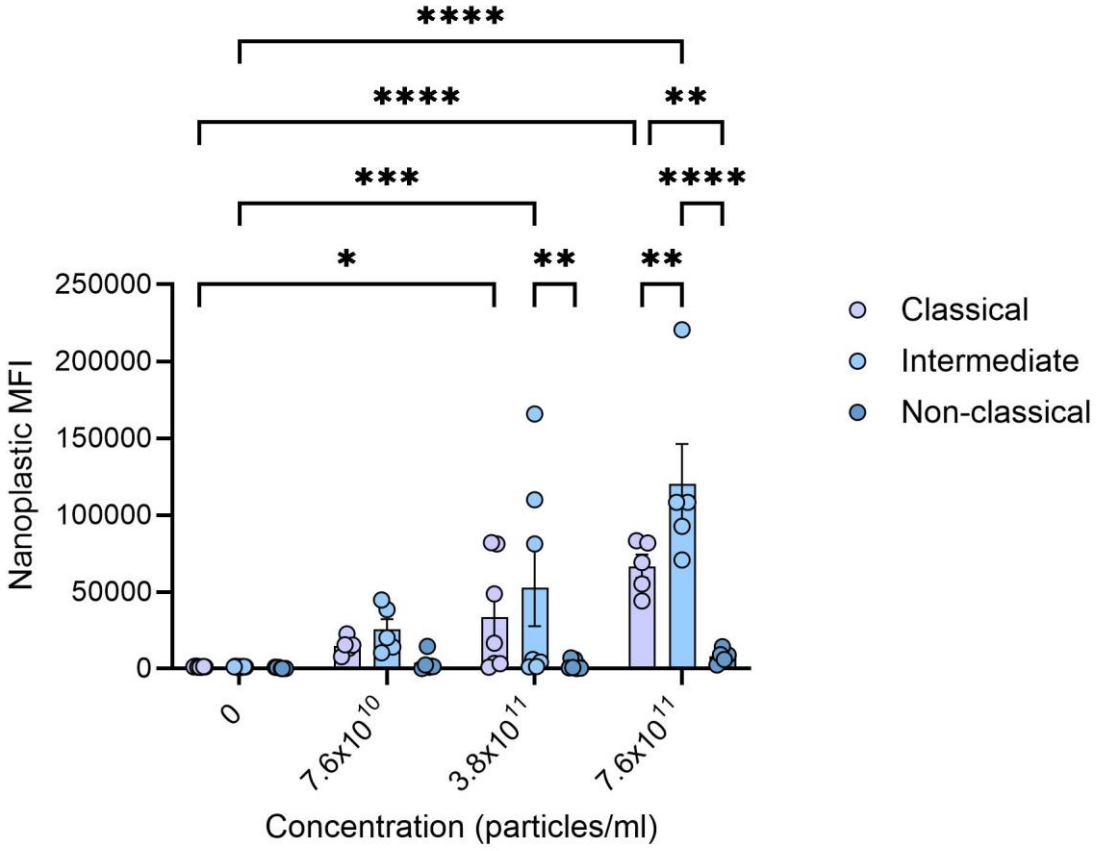

Figure 3.8. NP uptake in pregnant monocyte subsets. Pregnant whole blood collected into heparin-coated tubes was cultured with different NP concentrations for 0 and 2 hrs at 37°C and 5% CO_2 and analysed using the Cytek Aurora™ with Pacific Blue-CD14 and APC-CD16 anti-human antibodies for monocyte subset identification and subsequent NP MFI. Statistics were determined via conduction of a 2-way ANOVA with Tukey post-hoc tests and significance were accepted if $p < 0.05$. Classical; CD14++CD16-, intermediate; CD14++CD16+ and non-classical; $CD14^{dim}CD16+$. Each subset with NPs was compared to the same subsets' control (Classical; $7.6x10^{10}$ particles/ml $p = 0.7543$, $3.8x10^{11}$ particles/ml $p = 0.0498$, $7.6x10^{11}$ particles/ml $p < 0.0001$, intermediate; $7.6x10^{10}$ particles/ml $p = 0.3053$, $3.8x10^{11}$ particles/ml $p = 0.0005$, $7.6x10^{11}$ particles/ml $p < 0.0001$, non-classical; $7.6x10^{10}$ particles/ml $p = 0.9942$, $7.6x10^{11}$ particles/ml $p = 0.9984$, $7.6x10^{11}$ particles/ml $p = 0.9423$). Within each NP concentration, each monocyte subset was also compared to each other ($7.6x10^{10}$ particles/ml; classical vs intermediate $p = 0.7986$, classical vs non-classical $p = 0.7765$ and intermediate vs non-classical $p = 0.3894$, $3.8x10^{11}$ particles/ml; classical vs intermediate $p = 0.3619$, classical vs non-classical $p = 0.0679$, intermediate vs non-classical $p = 0.0015$, $7.6x10^{11}$ particles/ml; classical vs intermediate $p = 0.0049$, classical vs non-classical $p = 0.0019$, intermediate vs non-classical $p < 0.0001$). Data is presented as mean ± SEM, n = 5-12/group, * $p < 0.05$, ** $p < 0.01$, *** $p < 0.001$, **** $p < 0.0001$.

Comparing the uptake of NPs by subsets for monocytes from non-pregnant and pregnant women revealed differences between the subsets. There were no significant differences in NP uptake in non-classical monocytes from non-pregnant versus pregnant women for any NP concentration studies (figure 3.9C). However, NP uptake by both the classical (figure 3.9A) and intermediate (figure 3.9B) subsets was greater for pregnant compared to non-pregnant women for 7.6 x 10^{11} particles/ml; this significant difference was still evident for the classical subset at 3.8x10^{11} particles/ml.

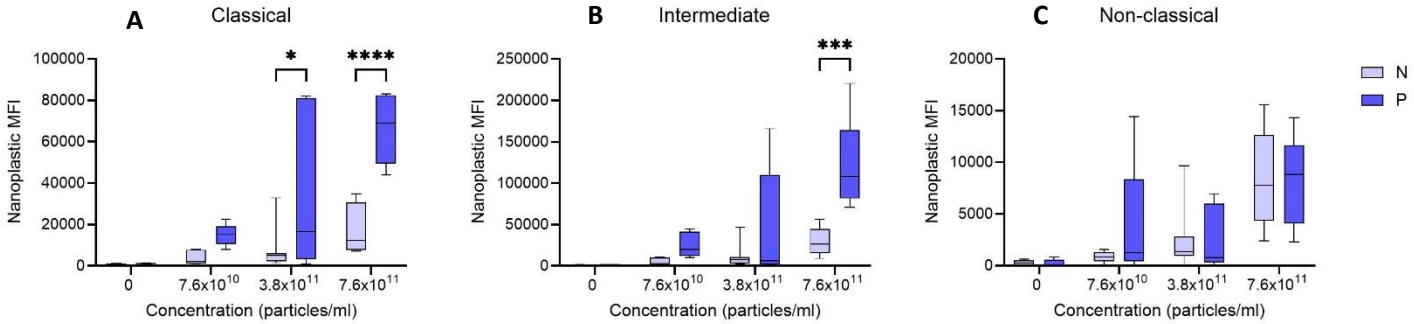

Figure 3.9. NP uptake by monocyte subsets in non-pregnant and pregnant women. Non-pregnant and pregnant whole blood collected into heparin-coated tubes was cultured with different NP concentrations for 0 and 2 hrs at 37°C and 5% CO_2 and analysed using the Cytek Aurora™ with Pacific Blue-CD14 and APC-CD16 anti-human antibodies for monocyte subset identification and subsequent NP MFI. Statistics were determined via conduction of a 2-way ANOVA with Tukey post-hoc tests and significance were accepted if $p < 0.05$. Classical; CD14++CD16-, intermediate; CD14++CD16+ and non-classical; $CD14^{dim}CD16+$. Within each subset, non-pregnant and pregnant monocytes were compared at each NP concentration (**A** classical; 7.6x10^{10} particles/ml p = 0.7063, 3.8x10^{11} particles/ml p = 0.0116 and 7.6x10^{11} p < 0.0001, **B** intermediate; 7.6x10^{10} particles/ml p 0.7742, 3.8x10^{11} particles/ml p = 0.0663, 7.6x10^{11} = 0.0001, **C** non-classical; 7.6x10^{10} particles/ml p = 0.4493, 3.8x10^{11} particles/ml p = 0.9998, 7.6x10^{11} particles/ml p = 0.9998). Data is presented as maximum and minimum, n = 5-12/group, * $p < 0.05$, *** $p < 0.001$, **** $p < 0.0001$.

3.6. Confirmation of NP uptake in monocytes and placental macrophages

As NPs have the potential to bind to the surface of cells as well be internalised, confocal microscopy was conducted to confirm NP internalisation in monocytes and placental macrophages (figure 3.10). The presence of green fluorescence in each NP concentration with monocytes and placental macrophages confirms that exposure to NP leads to uptake. On appearance, NPs are observed to deposit within the cytoplasm of phagocytes.

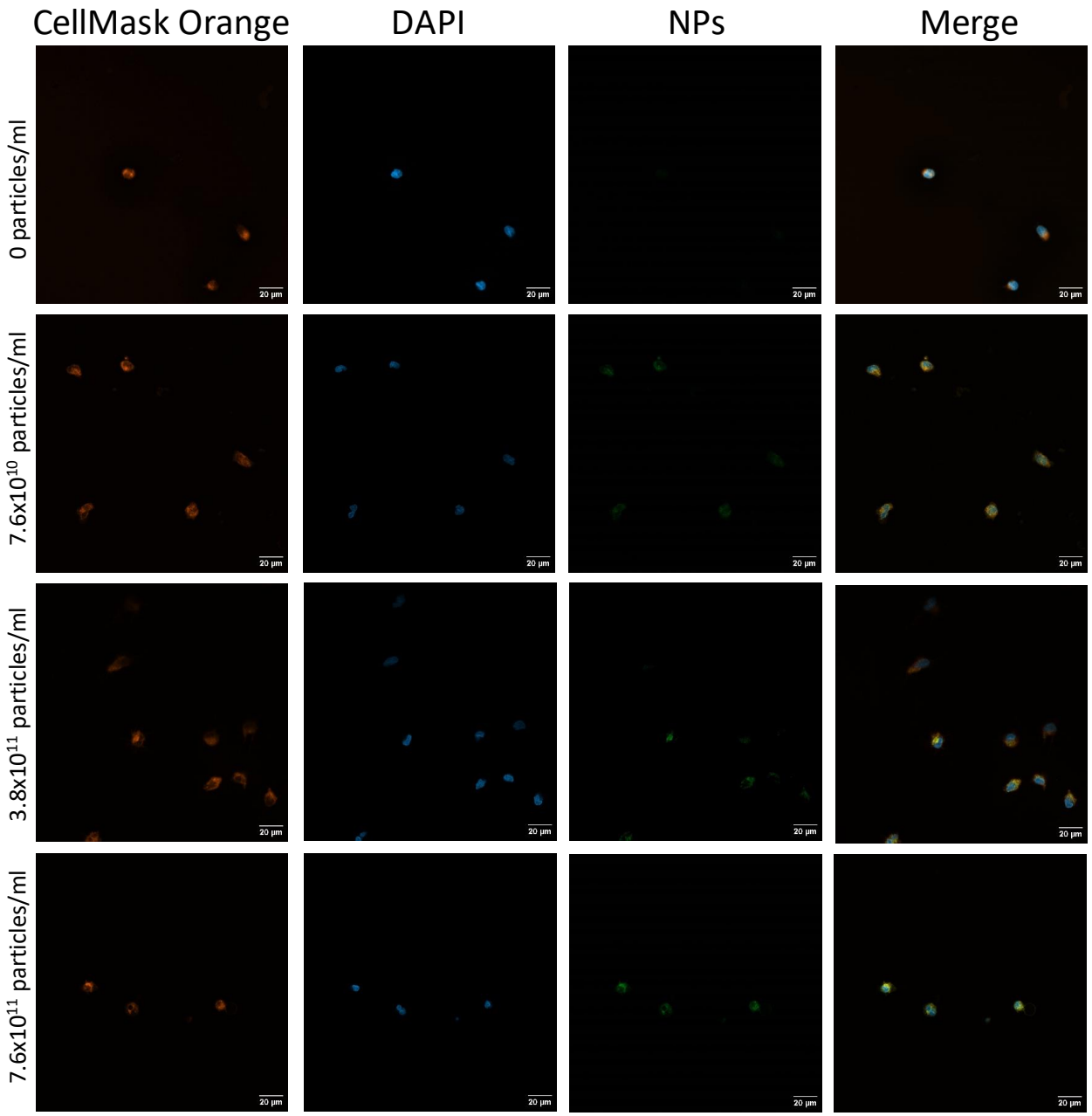

Figure 3.10. Visualisation of NP uptake in monocytes (non-pregnant). Isolated non-pregnant monocytes were cultured for 20 hrs with ascending nanoplastic concentrations at 37°C and 5% CO_2, followed by imaging with the ZEISS 980 Confocal with Airyscan to confirm NP (green). CellMask Orange was used as a cell membrane stain (orange) and DAPI was used a cell nuclei stain (blue) (n = 3).

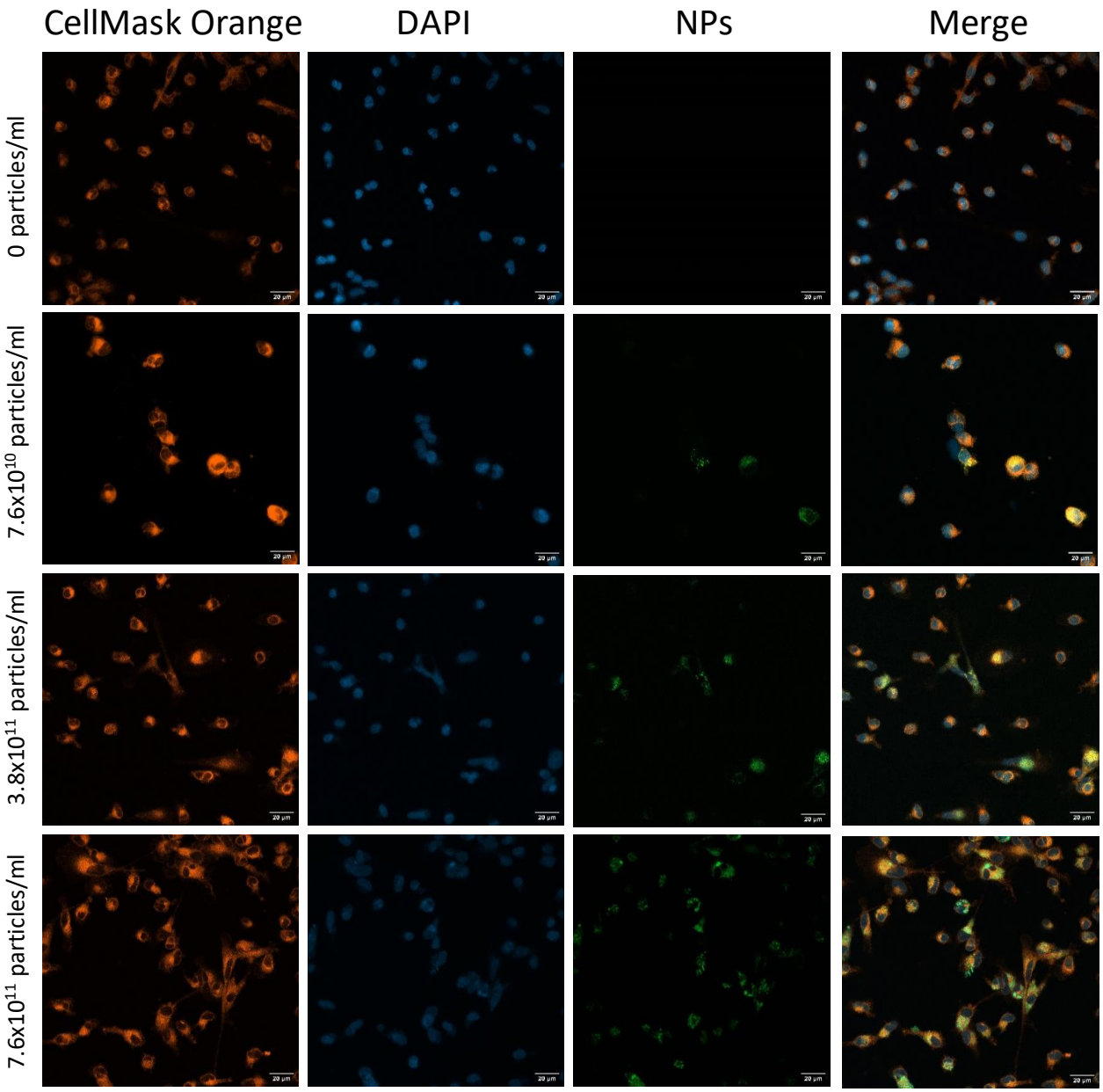

Figure 3.11. Visualisation of NP uptake in placental macrophages. Isolated placental macrophages were cultured for 24 hrs with ascending nanoplastic concentrations at 37°C and 5% CO_2, followed by imaging with the ZEISS 980 Confocal with Airyscan to confirm NP (green) uptake. CellMask Orange was used as a cell membrane stain (orange) and DAPI was used a cell nuclei stain (blue) (n = 3).

3.7. NP effect on TNFα production in monocytes from pregnant and non-pregnant women

The effects of NP alone on cytokine production and their ability to modulate LPS-stimulated cytokine production was then considered. LPS was chosen as a prototypic inflammatory stimulus that significantly increases TNF-α production from monocytes of non-pregnant (figure 3.12) and pregnant women (figure 3.13). NPs did not have any effect on production of TNF-α, in the absence of LPS stimulation for either non-pregnant (figure 3.12) or pregnant women (figure 3.13). Similarly, there

was no significant effect of NPs at any concentration on LPS-stimulated TNF-α from monocytes of non-pregnant (figure 3.12) and pregnant women (figure 3.13).

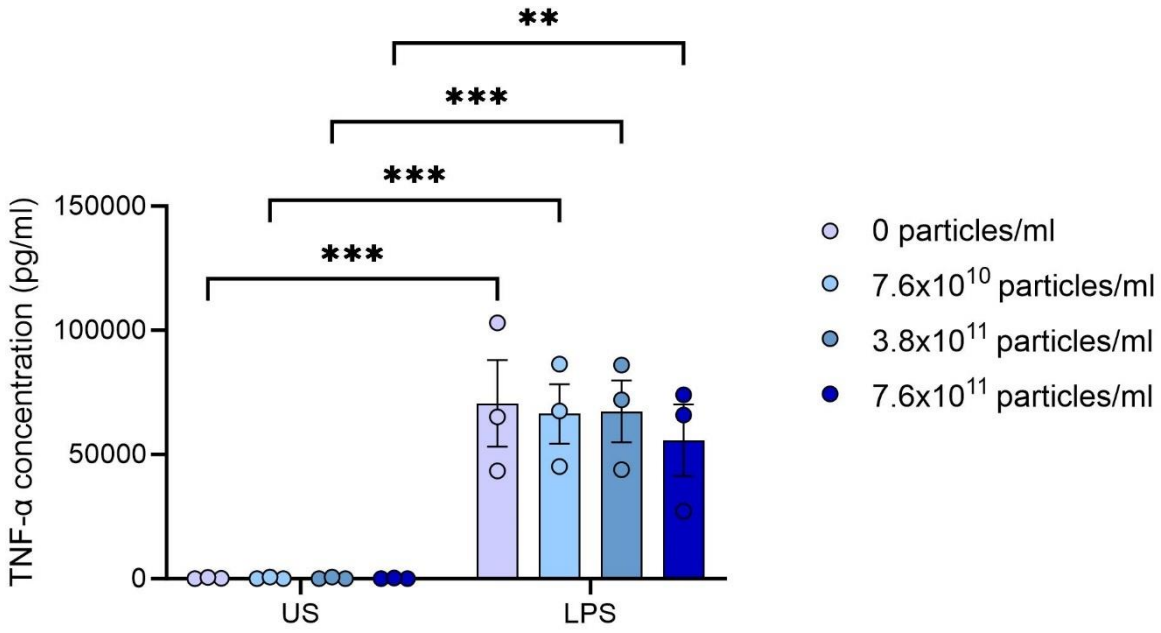

Figure 3.12. NP effect on TNFα production in monocytes from non-pregnant women. Monocytes were isolated from whole blood of non-pregnant women collected into heparin-coated tubes and cultured for 20 hrs with and without LPS (10ng/ml) and different NP concentrations at 37°C and 5% CO_2. The supernatants were analysed for TNF-α production via ELISA experiments. Statistical analysis was via a 2-way ANOVA with Tukey post hoc testing and significance was accepted if $p \leq 0.05$. Each unstimulated (US) NP concentration was compared with the LPS-stimulated counterpart; 0 particles/ml ($p = 0.0001$), $7.6x10^{10}$ particles/ml ($p = 0.0003$), $3.8x10^{11}$ particles/ml ($p = 0.0002$) and $7.6x10^{11}$ particles/ml ($p = 0.0013$). Each nanoparticle concentration was compared to the respective unstimulated or stimulated control; $7.6x10^{10}$ particles/ml (US $p > 0.9999$, LPS $p = 0.9907$), $3.8x10^{11}$ particles/ml (US $p > 0.9999$, LPS $p = 0.9956$) and $7.6x10^{11}$ particles/ml (US $p > 0.9999$, LPS $p = 0.7260$). Data is presented as mean ± SEM, n = 3/group, ** $p < 0.01$, *** $p < 0.001$.

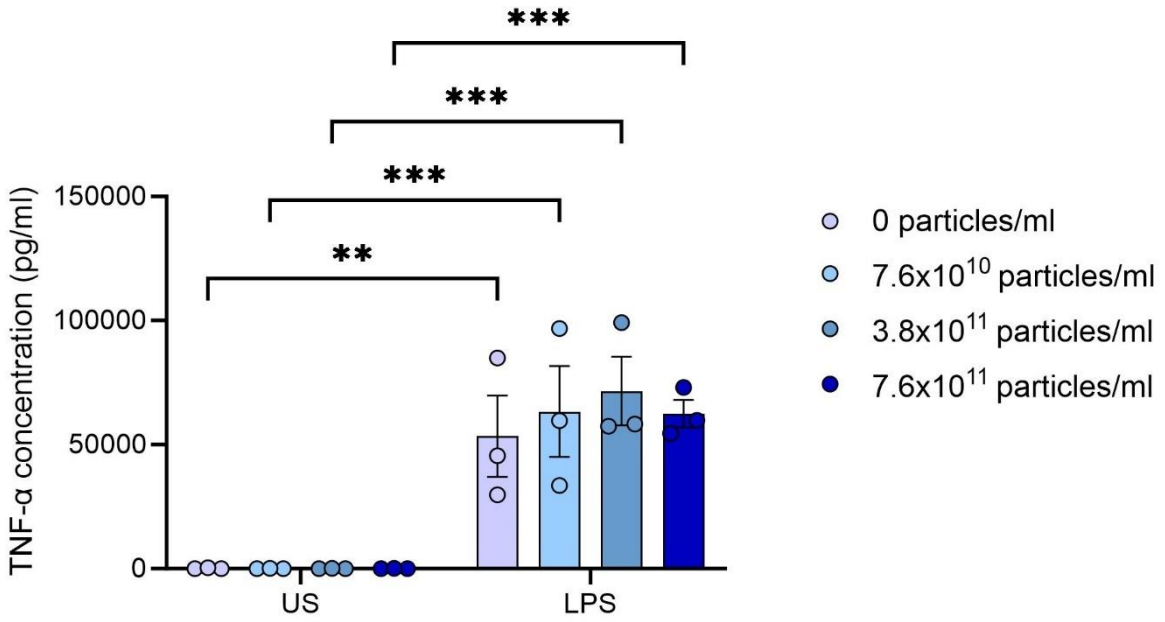

Figure 3.13. NP effect on TNF-α production in monocytes from pregnant women. Monocytes were isolated from whole blood of pregnant women collected into heparin-coated tubes and cultured for 20 hrs with and without LPS (10ng/ml) and different NP concentrations at 37°C and 5% CO_2. The supernatants were analysed for TNF-α production via ELISA experiments. Statistical analysis was via a 2-way ANOVA with Tukey post hoc testing and significance was accepted if $p \leq 0.05$. Each unstimulated (US) NP concentration was compared with the LPS-stimulated counterpart; 0 particles/ml ($p = 0.0019$), $7.6x10^{10}$ particles/ml ($p = 0.0004$), $3.8x10^{11}$ particles/ml ($p = 0.0002$) and $7.6x10^{11}$ particles/ml ($p = 0.0005$).Each nanoparticle concentration was compared to the respective unstimulated or stimulated control; $7.6x10^{10}$ particles/ml (US $p > 0.9999$, LPS $p = 0.9003$), $3.8x10^{11}$ particles/ml (US $p > 0.9999$, LPS $p = 0.5971$) and $7.6x10^{11}$ particles/ml (US $p > 0.9999$, LPS $p = 0.9209$). Data is presented as mean ± SEM, n = 3/group, ** $p < 0.01$, *** $p < 0.001$.

3.8. NP effect on IL-1β production in monocytes from pregnant and non-pregnant women

NP effect on IL-1β production in non-pregnant (figure 3.14) and pregnant (figure 3.15) monocytes was also considered. Unsurprisingly, NPs had no effect on IL-1β production in the presence or absence of LPS stimulation both non-pregnant (figure 3.14) and pregnant (figure 3.15) monocytes.

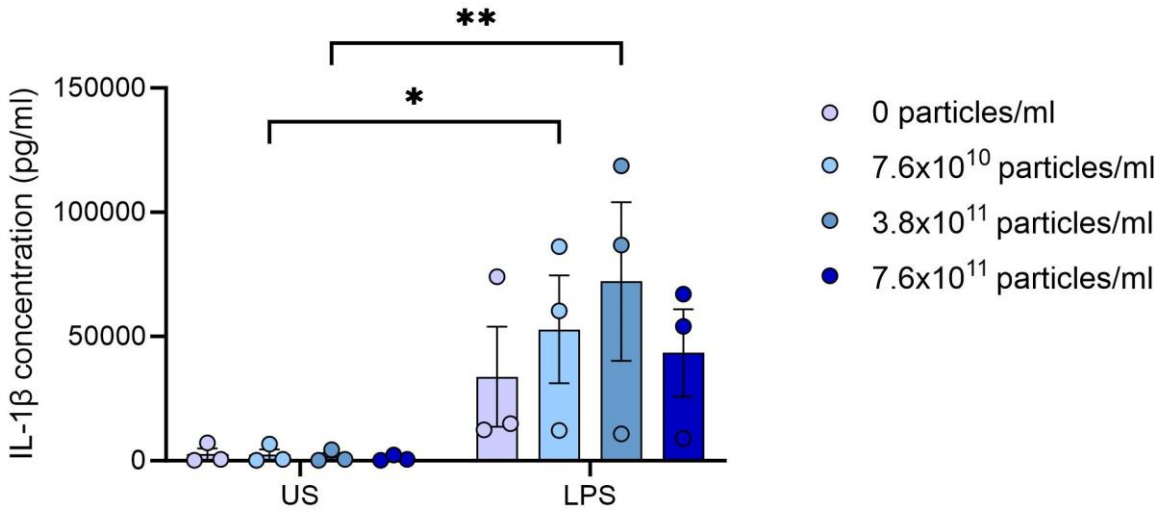

Figure 3.14. NP effect on IL-1β production in non-pregnant monocytes. Monocytes were isolated from whole blood of non-pregnant women collected into heparin-coated tubes and cultured for 20 hrs with and without LPS (10ng/ml) and different NP concentrations at 37°C and 5% CO_2. The supernatants were analysed for IL-1β production via ELISA experiments. Statistical analysis was via a 2-way ANOVA with Tukey post hoc testing and significance was accepted if $p \leq 0.05$. Each unstimulated (US) NP concentration was compared with the LPS-stimulated counterpart; 0 particles/ml ($p = 0.2043$), $7.6x10^{10}$ particles/ml ($p = 0.0482$), $3.8x10^{11}$ particles/ml ($p = 0.0087$) and $7.6x10^{11}$ particles/ml ($p = 0.0908$).Each nanoparticle concentration was compared to the respective unstimulated or stimulated control; $7.6x10^{10}$ particles/ml (US $p > 0.9999$, LPS $p = 0.8492$), $3.8x10^{11}$ particles/ml (US $p > 0.9999$, LPS $p = 0.3921$) and $7.6x10^{11}$ particles/ml (US $p = 0.9999$, LPS $p = 0.9765$). Data is presented as mean ± SEM, n = 3/group, * $p < 0.05$, ** $p < 0.01$.

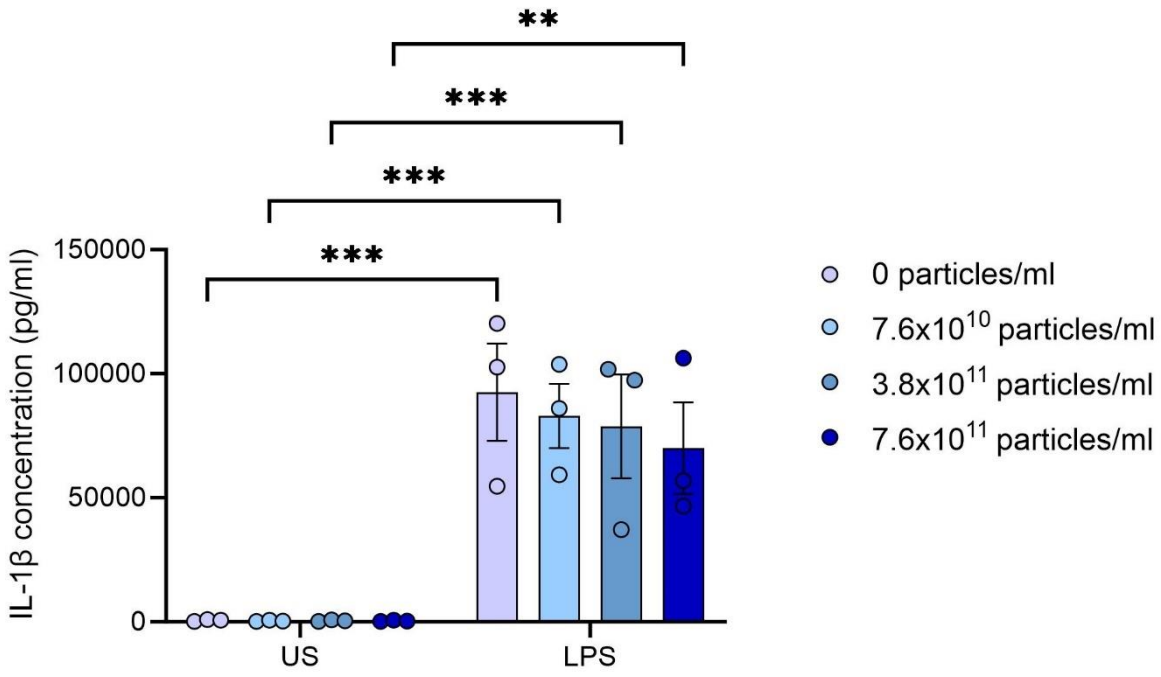

Figure 3.15. NP effect on IL-1β production in pregnant monocytes. Monocytes were isolated from whole blood of pregnant women collected into heparin-coated tubes and cultured for 20 hrs with and without LPS (10ng/ml) and different NP concentrations at 37°C and 5% CO_2. The supernatants were analysed for IL-1β production via ELISA experiments. Statistical analysis was via a 2-way ANOVA with Tukey post hoc testing and significance was accepted if $p \leq 0.05$. Each unstimulated (US) NP concentration was compared with the LPS-stimulated counterpart; 0 particles/ml ($p = 0.0001$), $7.6x10^{10}$ particles/ml ($p = 0.0003$), $3.8x10^{11}$ particles/ml ($p = 0.0005$) and $7.6x10^{11}$ particles/ml ($p = 0.0015$).Each nanoparticle concentration was compared to the respective unstimulated or stimulated control; $7.6x10^{10}$ particles/ml (US $p > 0.9999$, LPS $p = 0.9523$), $3.8x10^{11}$ particles/ml (US $p > 0.9999$, LPS $p = 0.8729$) and $7.6x10^{11}$ particles/ml (US $p > 0.9999$, LPS $p = 0.6127$). Data is presented as mean ± SEM, n = 3/group, ** $p < 0.01$, *** $p < 0.001$.

3.9. NP effect on IL-10 production in monocytes from pregnant and non-pregnant women

Finally, NP effect IL-10 production was also considered as it is a potent cytokine involved in the anti-inflammatory response in monocytes. IL-10 production in non-pregnant (figure 3.16) and pregnant (figure 3.17) monocytes were not affected by NP uptake in the absence of LPS stimulation. Likewise, NPs showed no effect on IL-10 production in non-pregnant (figure 3.16) and pregnant (figure 3.17) monocytes with LPS stimulation.

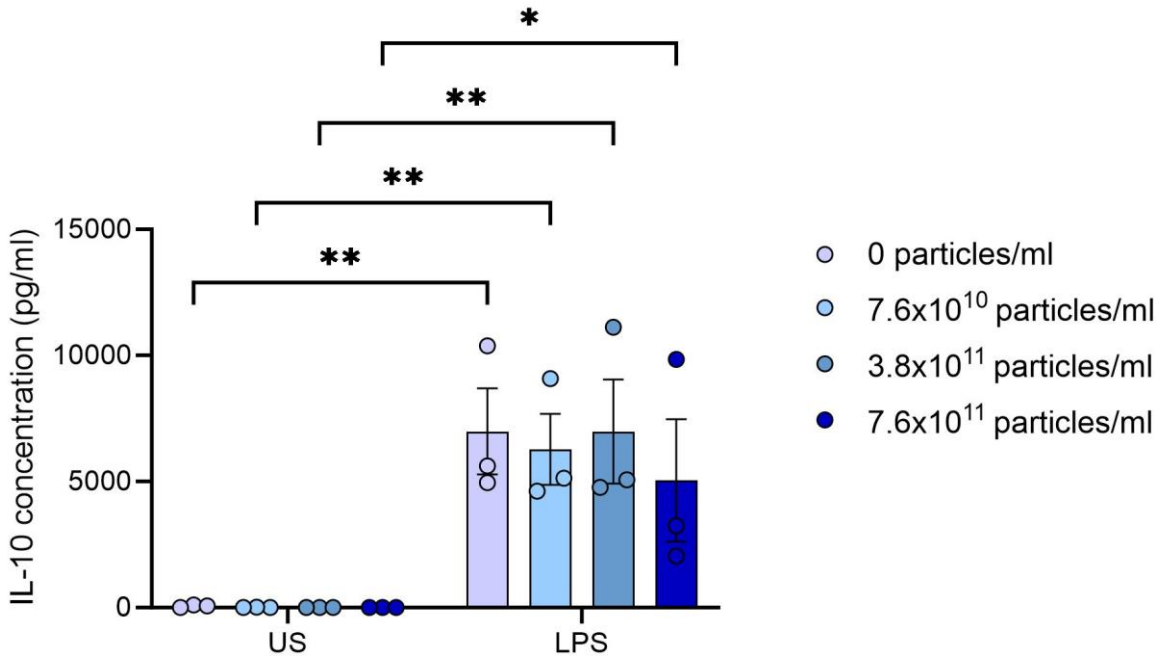

Figure 3.16. NP effect on IL-10 production in non-pregnant monocytes. Monocytes were isolated from whole blood of non-pregnant women collected into heparin-coated tubes and cultured for 20 hrs with and without LPS (10ng/ml) and different NP concentrations at 37°C and 5% CO_2. The supernatants were analysed for IL-10 production via ELISA experiments. Statistical analysis was via a 2-way ANOVA with Tukey post hoc testing and significance was accepted if $p \leq 0.05$. Each unstimulated (US) NP concentration was compared with the LPS-stimulated counterpart; 0 particles/ml ($p = 0.0026$), $7.6x10^{10}$ particles/ml ($p = 0.0052$), $3.8x10^{11}$ particles/ml ($p = 0.0024$) and $7.6x10^{11}$ particles/ml ($p = 0.0194$).Each nanoparticle concentration was compared to the respective unstimulated or stimulated control; $7.6x10^{10}$ particles/ml (US $p > 0.9999$, LPS $p = 0.9826$), $3.8x10^{11}$ particles/ml (US $p > 0.9999$, LPS $p > 0.9999$) and $7.6x10^{11}$ particles/ml (US $p > 0.9999$, LPS $p = 0.7504$). Data is presented as mean ± SEM, n = 3/group, * $p < 0.05$.

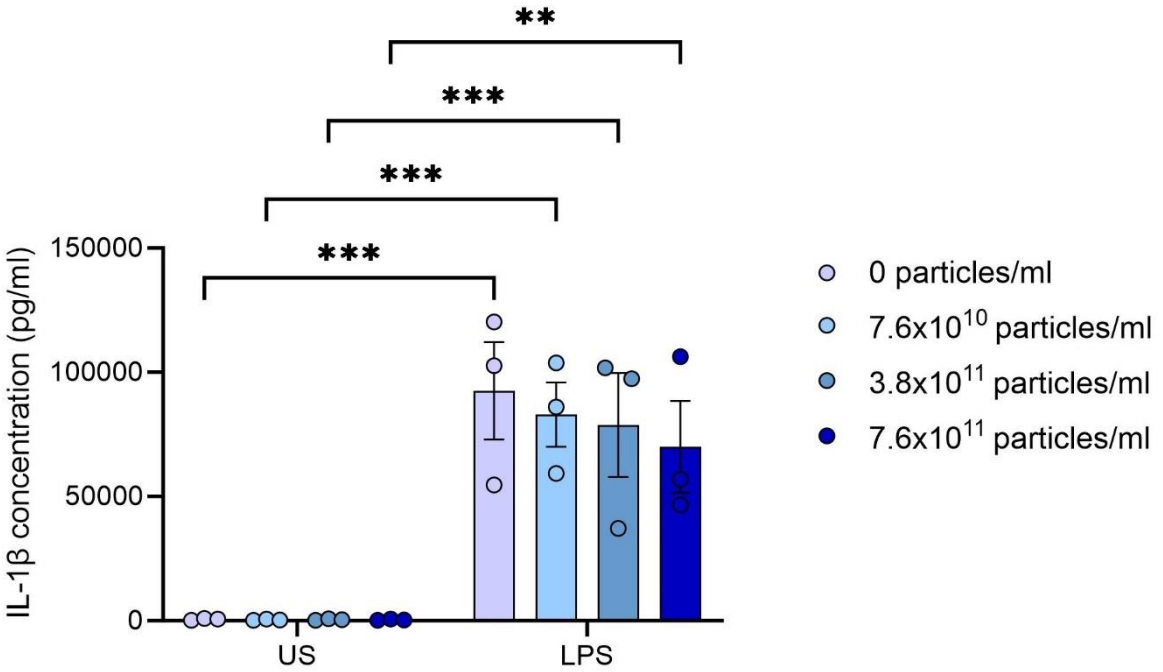

Figure 3.17. NP effect on IL-10 production in pregnant monocytes. Monocytes were isolated from whole blood of pregnant women collected into heparin-coated tubes and cultured for 20 hrs with and without LPS (10ng/ml) and different NP concentrations at 37°C and 5% CO_2. The supernatants were analysed via ELISA experiments. Statistical analysis was via a 2-way ANOVA with Tukey post hoc testing and significance was accepted if $p \leq 0.05$. Each unstimulated (US) NP concentration was compared with the LPS-stimulated counterpart; 0 particles/ml ($p = 0.0007$), $7.6x10^{10}$ particles/ml ($p = 0.0001$), $3.8x10^{11}$ particles/ml ($p = 0.0015$) and $7.6x10^{11}$ particles/ml ($p = 0.0207$).Each nanoparticle concentration was compared to the respective unstimulated or stimulated control; $7.6x10^{10}$ particles/ml (US $p > 0.9999$, LPS $p = 0.8234$), $3.8x10^{11}$ particles/ml (US $p > 0.9999$, LPS $p = 0.9863$) and $7.6x10^{11}$ particles/ml (US $p > 0.9999$, LPS $p = 0.4090$). Data is presented as mean ± SEM, n = 3/group, * $p < 0.05$.

3.10. Comparisons of NP effect on cytokine productions between non-pregnant and pregnant monocytes

When comparing cytokine production from both unstimulated and LPS stimulated monocytes of non-pregnant and pregnant women in the absence or presence of NPs, no significant difference was observed when comparing each group for production of TNF-α (figure 3.18), IL-1β (figure 3.19) or IL-10 (figure 3.20). Notably there was a difference in LPS-stimulated IL-1β in the absence of any NPs with levels significantly higher from monocytes of pregnant women (figure 3.19; p = 0.0415).

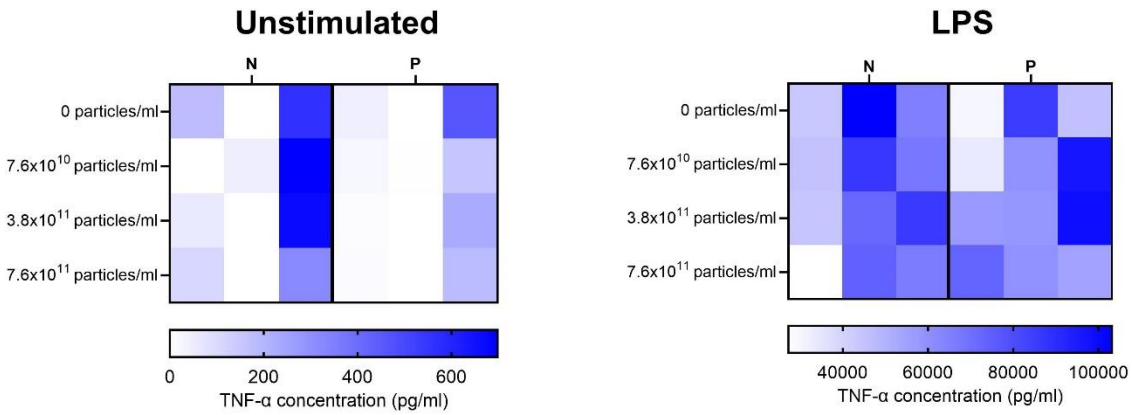

Figure 3.18. Heatmap of TNF-α production comparison between non-pregnant and pregnant monocytes. Isolated monocytes from whole non-pregnant (N) and pregnant (P) blood collected into heparin-coated tubes were cultured for 20 hrs with each NP concentration with and without LPS at 37°C and 5% CO_2. The supernatants were then used to analyse TNF-α production via ELISA experiments. Statistical analysis was via a 2-way ANOVA with Tukey post hoc testing and significance was accepted if $p \leq 0.05$. Each NP concentration was compared to the opposing group of cells with the same conditions; 0 particles/ml (US $p > 0.9999$, LPS $p = 0.6309$), $7.6x10^{10}$ particles/ml (US $p > 0.9999$, LPS $p = 0.9964$), $3.8x10^{11}$ particles/ml (US $p > 0.9999$, LPS $p = 0.9907$) and $7.6x10^{11}$ particles/ml (US $p > 0.9999$, LPS $p = 0.9645$). Data is presented as mean ± SEM, n = 3/group.

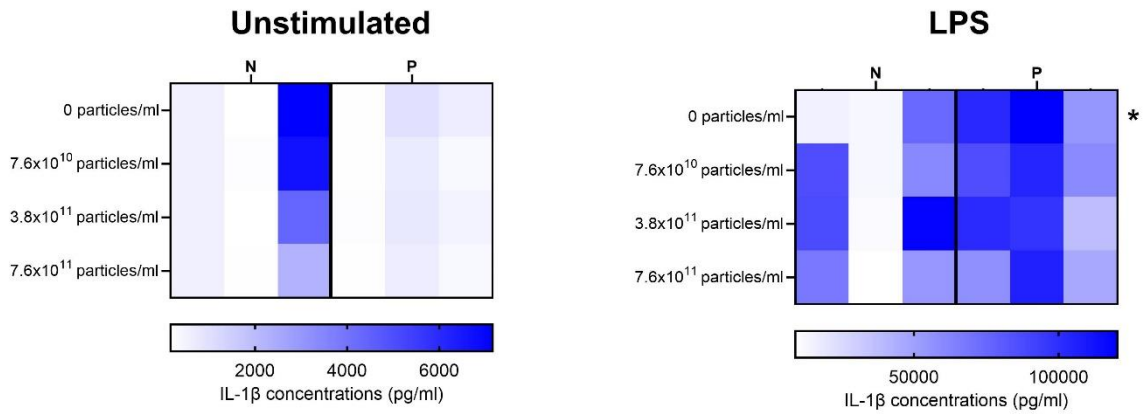

Figure 3.19. Comparison of NP effect on IL-1β production between non-pregnant and pregnant monocytes. Isolated monocytes from whole non-pregnant (N) and pregnant (P) blood collected into heparin-coated tubes were cultured for 20 hrs with each NP concentration with and without LPS at 37°C and 5% CO_2. The supernatants were then used to analyse IL-1β production via ELISA experiments. Statistical analysis was via a 2-way ANOVA with Tukey post hoc testing and significance was accepted if $p \leq 0.05$. Each NP concentration was compared to the second group of cells with the same conditions; 0 particles/ml (US p = 0.9997, LPS p = 0.0415), $7.6x10^{10}$ particles/ml (US p = 0.9997, LPS p = 0.4885), $3.8x10^{11}$ particles/ml (US p > 0.9999, LPS p = 0.9888) and $7.6x10^{11}$ particles/ml (US p > 0.9999, LPS p = 0.5912). Data is presented as mean ± SEM, n = 3/group, * $p < 0.05$.

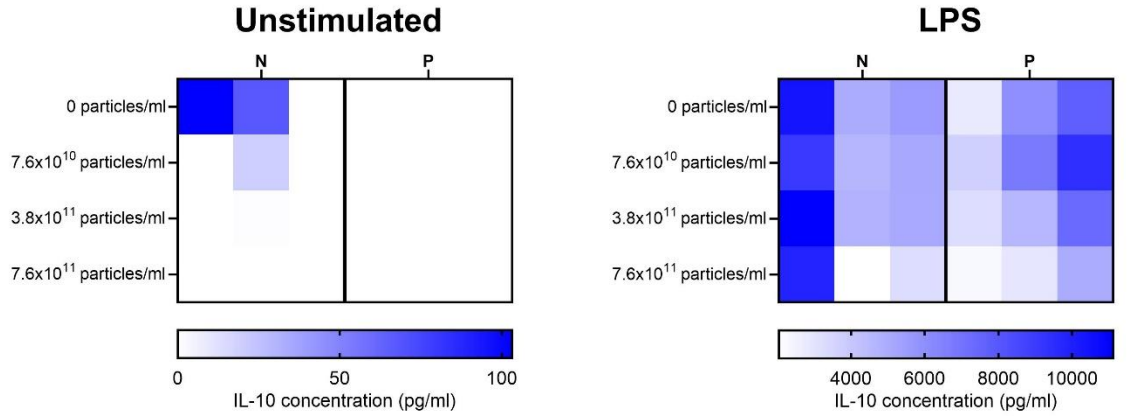

Figure 3.20. Comparison of NP effect on IL-10 production between non-pregnant and pregnant monocytes. Isolated monocytes from whole non-pregnant (N) and pregnant (P) blood collected into heparin-coated tubes were cultured for 20 hrs with each NP concentration with and without LPS at 37°C and 5% CO_2. The supernatants were then used to analyse IL-10 production via ELISA experiments. Statistical analysis was via a 2-way ANOVA with Tukey post hoc testing and significance was accepted if $p \leq 0.05$. Each NP concentration was compared to the second group of cells with the same conditions; 0 particles/ml (US p > 0.9999, LPS p = 0.8033), $7.6x10^{10}$ particles/ml (US p > 0.9999, LPS p = 0.9966), $3.8x10^{11}$ particles/ml (US p > 0.9999, LPS p = 0.6504) and $7.6x10^{11}$ particles/ml (US p > 0.9999, LPS p = 0.7513). Data is presented as mean ± SEM, n = 3/group.

3.11. NP effect on cytokine production in placental macrophages

Like their monocyte precursors, NPs had no effect on TNF-α production by unstimulated or LPS-stimulated placental macrophages (figure 3.21). There was a significant increase in TNF-α production when comparing LPS-stimulated to the unstimulated for each concentration as expected (figure 3.21). Interestingly, there appears to be increased IL-1β production for both unstimulated and stimulated placental macrophages with higher NP concentrations, however, this increase was insignificant (figure 3.22). IL-10 production in unstimulated or LPS-stimulated placental macrophages was not significantly affected by NPs of any concentration studied (figure 3.23). Unexpectedly, there was no significant increase in IL-10 production in placental macrophages when comparing each LPS-stimulated NP concentration to the unstimulated counterpart (figure 3.23).

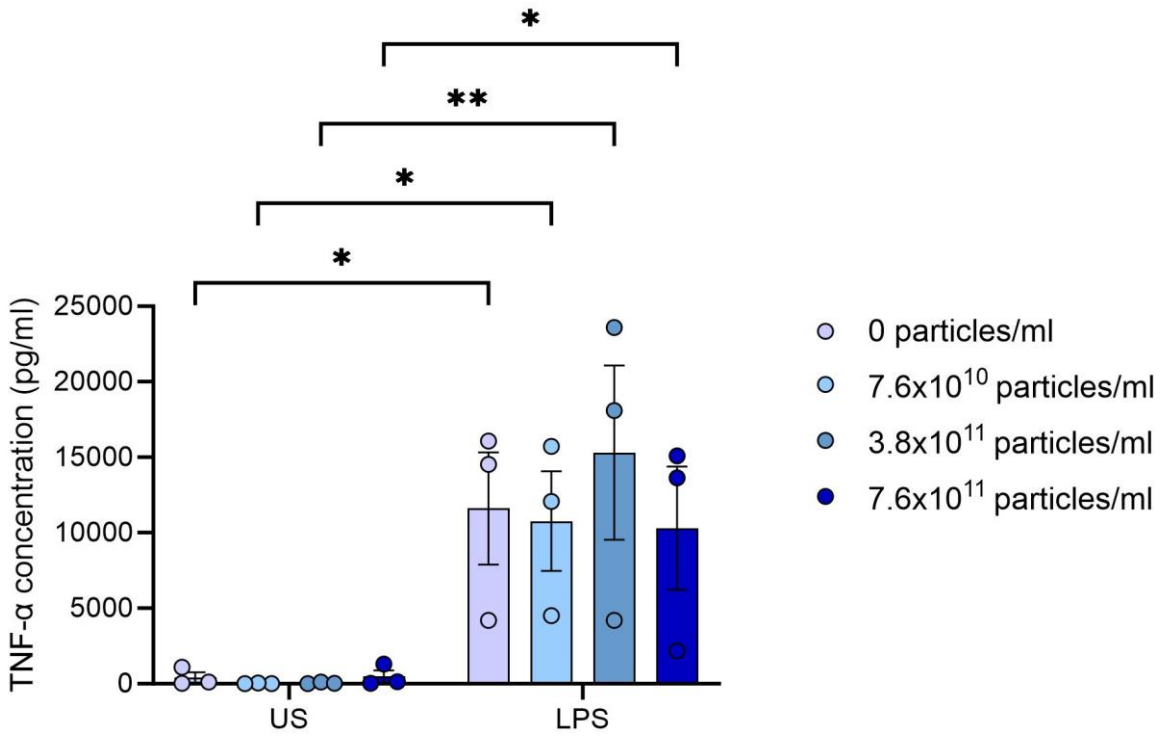

Figure 3.21. NP effect on TNF-α production in placental macrophages. Placental macrophages were enzymatically digested from placental tissue and cultured with different NP concentrations, with and without LPS for 24 hrs at 37°C and 5% CO_2. The supernatants were analysed for TNF-α production via ELSIA experiments. Statistical analysis was via a 2-way ANOVA with Tukey post hoc testing and significance was accepted if $p \leq 0.05$. Each unstimulated (US) NP concentration was compared with the LPS-stimulated counterpart; 0 particles/ml ($p = 0.0199$), $7.6x10^{10}$ particles/ml ($p = 0.0246$), $3.8x10^{11}$ particles/ml ($p = 0.0028$) and $7.6x10^{11}$ particles/ml ($p = 0.0375$).Each nanoparticle concentration was compared to the respective unstimulated or stimulated control; $7.6x10^{10}$ particles/ml (US $p = 0.9997$, LPS $p = 0.9973$), $3.8x10^{11}$ particles/ml (US $p = 0.9998$, LPS $p = 0.8288$) and $7.6x10^{11}$ particles/ml (US $p > 0.9999$, LPS $p = 0.9901$). Data is presented as mean ± SEM, n = 3/group, * $p < 0.05$, ** $p < 0.01$.

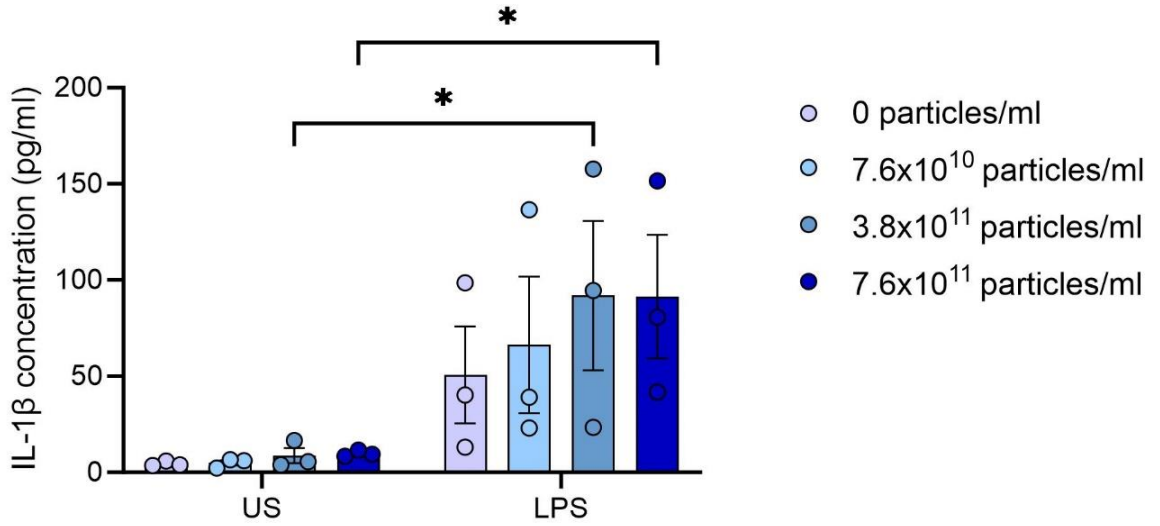

Figure 3.22. NP effect on IL-1β production in placental macrophages. Placental macrophages were enzymatically digested from placental tissue and cultured with different NP concentrations, with and without LPS for 24 hrs at 37°C and 5% CO_2. The supernatants were analysed for IL-1β production via ELSIA experiments. Statistical analysis was via a 2-way ANOVA with Tukey post hoc testing and significance was accepted if $p \leq 0.05$. Each unstimulated (US) NP concentration was compared with the LPS-stimulated counterpart; 0 particles/ml ($p = 0.1859$), $7.6x10^{10}$ particles/ml ($p = 0.0848$), $3.8x10^{11}$ particles/ml ($p = 0.0240$) and $7.6x10^{11}$ particles/ml ($p = 0.0265$).Each nanoparticle concentration was compared to the respective unstimulated or stimulated control; $7.6x10^{10}$ particles/ml (US $p > 0.9999$, LPS $p = 0.9650$), $3.8x10^{11}$ particles/ml (US $p = 0.9993$, LPS $p = 0.6141$) and $7.6x10^{11}$ particles/ml (US $p = 0.9985$, LPS $p = 0.6234$). Data is presented as mean ± SEM, n = 3/group, * $p < 0.05$.

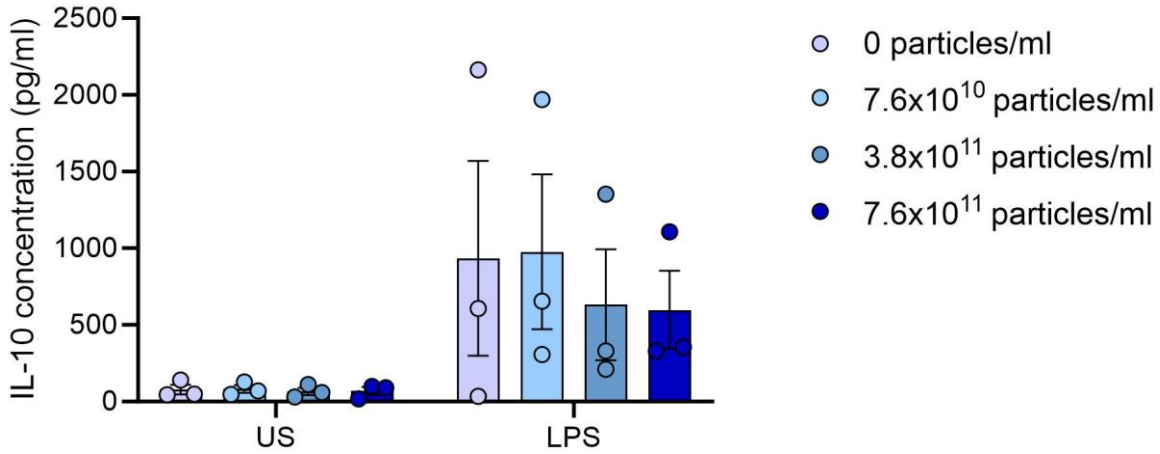

Figure 3.23. NP effect on IL-10 production in placental macrophages. Placental macrophages were enzymatically digested from placental tissue and cultured with different NP concentrations, with and without LPS for 24 hrs at 37°C and 5% CO_2. The supernatants were analysed for IL-10 production via ELSIA experiments. Statistical analysis was via a 2-way ANOVA with Tukey post hoc testing and significance was accepted if $p \leq 0.05$. Each unstimulated (US) NP concentration was compared with the LPS-stimulated counterpart; 0 particles/ml ($p = 0.0831$), $7.6x10^{10}$ particles/ml ($p = 0.0714$), $3.8x10^{11}$ particles/ml ($p = 0.2415$) and $7.6x10^{11}$ particles/ml ($p = 0.2711$). Each nanoparticle concentration was compared to the

respective unstimulated or stimulated control; $7.6x10^{10}$ particles/ml (US $p > 0.9999$, LPS $p = 0.9997$), $3.8x10^{11}$ particles/ml (US $p > 0.9999$, LPS $p = 0.9124$) and $7.6x10^{11}$ particles/ml (US $p > 0.9999$, LPS $p = 0.8843$). Data is presented as mean ± SEM, $n = 3$/group, * $p < 0.05$.

3.12. Comparisons of NP effect of cytokine production between placental macrophages, non—pregnant and pregnant monocytes

When comparing TNF-α, IL-1β and IL-10 between non-pregnant or pregnant monocytes and placental macrophages, unstimulated populations with each concentration did not show any significant differences (figure 3.24 – 3.26). LPS stimulation showed a significantly lower TNF-α production for each concentration with placental macrophages when compared to the non-pregnant and pregnant monocytes (figure 3.24). Stimulation with LPS showed a significantly reduced IL-1β production in placental macrophages when compared to non-pregnant monocytes, but only at $3.8x10^{11}$ particles/ml (figure 3.25: $p = 0.0008$). IL-1β production was significantly reduced in all LPS-stimulated groups of placental macrophages when compared to pregnant monocytes (figure 3.25). Likewise, IL-10 production in placental macrophages is significantly reduced when compared to the non-pregnant and pregnant monocytes for all concentrations (figure 3.26).

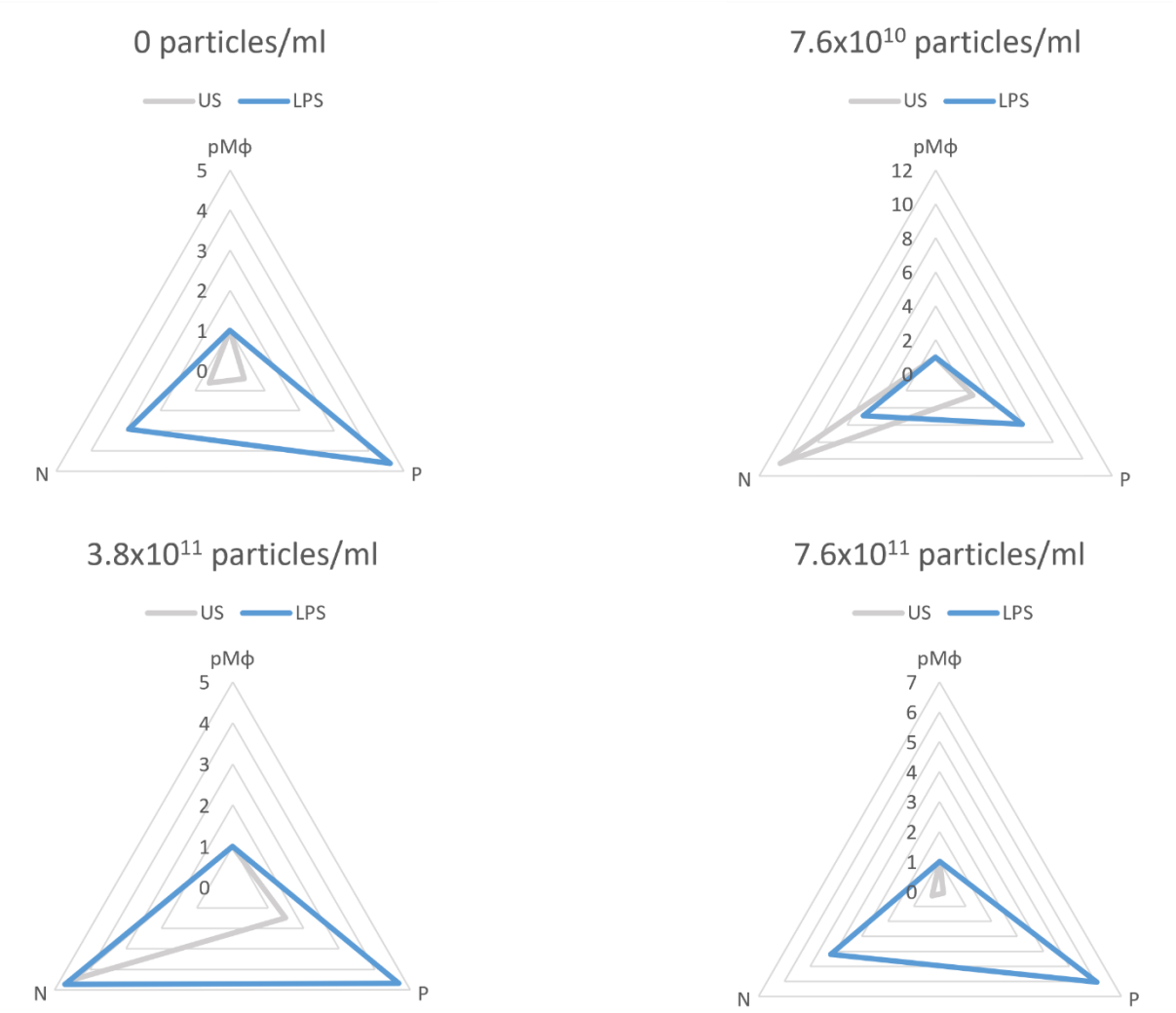

Figure 3.24. TNF-α production comparisons between placental macrophages, non-pregnant monocytes and pregnant monocytes with NP concentrations. Isolated non-pregnant (N) and pregnant (P) monocytes were isolated from whole blood collected in heparin-coated tubes and placental macrophages (pMϕ) were enzymatically digested from placental tissue. All cell types were cultured for 20-24 hrs with different nanoplastic concentrations with and without LPS at 37°C and 5% CO_2. The supernatants were analysed for TNF-α production via ELISA experiments. Statistical analysis was via a 2-way ANOVA with Tukey post hoc testing and significance was accepted if $p \leq 0.05$. TNF-α production in placental macrophages were compared to non-pregnant monocyte production (US 0 particles/ml $p > 0.9999$, $7.6x10^{10}$ particles/ml $p = 0.9999$, $3.8x10^{11}$ particles/ml $p > 0.9999$, $7.6x10^{11}$ particles/ml $p > 0.9999$; LPS 0 particles/ml $p < 0.0001$, $7.6x10^{10}$ particles/ml $p < 0.0001$, $3.8x10^{11}$ particles/ml $p = 0.0001$, $7.6x10^{11}$ particles/ml $p = 0.0008$) and pregnant monocytes (0 particles/ml $p > 0.9999$, $7.6x10^{10}$ particles/ml $p > 0.9999$, $3.8x10^{11}$ particles/ml $p > 0.9999$, $7.6x10^{11}$ particles/ml $p > 0.9999$; LPS 0 particles/ml $p = 0.0022$, $7.6x10^{10}$ particles/ml $p = 0.0001$, $3.8x10^{11}$ particles/ml $p < 0.0001$, $7.6x10^{11}$ particles/ml $p < 0.0001$). Radar plots displayed are normalised to represent the means of cytokine production of non-pregnant monocytes and pregnant monocytes means with respect to the means of placental macrophages per NP concentration, n = 3/group.

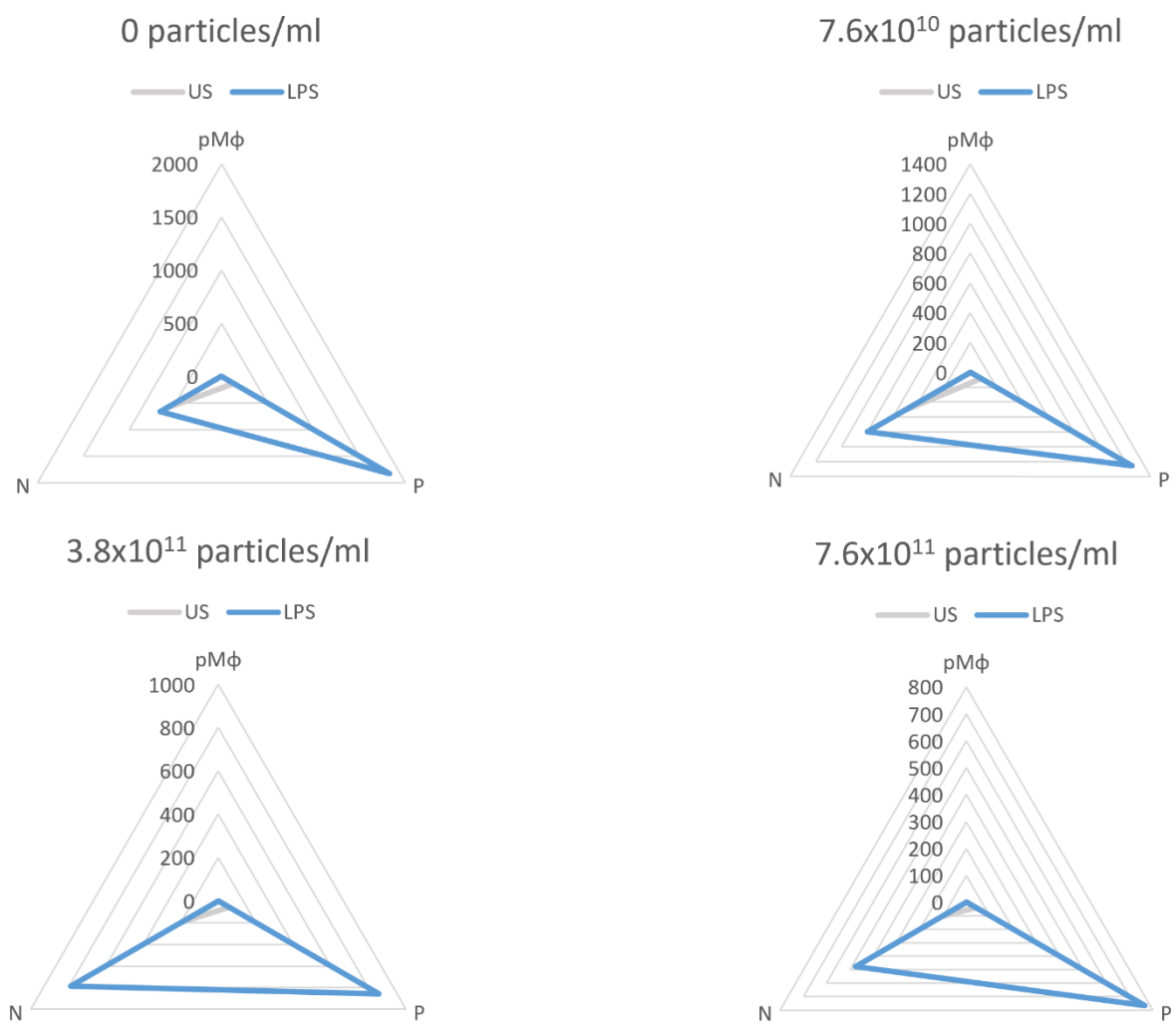

Figure 3.25. IL-1β production comparisons between placental macrophages, non-pregnant monocytes and pregnant monocytes with NP concentrations. Isolated non-pregnant (N) and pregnant (P) monocytes were isolated from whole blood collected in heparin-coated tubes and placental macrophages (pMϕ) were enzymatically digested from placental tissue. All cell types were cultured for 20-24 hrs with different nanoplastic concentrations with and without LPS at 37°C and 5% CO_2. The supernatants were analysed for IL-1β production via ELISA experiments. Statistical analysis was conducted via a 2-way ANOVA with Tukey post hoc testing and significance was accepted if $p \leq 0.05$. IL-1β production in placental macrophages were compared to non-pregnant monocyte production (US 0 particles/ml $p = 0.9986$, $7.6x10^{10}$ particles/ml $p = 0.9988$, $3.8x10^{11}$ particles/ml $p = 0.9996$, $7.6x10^{11}$ particles/ml $p > 0.9999$; LPS 0 particles/ml $p = 0.1997$, $7.6x10^{10}$ particles/ml $p = 0.168$, $3.8x10^{11}$ particles/ml $p = 0.0008$, $7.6x10^{11}$ particles/ml $p = 0.0639$) and pregnant monocytes (0 particles/ml $p > 0.9999$, $7.6x10^{10}$ particles/ml $p > 0.9999$, $3.8x10^{11}$ particles/ml $p > 0.9999$, $7.6x10^{11}$ particles/ml $p > 0.9999$; LPS 0 particles/ml $p < 0.0001$, $7.6x10^{10}$ particles/ml $p < 0.0001$, $3.8x10^{11}$ particles/ml $p < 0.0001$, $7.6x10^{11}$ particles/ml $p < 0.0001$). Radar plots displayed are normalised to represent the means of cytokine production of non-pregnant monocytes and pregnant monocytes means with respect to the means of placental macrophages per NP concentration , n = 3/group.

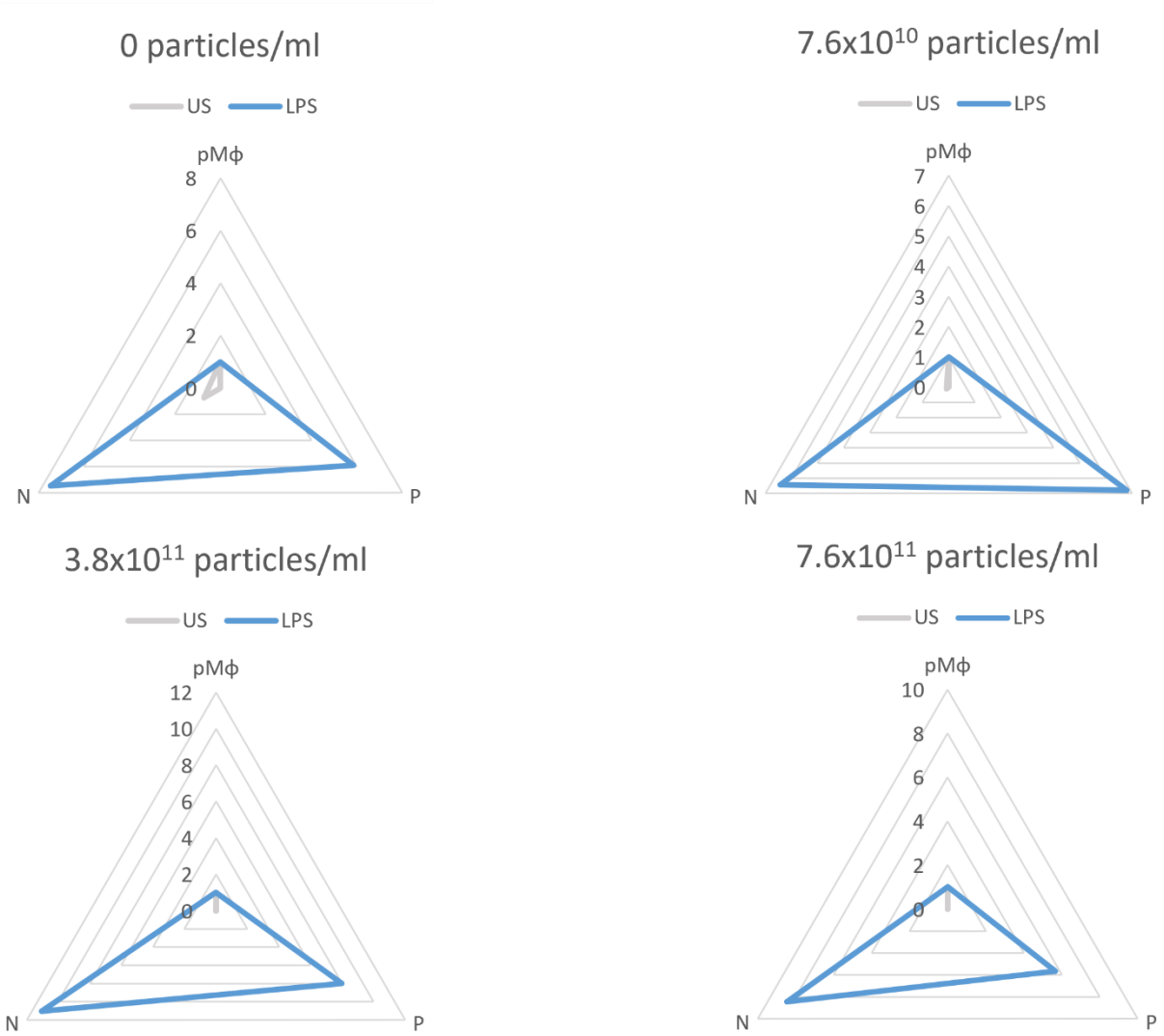

Figure 3.26. IL-10 production comparisons between placental macrophages, non-pregnant monocytes and pregnant monocytes with NP concentrations. Isolated non-pregnant (N) and pregnant (P) monocytes were isolated from whole blood collected in heparin-coated tubes and placental macrophages (pMϕ) were enzymatically digested from placental tissue. All cell types were cultured for 20-24 hrs with different nanoplastic concentrations with and without LPS at 37°C and 5% CO_2. The supernatants were analysed for IL-1β production via ELISA experiments. Statistical analysis was via a 2-way ANOVA with Tukey post hoc testing and significance was accepted if $p \leq 0.05$. IL-10 production in placental macrophages were compared to non-pregnant monocyte production (US 0 particles/ml $p > 0.9999$, $7.6x10^{10}$ particles/ml $p > 0.9999$, $3.8x10^{11}$ particles/ml $p > 0.9999$, $7.6x10^{11}$ particles/ml $p > 0.9999$; LPS 0 particles/ml $p = 0.0008$, $7.6x10^{10}$ particles/ml $p = 0.0037$, $3.8x10^{11}$ particles/ml $p = 0.0005$, $7.6x10^{11}$ particles/ml $p = 0.0176$) and pregnant monocytes (0 particles/ml $p = 0.9998$, $7.6x10^{10}$ particles/ml $p = 0.9998$, $3.8x10^{11}$ particles/ml $p > 0.9999$, $7.6x10^{11}$ particles/ml $p > 0.9999$; LPS 0 particles/ml $p = 0.0003$, $7.6x10^{10}$ particles/ml $p < 0.0001$, $3.8x10^{11}$ particles/ml $p = 0.0005$, $7.6x10^{11}$ particles/ml $p = 0.0389$). Radar plots displayed are normalised to represent the means of cytokine production of non-pregnant monocytes and pregnant monocytes means with respect to the means of placental macrophages per NP concentration n = 3/group.

Chapter 4: General discussion and conclusion

4.1. Discussion

The results presented in this thesis provide evidence to show that monocytes are a key cell type within blood that take up NPs. This is likely due to monocytes' being more adept to engulf and digest foreign objects when compared to neutrophils (Bain, 2017). Lymphocytes', and platelets' main functions antigen recognition, response, and immune regulation, and coagulation, respectively (Bain, 2017). Along with this, monocytes are the largest of the cell types (15-22µm in diameter) analysed within blood, therefore, they have an increased intracellular capacity suggesting that they can sustain increased uptake of NPs compared neutrophils, lymphocytes and platelets (Saidani et al., 2024; Schmid-Schöbein, Shih & Chien, 1980). Tissue resident counterparts of monocytes, in this case placental macrophages, also internalise the NPs. While flow cytometry was used to determine uptake of NPs due to their fluorescent nature, Raman spectrometry could be used in future to quantify the number of NPs internalised into cells, as well as accurately determined the true stock concentration of both non-fluorescent and fluorescent NPs. This would be valuable as the NP concentrations used to stimulate cells does not necessarily reflect the true amount of NPs that are internalised by monocytes and placental macrophages. Increasing the concentrations of NP exposure to placental macrophages did show a significant increase in uptake, however, prolonged exposure over 24 hours did not show any significance. This suggests that NP internalisation occurs relatively quickly once cells have been exposed. Non-pregnant monocytes were not significantly affected by increased concentration of NPs or length of exposure with regards to uptake but due to the variations of values within these datasets, further repeats may lead to significance between concentrations and/or exposure times. With each dosage at increasing timepoints for both non-pregnant monocytes and placental macrophages, NP uptake was identified and further confirmed with confocal microscopy. Like NP uptake over time in placental macrophages, the prolonged exposure appeared to have negligible effects on placental macrophage viability, however, as the cells were cultured for only 24 hours, further work could include prolonged culture over several days to see the long term effects of exposure and identify possible pathologies NPs could induce in the placenta. Similarly, prolonged NP exposure of peripheral monocytes can be used to observe their effects on cell viability as well as any inhibition or dysfunctional differentiation into macrophages. NPs in rat basophilic leukaemia (RBL-2H3) cells have been shown to adopt both endocytic and pinocytotic pathways for uptake depending on size (Liu et al., 2021). This evidence shows that NPs may adopt varying pathways to be internalised and may be cell type specific. Further work would explore this by inhibiting phagocytic and endocytic pathways of phagocytes followed by exposure to NPs to identify the mode of uptake NPs used for cellular internalisation, which in turn, will also provide evidence as to whether NPs have the potential to passively diffuse across cellular

membranes. While confocal microscopy was utilised to confirm nanoplastic uptake, addition of focus stacking within confocal microscopy could be implemented in future studies to produce a 3D image of cells with NPs and confirm internalisation. Likewise, TEM has been used to previously to confirm internalisation of polystyrene NPs to neural stem cells, as well as the exact intracellular location of the NPs, size of NPs and their subsequent agglomerates (González-Caballero et al., 2024). These methods could be used in future studies to support the claim that NPs are internalised into monocytes, as well as characterise the size of plastics and agglomerates intracellularly. The use of TEM in future studies could also aid in driving further investigation to how NPs interact with monocyte organelles and subsequent functionality by identifying where NPs deposit intracellularly.

One of the main findings of this work is that monocytes from pregnant women show greater uptake of NPs than non-pregnant women. This is in keeping with Rees et al. (2024), who concluded that monocytes in pregnancy have increased expression of proteins related to phagocytosis and further emphasised by increased phagocytosis via pHrodo™ analysis modelling bacteria uptake. While this research logically leads to the theory that these NPs are taken up more in pregnancy via phagocytosis, the evidence in this thesis did not analyse this mechanism and therefore it cannot be concluded that phagocytosis is responsible for the observed NP uptake in pregnant monocytes. Regardless, the significant increase of NP internalisation in pregnant monocytes suggests the possibility that the effects of NPs might be exacerbated in pregnant women as they will have a greater intracellular load.

Further work showed that intermediate monocytes tended to have the greater NP load than classical monocytes. This was true for both pregnant and non-pregnant women and the elevated uptake by total monocytes from pregnant women was seen for both the classical and the intermediate subset. This indicates that the functionality of these subsets encompasses NP uptake in pregnancy and the clearance of pathogens/foreign bodies in the blood, however this mechanism was not investigated herein. Furthermore, as the presence of CD14++ in tandem with CD16+ expression on monocytes (intermediate monocytes) lead to increased uptake compared to classical and non-classical (which had no change in pregnancy), further work into how these markers facilitate NP uptake is warranted. As CD16 (FcγRIIIa) is involved in phagocytosis, the evidence does not indicate NPs are internalised in pregnant monocytes solely via CD16-mediated phagocytosis as NP uptake was not effected in non-classical monocytes (Sampath, Moideen, Ranganathan & Bethunaickan, 2018). Further work could include inhibition of uptake pathways in monocytes to identify uptake mechanisms such as CD36 or

CD64 (involved in non-opsonised and opsonised phagocytosis, respectively, with CD64 being upregulated in CD16+ monocytes) to identify if NP uptake is facilitated via alternative phagocytic pathways (Patel et al., 2007; Rees et al., 2024). MPs have been shown to have increased uptake after being environmentally exposed and allowed to create a corona composed of carbohydrates, nucleic acids and amino acids suggesting that these molecules can potentially act as opsonins and allow for opsonin-mediated phagocytosis (Ramsperger et al., 2020).

There is also evidence to support the hypothesis that NPs could modulate immune function of mononuclear phagocytes. However, due to lack of significant results, this cannot be concluded here. It is worth noting that the methods used throughout this thesis consistently used polystyrene materials (culture plates etc.) and are therefore likely to be relatively inert with regards with cellular interaction in immune response invocation, also suggesting that the carboxylated polystyrene NPs used would lack an effect on inflammation. Changes in plastic type (whether it be the NPs or the materials) used may have yielded different results as the literature has shown that the use different plastic types lead to variances in the results. For example, polyethylene was the predominant contaminant in placentas involved in IUGR pregnancies suggesting polyethylene could have more potent adverse effects than polystyrene, warranting further investigation in future (Amereh et al., 2022).

It was hypothesised that NPs would alter the production of cytokines with potential differences between pregnant and non-pregnant women, due to the shift to anti-inflammatory responses of phagocytes during pregnancy. In normal pregnancy, the immune system presents as anti-inflammatory partially supported by phagocyte function shifting to M2-like while pro-inflammatory cytokine production is decreased to reduce the potential for immune attacks to the semi-allogenic fetus (Joerink, Rindsjö, van Riel, Alm & Papadogiannakis, 2011; Liu et al., 2022; Mendoza-Cabrera et al., 2020). The three cytokines analysed in this thesis were TNF-α, IL-1β and IL-10. These were chosen for their important roles at different stages of pregnancy.

Increased TNF-α production in placental tissue has been associated with intrauterine growth restriction, with this restriction also observed with increased NP exposure and translocation (paired with varying plastic types) in pregnant mice and human placentas, overall leading to reduced birth weights, lengths and head circumference, suggesting that NPs interfere and reduce nutrient

transport to the fetus (Holcberg et al., 2001; Aghaei et al., 2022; Amereh et al., 2022). However, the evidence presented in this thesis does not support the previous literature as TNF-α production did not significantly change with increasing NP concentrations in any cell type investigated. Increased TNF-α production in monocytes has been associated with monocyte differentiation into dendritic and macrophage cells as well as a response to tissue damage (Iwamoto et al., 2007). Despite insignificances, an increase of TNF-α production observed in pregnant monocytes with increased NP dosages suggests that NPs could induce monocyte differentiation in an effort for tissue repair and maintenance of homeostasis in pregnancy, however, further work would be required to conclude this. Further work analysing pregnant monocyte-derived macrophages and dendritic cells after prolonged NP exposure could also provide evidence to support this suggestion.

Like TNF-α, increased IL-1β production promotes monocyte differentiation into dendritic cells and macrophages (specifically M1 phenotypes) (Kaneko et al., 2019). Increasing NP concentrations lead to decreased IL-1β production in non-pregnant monocytes and placental macrophages with the opposite seen in pregnant monocytes. From this, there is some evidence to suggest that NP increase leads to a greater likelihood of pregnant monocyte differentiation to M1/pro-inflammatory macrophages which could potentially lead to pathologies in pregnancy as pregnancy relies on well-regulated control of inflammation and maintenance of tissue homeostasis via M2 phagocytes, however, lack of significance calls for further work to support this.

A possible explanation to the opposite trends observed for pro-inflammatory cytokine productions in non-pregnant and pregnant monocytes might lie in the fact that NPs are regularly taken up at an increased rate in pregnant monocytes when compared to non-pregnant and a greater internal load might increase disruption to intracellular pathways. However, further work would need to be undertaken to explore this suggestion as the mechanisms of uptake and therefore effects inside the cell are not yet known.

Finally, IL-10 is an anti-inflammatory cytokine that reduces the production of TNF-α and IL-1β (Armstrong, Jordan & Millar, 1996; Sun et al., 2019). IL-10 is also a mediator in placental growth, repair and remodelling during pregnancy as well as an apoptotic moderator (Iyer & Chen, 2012; Thaxton & Sharma, 2010). Increased NP concentrations lead to a decrease in IL-10 production across all cell types analysed in this thesis, logically suggesting that NPs could reduce placental maintenance

and reduce the efficiency of inflammation leading to further tissue damage both peripherally and within tissues, however this will need to be further investigated due to insignificant results.

Placental macrophages when compared to each monocyte population showed a significantly lower production of each cytokine analysed which is expected as the function of placental macrophages is mainly for tissue repair and immunomodulation in the placenta rather than invocation of inflammation (Mezouar, Katsogiannou, Amara, Bretelle & Mege, 2021). Therefore, future investigations into cytokines produced for tissue modulation by placental macrophages such as VEGF, GDF-15 and FGF-21 should be considered to understand how NPs potentially affect tissue homeostasis in the placenta.

Prolonged exposure of NPs to cells and mouse models has shown to induce an increase in inflammation as well as neurodegeneration and cardiovascular issues (Liang et al., 2022; W. Wang et al., 2023). As physiological exposure to NPs is constant and prolonged, further work looking at repeated exposure of NPs to monocytes and placental macrophages over extended periods of time may reveal further cellular dysfunction, however this is just speculation. Implementation of metabolomics and transcriptomics could be utilised to obtain a better understanding of the effects of NPs on monocytes and placental macrophages.

It is reported that monocytes in pregnancy differs in cytokine response of monocytes from non-pregnant and pregnant women is dependent on the stimulus used to induce cytokine production. MDP – that activates the nucleotide oligomerization domain 2 (NOD2) receptor - has been shown have reduced inflammatory effects in pregnant monocytes when compared to non-pregnant, however LPS - that activates toll-like receptor 4 (TLR4) - was shown to have no effect (Faas, Spaans & de Vos, 2014; Rees et al., 2024). Research has shown these stimulant-dependent variances in cytokine production relates to LPS switching the monocytes to glycolysis for energy whereas MDP switches the monocytes to favour oxidative phosphorylation (OXPHOS), which is reduced in pregnancy (Rees et al., 2024). The results presented in this thesis support this statement as no significant differences were seen for any cytokine production between the monocyte populations stimulated with LPS. Further work lies in investigating the effects of NPs on glycolysis and OXPHOS and possibly other immune stimulants such as R848, R837 and TL8 that preferentially activate TLR7 and TLR8 and have a critical anti-viral role.

4.2. Limitations

Throughout this project, some limitations were encountered. Firstly, analysis of TNF-α and IL-10 production in monocytes in some samples resulted in no detection. This is due to the production of said cytokines by monocytes being so minimal that they were not within the range of the standards produced in the ELISA kits. Sensitive ELISA experiments would be useful as incredibly little cytokine production would have been detected and thus provide more informative data and come to more solid conclusions.

Another limitation is, although concentrations of NPs used remained consistent throughout the project, the number of cells used varied depending on the experiment conducted. From this, particles/cell will vary and could potentially result in incohesive data. A solution to this would be to use particles/cell in future studies to ensure that cell exposure and thus immune response remains consistent throughout.

Methodical limitations were also encountered. NP uptake in monocytes was observed by flow cytometry with whole blood. It would be incorrect to say that NPs would solely interact with monocytes in whole blood and would likely interact with many other cells such as red blood cells, neutrophils and lymphocytes. Monocyte isolation would need to be conducted in future work specifically for NP uptake analysis via flow cytometry for consistency with the other experiments conducted in this project. With this, most of the apparatus used throughout this thesis were made of plastic and therefore likely caused further plastic contamination to the investigated phagocytes, therefore inflammatory responses may not solely by due to NPs added to the cells but also from the surrounding plastic environment.

Finally, daily time constraints and incubation periods proved to be a limitation in this project. Monocytes in whole blood were cultured for 2 hrs (flow cytometry) while isolated monocytes were cultured for 20 hrs (ELISAs) as this provided most appropriate conditions for the experiments. Along with this, sample acquisition was not allocated to a set time, resulting in placenta and pregnant blood samples being processed at various times throughout the day. In future experiments, optimisation of timepoints would need to be decided to ensure consistency throughout the project.

4.3. Conclusion

This thesis investigated the effect of NP exposure in innate immune cells in pregnancy, namely peripheral monocytes and placental macrophages. Different dosages of NP lead to increased rate of uptake in both monocytes and placental macrophages, with pregnant monocytes having an increased uptake when compared to non-pregnant monocytes. Despite variations in NP effect on

pro- and anti-inflammatory cytokine productions, NPs did not significantly affect this production and therefore NP leading to modulation of inflammation could not be concluded. While the results presented provide insights to NP effect on the mechanical and immunological function of phagocytes, it also calls for further work including extended culture studies, proteomics, metabolomics and uptake mechanism inhibition to gain a better understanding of how NPs are internalised in phagocytes and at what part of cytokine signalling pathways they up/downregulate or disrupt in order to invoke the observed immune responses.

Bibliography

Abrams, E. T., Brown, H., Chensue, S. W., Turner, G. D. H., Tadesse, E., Lema, V. M., Molyneux, M. E., Rochford, R., Meshnick, S. R., & Rogerson, S. J. (2003). Host Response to Malaria During Pregnancy: Placental Monocyte Recruitment Is Associated with Elevated β Chemokine Expression. *Journal of Immunology*, *170*(5), 2759–2764. https://doi.org/10.4049/jimmunol.170.5.2759

Abumaree, M. H., Al Jumah, M. A., Kalionis, B., Jawdat, D., Al Khaldi, A., Abomaray, F. M., Fatani, A. S., Chamley, L. W., & Knawy, B. A. (2013). Human Placental Mesenchymal Stem Cells (pMSCs) Play a Role as Immune Suppressive Cells by Shifting Macrophage Differentiation from Inflammatory M1 to Anti-inflammatory M2 Macrophages. *Stem Cell Reviews and Reports*, *9*(5), 620–641. https://doi.org/10.1007/s12015-013-9455-2

Abu-Raya, B., Michalski, C., Sadarangani, M., & Lavoie, P. M. (2020). Maternal Immunological Adaptation During Normal Pregnancy. *Frontiers in Immunology*, *11*, 575197–575197. https://doi.org/10.3389/fimmu.2020.575197

Aghaei, Z., Sled, J. G., Kingdom, J. C., Baschat, A. A., Helm, P. A., Jobst, K. J., & Cahill, L. S. (2022). Maternal Exposure to Polystyrene Micro- and Nanoplastics Causes Fetal Growth Restriction in Mice. *Environmental Science and Technology Letters*, *9*(5), 426–430. https://doi.org/10.1021/acs.estlett.2c00186

Alma, A. M., de Groot, G. S., & Buteler, M. (2023). Microplastics incorporated by honeybees from food are transferred to honey, wax and larvae. *Environmental Pollution*, *320*. https://doi.org/10.1016/j.envpol.2023.121078

Amereh, F., Amjadi, N., Mohseni-Bandpei, A., Isazadeh, S., Mehrabi, Y., Eslami, A., Naeiji, Z., & Rafiee, M. (2022). Placental plastics in young women from general population correlate with reduced foetal growth in IUGR pregnancies. *Environmental Pollution*, *314*. https://doi.org/10.1016/j.envpol.2022.120174

Armstrong, L., Jordan, N., & Millar, A. (1996). Interleukin 10 (IL-10) regulation of tumour necrosis factor alpha (TNF-alpha) from human alveolar macrophages and peripheral blood monocytes. *Thorax*, *51*(2), 143-149. https://doi.org/10.1136/thx.51.2.143

Auta, H. S., Emenike, C. U., & Fauziah, S. H. (2017). Distribution and importance of microplastics in the marine environment: A review of the sources, fate, effects, and potential

solutions. *Environment International*, *102*, 165–176. https://doi.org/10.1016/j.envint.2017.02.013

Bai, K., Lee, C. L., Liu, X., Li, J., Cao, D., Zhang, L., Hu, D., Li, H., Hou, Y., Xu, Y., Kan, A. S. Y., Cheung, K. W., Ng, E. H. Y., Yeung, W. S. B., & Chiu, P. C. N. (2022). Human placental exosomes induce maternal systemic immune tolerance by reprogramming circulating monocytes. *Journal of Nanobiotechnology*, *20*(1). https://doi.org/10.1186/s12951-022-01283-2

Bain, B. J. (2017). Structure and function of red and white blood cells. *Medicine*, *45*(4), 187–193. https://doi.org/10.1016/j.mpmed.2017.01.011

Bakos, E., Thaiss, C. A., Kramer, M. P., Cohen, S., Radomir, L., Orr, I., Kaushansky, N., Ben-Nun, A., Becker-Herman, S., & Shachar, I. (2017). CCR2 Regulates the Immune Response by Modulating the Interconversion and Function of Effector and Regulatory T Cells. *Journal of Immunology*, *198*(12), 4659–4671. https://doi.org/10.4049/jimmunol.1601458

Barnes, D. K. A., Galgani, F., Thompson, R. C., & Barlaz, M. (2009). Accumulation and fragmentation of plastic debris in global environments. *Philosophical Transactions of the Royal Society of London. Series B. Biological Sciences*, *364*(1526), 1985–1998. https://doi.org/10.1098/rstb.2008.0205

BioLegend. (2024). *DRAQ7™*. Retrieved December 14, 2024, from https://www.biolegend.com/en-gb/products/draq7-9628#:~:text=DRAQ7%E2%84%A2%20is%20a%20far,%2C%20715LP%2C%20and%20780LP%20filters.

Burton, G. J., & Fowden, A. L. (2015). The placenta: a multifaceted, transient organ. *Philosophical Transactions of the Royal Society of London. Series B. Biological Sciences*, *370*(1663), 20140066–20140066. https://doi.org/10.1098/rstb.2014.0066

Cai, L., Hu, L., Shi, H., Ye, J., Zhang, Y., & Kim, H. (2018). Effects of inorganic ions and natural organic matter on the aggregation of nanoplastics. *Chemosphere*, *197*, 142–151. https://doi.org/10.1016/j.chemosphere.2018.01.052

Cary, C. M., DeLoid, G. M., Yang, Z., Bitounis, D., Polunas, M., Goedken, M. J., Buckley, B., Cheatham, B., Stapleton, P. A., & Demokritou, P. (2023a). Ingested Polystyrene Nanospheres Translocate to Placenta and Fetal Tissues in Pregnant Rats: Potential Health Implications. *Nanomaterials*, *13*(4). https://doi.org/10.3390/nano13040720

Cary, C. M., Seymore, T. N., Singh, D., Vayas, K. N., Goedken, M. J., Adams, S., Polunas, M., Sunil, V. R., Laskin, D. L., Demokritou, P., & Stapleton, P. A. (2023b). Single inhalation exposure to polyamide micro and nanoplastic particles impairs vascular dilation without generating pulmonary inflammation in virgin female Sprague Dawley rats. *Particle and Fibre Toxicology*, *20*(1). https://doi.org/10.1186/s12989-023-00525-x

Cella, C., La Spina, R., Mehn, D., Fumagalli, F., Ceccone, G., Valsesia, A., & Gilliland, D. (2022). Detecting Micro- and Nanoplastics Released from Food Packaging: Challenges and Analytical Strategies. *Polymers*, *14*(6), 1238-. https://doi.org/10.3390/polym14061238

Chai, G., Nie, Z., Liu, G., Huang, X., Chen, Y., Yang, X., & Meng, Y. (2023). Microplastic Pollution in the Qinghai–Tibet Plateau: Current State and Future Perspectives. *Reviews of Environmental Contamination and Toxicology*, *261*(1), 19-. https://doi.org/10.1007/s44169-023-00044-y

Chambers, M., Rees, A., Cronin, J. G., Nair, M., Jones, N., & Thornton, C. A. (2021). Macrophage Plasticity in Reproduction and Environmental Influences on Their Function. *Frontiers in Immunology*, *11*, 607328–607328. https://doi.org/10.3389/fimmu.2020.607328

Chen, J., Ma, R., Shi, Q., Mei, A., & Xu, Z. (2023). Aggregation of positively charged polystyrene nanoplastics in soil–root systems. *Environmental Chemistry Letters*, *21*(5), 2483–2488. https://doi.org/10.1007/s10311-023-01615-0

Cheng, S., Hu, J., Guo, C., Ye, Z., Shang, Y., Lian, C., & Liu, H. (2023). The effects of size and surface functionalization of polystyrene nanoplastics on stratum corneum model membranes: An experimental and computational study. *Journal of Colloid and Interface Science*, *638*, 778–787. https://doi.org/10.1016/j.jcis.2023.02.008

Clark, N. J., Khan, F. R., Mitrano, D. M., Boyle, D., & Thompson, R. C. (2022). Demonstrating the translocation of nanoplastics across the fish intestine using palladium-doped polystyrene in a salmon gut-sac. *Environment International*, *159*. https://doi.org/10.1016/j.envint.2021.106994

Claudia, C., La Spina, R., Mehn, D., Fumagalli, F., Ceccone, G., Valsesia, A., & Gilliland, D. (2022). Detecting Micro-and Nanoplastics Released from Food Packaging: Challenges and Analytical Strategies. *Polymers*, *14*(6). https://doi.org/10.3390/polym14061238

Correia, M., & Loeschner, K. (2018). Detection of nanoplastics in food by asymmetric flow field-flow fractionation coupled to multi-angle light scattering: possibilities, challenges and analytical limitations. *Analytical and Bioanalytical Chemistry*, *410*(22), 5603–5615. https://doi.org/10.1007/s00216-018-0919-8

Davis, D., Kaufmann, R., & Moticka, E. J. (1998). Nonspecific immunity in pregnancy: monocyte surface Fc γ receptor expression and function. *Journal of Reproductive Immunology*, *40*(2), 119–128. https://doi.org/10.1016/S0165-0378(98)00076-X

Denney, J. M., Nelson, E. L., Wadhwa, P. D., Waters, T. P., Mathew, L., Chung, E. K., Goldenberg, R. L., & Culhane, J. F. (2011). Longitudinal modulation of immune system cytokine profile during pregnancy. *Cytokine*, *53*(2), 170–177. https://doi.org/10.1016/j.cyto.2010.11.005

Dissanayake, P. D., Kim, S., Sarkar, B., Oleszczuk, P., Sang, M. K., Haque, M. N., Ahn, J. H., Bank, M. S., & Ok, Y. S. (2022). Effects of microplastics on the terrestrial environment: A critical review. *Environmental Research*, *209*. https://doi.org/10.1016/j.envres.2022.112734

Dong, Z., Hou, Y., Han, W., Liu, M., Wang, J., & Qiu, Y. (2020). Protein corona-mediated transport of nanoplastics in seawater-saturated porous media. *Water Research*, *182*. https://doi.org/10.1016/j.watres.2020.115978

Dusza, H. M., Katrukha, E. A., Nijmeijer, S. M., Akhmanova, A., Vethaak, A. D., Walker, D. I., & Legler, J. (2022). Uptake, Transport, and Toxicity of Pristine and Weathered Micro-and Nanoplastics in Human Placenta Cells. *Environmental Health Perspectives*, *130*(9). https://doi.org/10.1289/EHP10873

El Hadri, H., Gigault, J., Maxit, B., Grassl, B., & Reynaud, S. (2020). Nanoplastic from mechanically degraded primary and secondary microplastics for environmental assessments. *NanoImpact*, *17*. https://doi.org/10.1016/j.impact.2019.100206

Faas, M. M., & de Vos, P. (2017). Maternal monocytes in pregnancy and preeclampsia in humans and in rats. *Journal of Reproductive Immunology*, *119*, 91–97. https://doi.org/10.1016/j.jri.2016.06.009

Faas, M. M., Spaans, F., & De Vos, P. (2014). Monocytes and macrophages in pregnancy and pre-eclampsia. *Frontiers in Immunology*, *5*, 298–298. https://doi.org/10.3389/fimmu.2014.00298

Fadare, O. O., Wan, B., Liu, K., Yang, Y., Zhao, L., & Guo, L. H. (2020). Eco-Corona vs Protein Corona: Effects of Humic Substances on Corona Formation and Nanoplastic Particle Toxicity in Daphnia magna. *Environmental Science and Technology*, *54*(13), 8001–8009. https://doi.org/10.1021/acs.est.0c00615

Fournier, S. B., D'Errico, J. N., Adler, D. S., Kollontzi, S., Goedken, M. J., Fabris, L., Yurkow, E. J., & Stapleton, P. A. (2020). Nanopolystyrene translocation and fetal deposition after acute lung

exposure during late-stage pregnancy. *Particle and Fibre Toxicology*, *17*(1). https://doi.org/10.1186/s12989-020-00385-9

Fowden, A. L., Sferruzzi-Perri, A. N., Coan, P. M., Constancia, M., & Burton, G. J. (2009). Placental efficiency and adaptation: Endocrine regulation. *Journal of Physiology*, *587*(14), 3459–3472. https://doi.org/10.1113/jphysiol.2009.173013

Francisco, V., Pino, J., Campos-Cabaleiro, V., Ruiz-Fernández, C., Mera, A., Gonzalez-Gay, M. A., Gómez, R., & Gualillo, O. (2018). Obesity, Fat Mass and Immune System: Role for Leptin. *Frontiers in physiology*, *9*, 640. https://doi.org/10.3389/fphys.2018.00640

Gallo, F., Fossi, C., Weber, R., Santillo, D., Sousa, J., Ingram, I., Nadal, A., & Romano, D. (2018). Marine litter plastics and microplastics and their toxic chemicals components: the need for urgent preventive measures. *Environmental Sciences Europe*, *30*(1), 1–14. https://doi.org/10.1186/s12302-018-0139-z

Garcia-Torné, M., Abad, E., Almeida, D., Llorca, M., & Farré, M. (2023). Assessment of Micro- and Nanoplastic Composition (Polymers and Additives) in the Gastrointestinal Tracts of Ebro River Fishes. *Molecules*, *28*(1). https://doi.org/10.3390/molecules28010239

Gautam, R., Jo, J. H., Acharya, M., Maharjan, A., Lee, D. E., Pramod, P. B., Kim, C. Y., Kim, K. S., Kim, H. A., & Heo, Y. (2022). Evaluation of potential toxicity of polyethylene microplastics on human derived cell lines. *Science of the Total Environment*, *838*. https://doi.org/10.1016/j.scitotenv.2022.156089

Gigault, J., Halle, A. ter, Baudrimont, M., Pascal, P.-Y., Gauffre, F., Phi, T.-L., El Hadri, H., Grassl, B., & Reynaud, S. (2018). Current opinion: What is a nanoplastic? *Environmental Pollution (1987)*, *235*, 1030–1034. https://doi.org/10.1016/j.envpol.2018.01.024

Gimeno-Molina, B., Muller, I., Kropf, P., & Sykes, L. (2022). The Role of Neutrophils in Pregnancy, Term and Preterm Labour. *Life*, *12*(10), 1512-. https://doi.org/10.3390/life12101512

Goasguen, J. E., Bennett, J. M., Bain, B. J., Vallespi, T., Brunning, R., & Mufti, G. J. (2009). Morphological evaluation of monocytes and their precursors. *Haematologica*, *94*(7), 994–997. https://doi.org/10.3324/haematol.2008.005421

González-Caballero, M. C., de Alba González, M., Torres-Ruiz, M., Iglesias-Hernández, P., Zapata, V., Terrón, M. C., Sachse, M., Morales, M., Martin-Folgar, R., Liste, I., & Cañas-Portilla, A. I. (2024). Internalization and toxicity of polystyrene nanoplastics on immortalized human neural stem cells. *Chemosphere*, *355*. https://doi.org/10.1016/j.chemosphere.2024.141815

González-Pleiter, M., Tamayo-Belda, M., Pulido-Reyes, G., Amariei, G., Leganés, F., Rosal, R., & Fernández-Piñas, F. (2019). Secondary nanoplastics released from a biodegradable microplastic severely impact freshwater environments. *Environmental Science: Nano*, *6*(5), 1382–1392. https://doi.org/10.1039/c8en01427b

Gschwandtner, M., Derler, R., & Midwood, K. S. (2019). More Than Just Attractive: How CCL2 Influences Myeloid Cell Behavior Beyond Chemotaxis. *Frontiers in Immunology*, *10*, 2759–2759. https://doi.org/10.3389/fimmu.2019.02759

Halimu, G., Zhang, Q., Liu, L., Zhang, Z., Wang, X., Gu, W., Zhang, B., Dai, Y., Zhang, H., Zhang, C., & Xu, M. (2022). Toxic effects of nanoplastics with different sizes and surface charges on epithelial-to-mesenchymal transition in A549 cells and the potential toxicological mechanism. *Journal of Hazardous Materials*, *430*. https://doi.org/10.1016/j.jhazmat.2022.128485

He, P., Chen, L., Shao, L., Zhang, H., & Lü, F. (2019). Municipal solid waste (MSW)landfill: A source of microplastics? -Evidence of microplastics in landfill leachate. *Water Research*, *159*, 38–45. https://doi.org/10.1016/j.watres.2019.04.060

Holcberg, G., Huliehel, M., Sapir, O., Katz, M., Tsadkin, M., Furman, B., Mazor, M., & Myatt, L. (2001). Increased production of tumor necrosis factor-α TNF-α by IUGR human placentae. *European Journal of Obstetrics & Gynecology and Reproductive Biology*, *94*(1), 69–72. https://doi.org/10.1016/S0301-2115(00)00321-3

Hou, Z., Meng, R., Chen, G., Lai, T., Qing, R., Hao, S., Deng, J., & Wang, B. (2022). Distinct accumulation of nanoplastics in human intestinal organoids. *Science of the Total Environment*, *838*. https://doi.org/10.1016/j.scitotenv.2022.155811

Huang, T., Zhang, W., Lin, T., Liu, S., Sun, Z., Liu, F., Yuan, Y., Xiang, X., Kuang, H., Yang, B., & Zhang, D. (2022). Maternal exposure to polystyrene nanoplastics during gestation and lactation induces hepatic and testicular toxicity in male mouse offspring. *Food and Chemical Toxicology*, *160*. https://doi.org/10.1016/j.fct.2021.112803

Huang, X., Liu, L., Xu, C., Peng, X., Li, D., Wang, L., & Du, M. (2020). Tissue-resident CD8+T memory cells with unique properties are present in human decidua during early pregnancy. *American Journal of Reproductive Immunology*, *84*(1). https://doi.org/10.1111/aji.13254

Hüffer, T., Praetorius, A., Wagner, S., Von Der Kammer, F., & Hofmann, T. (2017). Microplastic Exposure Assessment in Aquatic Environments: Learning from Similarities and Differences to

Engineered Nanoparticles. *Environmental Science and Technology*, *51*(5), 2499–2507. https://doi.org/10.1021/acs.est.6b04054

Iwamoto, S., Iwai, S., Tsujiyama, K., Kurahashi, C., Takeshita, K., Naoe, M., Masunaga, A., Ogawa, Y., Oguchi, K., & Miyazaki, A. (2007). TNF-α Drives Human CD14+ Monocytes to Differentiate into CD70+ Dendritic Cells Evoking Th1 and Th17 Responses. *Journal of Immunology*, *179*(3), 1449–1457. https://doi.org/10.4049/jimmunol.179.3.1449

Iyer, S. S., & Cheng, G. (2012). Role of interleukin 10 transcriptional regulation in inflammation and autoimmune disease. *Critical reviews in immunology*, *32*(1), 23–63. https://doi.org/10.1615/critrevimmunol.v32.i1.30

Jansen, C. H. J. R., Kastelein, A. W., Kleinrouweler, C. E., Van Leeuwen, E., De Jong, K. H., Pajkrt, E., & Van Noorden, C. J. F. (2020). Development of placental abnormalities in location and anatomy. *Acta Obstetricia et Gynecologica Scandinavica*, *99*(8), 983–993. https://doi.org/10.1111/aogs.13834

Jenkins, B. J., Rees, A., Jones, N., & Thornton, C. A. (2021). Does Altered Cellular Metabolism Underpin the Normal Changes to the Maternal Immune System during Pregnancy? *Immunometabolism*, *3*(4). https://doi.org/10.20900/immunometab20210031

Jeong, B., Baek, J. Y., Koo, J., Park, S., Ryu, Y. K., Kim, K. S., Zhang, S., Chung, C. H., Dogan, R., Choi, H. S., Um, D., Kim, T. K., Lee, W. S., Jeong, J., Shin, W. H., Lee, J. R., Kim, N. S., & Lee, D. Y. (2022). Maternal exposure to polystyrene nanoplastics causes brain abnormalities in progeny. *Journal of Hazardous Materials*, *426*. https://doi.org/10.1016/j.jhazmat.2021.127815

Jin, Y. J., Kim, J. E., Roh, Y. J., Song, H. J., Seol, A., Park, J., Lim, Y., Seo, S., & Hwang, D. Y. (2023). Characterisation of changes in global genes expression in the lung of ICR mice in response to the inflammation and fibrosis induced by polystyrene nanoplastics inhalation. *Toxicological Research*, *39*(4), 575–599. https://doi.org/10.1007/s43188-023-00188-y

Joerink, M., Rindsjö, E., Van Riel, B., Alm, J., & Papadogiannakis, N. (2011). Placental macrophage (Hofbauer cell) polarization is independent of maternal allergen-sensitization and presence of chorioamnionitis. *Placenta*, *32*(5), 380–385. https://doi.org/10.1016/j.placenta.2011.02.003

Kaneko, N., Kurata, M., Yamamoto, T., Morikawa, S., & Masumoto, J. (2019). The role of interleukin-1 in general pathology. *Inflammation and Regeneration*, *39*, 12–12. https://doi.org/10.1186/s41232-019-0101-5

Kang, S., & Kumanogoh, A. (2020). The spectrum of macrophage activation by immunometabolism. *International Immunology*, *32*(7), 467–473. https://doi.org/10.1093/intimm/dxaa017

Kantha, P., Liu, S. T., Horng, J. L., & Lin, L. Y. (2022). Acute exposure to polystyrene nanoplastics impairs skin cells and ion regulation in zebrafish embryos. *Aquatic Toxicology*, *248*. https://doi.org/10.1016/j.aquatox.2022.106203

Kihara, S., Ghosh, S., McDougall, D. R., Whitten, A. E., Mata, J. P., Köper, I., & McGillivray, D. J. (2020). Structure of soft and hard protein corona around polystyrene nanoplastics—Particle size and protein types. *Biointerphases*, *15*(5), 051002. https://doi.org/10.1116/6.0000404

Kim, H. S., Cho, J. H., Park, H. W., Yoon, H., Kim, M. S., & Kim, S. C. (2002). Endotoxin-Neutralizing Antimicrobial Proteins of the Human Placenta. *Journal of Immunology*, *168*(5), 2356–2364. https://doi.org/10.4049/jimmunol.168.5.2356

Kim, J. S., Romero, R., Cushenberry, E., Kim, Y. M., Erez, O., Nien, J. K., Yoon, B. H., Espinoza, J., & Kim, C. J. (2007). Distribution of CD14+ and CD68+ Macrophages in the Placental Bed and Basal Plate of Women With Preeclampsia and Preterm Labor. *Placenta*, *28*(5), 571–576. https://doi.org/10.1016/j.placenta.2006.07.007

Kim, M. J., Herchenova, Y., Chung, J., Na, S. H., & Kim, E. J. (2022). Thermodynamic investigation of nanoplastic aggregation in aquatic environments. *Water Research*, *226*. https://doi.org/10.1016/j.watres.2022.119286

Kirchsteiger, B., Materić, D., Happenhofer, F., Holzinger, R., & Kasper-Giebl, A. (2023). Fine micro- and nanoplastics particles (PM2.5) in urban air and their relation to polycyclic aromatic hydrocarbons. *Atmospheric Environment*, *301*. https://doi.org/10.1016/j.atmosenv.2023.119670

Kulvietis, V., Zalgeviciene, V., Didziapetriene, J., & Rotomskis, R. (2011). Transport of nanoparticles through the placental barrier. *Tohoku Journal of Experimental Medicine*, *225*(4), 225–234. https://doi.org/10.1620/tjem.225.225

Kumar, A., & Samadder, S. R. (2017). A review on technological options of waste to energy for effective management of municipal solid waste. *Waste Management*, *69*, 407–422. https://doi.org/10.1016/j.wasman.2017.08.046

La Rocca, C., Carbone, F., Longobardi, S., & Matarese, G. (2014). The immunology of pregnancy: Regulatory T cells control maternal immune tolerance toward the fetus. In *Immunology Letters* (Vol. 162, Issue 1, pp. 41–48). Elsevier. https://doi.org/10.1016/j.imlet.2014.06.013

Lambert, S., & Wagner, M. (2016). Characterisation of nanoplastics during the degradation of polystyrene. *Chemosphere*, *145*, 265–268. https://doi.org/10.1016/j.chemosphere.2015.11.078

Leslie, H. A., van Velzen, M. J. M., Brandsma, S. H., Vethaak, A. D., Garcia-Vallejo, J. J., & Lamoree, M. H. (2022). Discovery and quantification of plastic particle pollution in human blood. *Environment International*, *163*. https://doi.org/10.1016/j.envint.2022.107199

Li, C., Chen, X., Du, Z., Geng, X., Li, M., Yang, X., Bo, C., Jia, Q., Yu, G., & Shi, L. (2024). Inhibiting ferroptosis in brain microvascular endothelial cells: A potential strategy to mitigate polystyrene nanoplastics–induced blood–brain barrier dysfunction. *Environmental Research*, *250*. https://doi.org/10.1016/j.envres.2024.118506

Li, J., Wang, G., Gou, X., Xiang, J., Huang, Q. T., & Liu, G. (2022). Revealing Trace Nanoplastics in Food Packages An Electrochemical Approach Facilitated by Synergistic Attraction of Electrostatics and Hydrophobicity. *Analytical Chemistry*, *94*(37), 12657–12663. https://doi.org/10.1021/acs.analchem.2c01703

Li, L., Xu, Y., Li, S., Zhang, X., Feng, H., Dai, Y., Zhao, J., & Yue, T. (2022). Molecular modeling of nanoplastic transformations in alveolar fluid and impacts on the lung surfactant film. *Journal of Hazardous Materials*, *427*. https://doi.org/10.1016/j.jhazmat.2021.127872

Liang, B., Huang, Y., Zhong, Y., Li, Z., Ye, R., Wang, B., Zhang, B., Meng, H., Lin, X., Du, J., Hu, M., Wu, Q., Sui, H., Yang, X., & Huang, Z. (2022). Brain single-nucleus transcriptomics highlights that polystyrene nanoplastics potentially induce Parkinson's disease-like neurodegeneration by causing energy metabolism disorders in mice. *Journal of Hazardous Materials*, *430*. https://doi.org/10.1016/j.jhazmat.2022.128459

Liu, L., Xu, K., Zhang, B., Ye, Y., Zhang, Q., & Jiang, W. (2021). Cellular internalization and release of polystyrene microplastics and nanoplastics. *Science of the Total Environment*, *779*. https://doi.org/10.1016/j.scitotenv.2021.146523

Liu, X., Ahmad, S., Ma, J., Wang, D., & Tang, J. (2023). Comparative study on the toxic effects of secondary nanoplastics from biodegradable and conventional plastics on Streptomyces coelicolor M145. *Journal of Hazardous Materials*, *460*. https://doi.org/10.1016/j.jhazmat.2023.132343

Liu, Y. Y., Liu, J., Wu, H., Zhang, Q., Tang, X. R., Li, D., Li, C. S., Liu, Y., Cao, A., & Wang, H. (2023). Endocytosis, Distribution, and Exocytosis of Polystyrene Nanoparticles in Human Lung Cells. *Nanomaterials*, *13*(1). https://doi.org/10.3390/nano13010084

Liu, Y., Na, Q., Liu, J., Liu, A., Oppong, A., Lee, J. Y., Chudnovets, A., Lei, J., Sharma, R., Kannan, S., Kannan, R. M., & Burd, I. (2022). Dendrimer-Based N-Acetyl Cysteine Maternal Therapy Ameliorates Placental Inflammation via Maintenance of M1/M2 Macrophage Recruitment. *Frontiers in Bioengineering and Biotechnology*, *10*. https://doi.org/10.3389/fbioe.2022.819593

Lunghi, L., Ferretti, M. E., Medici, S., Biondi, C., & Vesce, F. (2007). Control of human trophoblast function. *Reproductive Biology and Endocrinology*, *5*. https://doi.org/10.1186/1477-7827-5-6

Magon, N., & Kumar, P. (2012). Hormones in pregnancy. *Nigerian Medical Journal*, *53*(4), 179. https://doi.org/10.4103/0300-1652.107549

Martinez, F. O., Sica, A., Mantovani, A., & Locati, M. (2008). Macrophage activation and polarization. *Frontiers in bioscience*, *13*, 453–461. https://doi.org/10.2741/2692

Meijer, L. J. J., van Emmerik, T., van der Ent, R., Schmidt, C., & Lebreton, L. (2021). More than 1000 rivers account for 80% of global riverine plastic emissions into the ocean. *Science Advances*, *7*(18). https://doi.org/10.1126/sciadv.aaz5803

Mendoza-Cabrera, M. I., Navarro-Hernández, R. E., Santerre, A., Ortiz-Lazareno, P. C., Pereira-Suárez, A. L., & Estrada-Chávez, C. (2020). Effect of pregnancy hormone mixtures on cytokine production and surface marker expression in naïve and LPS-activated THP-1 differentiated monocytes/macrophages. *Innate Immunity*, *26*(2), 84–96. https://doi.org/10.1177/1753425919864658

Meng, X., Ge, L., Zhang, J., Xue, J., Gonzalez-Gil, G., Vrouwenvelder, J. S., & Li, Z. (2023). Systemic effects of nanoplastics on multi-organ at the environmentally relevant dose: The insights in physiological, histological, and oxidative damages. *Science of the Total Environment*, *892*. https://doi.org/10.1016/j.scitotenv.2023.164687

Mercnik, M. H., Schliefsteiner, C., Fluhr, H., & Wadsack, C. (2023). Placental macrophages present distinct polarization pattern and effector functions depending on clinical onset of preeclampsia. *Frontiers in Immunology*, *13*. https://doi.org/10.3389/fimmu.2022.1095879

Mezouar, S., Katsogiannou, M., Ben Amara, A., Bretelle, F., & Mege, J. L. (2021). Placental macrophages: Origin, heterogeneity, function and role in pregnancy-associated infections. *Placenta*, *103*, 94–103. https://doi.org/10.1016/j.placenta.2020.10.017

Moffett, A., & Colucci, F. (2014). Uterine NK cells: active regulators at the maternal-fetal interface. *The Journal of Clinical Investigation*, *124*(5), 1872–1879. https://doi.org/10.1172/jci68107

Morales, A. C., Tomlin, J. M., West, C. P., Rivera-Adorno, F. A., Peterson, B. N., Sharpe, S. A. L., Noh, Y., Sendesi, S. M. T., Boor, B. E., Howarter, J. A., Moffet, R. C., China, S., O'Callahan, B. T., El-Khoury, P. Z., Whelton, A. J., & Laskin, A. (2022). Atmospheric emission of nanoplastics from sewer pipe repairs. *Nature Nanotechnology*, *17*(11), 1171–1177. https://doi.org/10.1038/s41565-022-01219-9

Muzzio, D., Zenclussen, A. C., & Jensen, F. (2013). The Role of B Cells in Pregnancy: the Good and the Bad. *American Journal of Reproductive Immunology*, *69*(4), 408–412. https://doi.org/10.1111/aji.12079

Netea, M. G., Nold-Petry, C. A., Nold, M. F., Joosten, L. A. B., Opitz, B., van der Meer, J. H. M., van de Veerdonk, F. L., Ferwerda, G., Heinhuis, B., Devesa, I., Funk, C. J., Mason, R. J., Kullberg, B. J., Rubartelli, A., van der Meer, J. W. M., & Dinarello, C. A. (2009). Differential requirement for the activation of the inflammasome for processing and release of IL-1β in monocytes and macrophages. *Blood*, *113*(10), 2324–2335. https://doi.org/10.1182/blood-2008-03-146720

Okada, K., Arai, S., Itoh, H., Adachi, S., Hayashida, M., Nakase, H., & Ikemoto, M. (2016). CD68 on rat macrophages binds tightly to S100A8 and S100A9 and helps to regulate the cells' immune functions. *Journal of Leukocyte Biology*, *100*(5), 1093–1104. https://doi.org/10.1189/jlb.2a0415-170rrr

Ortega, D. E., & Cortés-Arriagada, D. (2023). Atmospheric microplastics and nanoplastics as vectors of primary air pollutants - A theoretical study on the polyethylene terephthalate (PET) case. *Environmental Pollution*, *318*. https://doi.org/10.1016/j.envpol.2022.120860

Palani, S., Maksimow, M., Miiluniemi, M., Auvinen, K., Jalkanen, S., & Salmi, M. (2011). Stabilin-1/CLEVER-1, a type 2 macrophage marker, is an adhesion and scavenging molecule on human placental macrophages. *European Journal of Immunology*, *41*(7), 2052–2063. https://doi.org/10.1002/eji.201041376

Pamer, E. G., & Shi, C. (2011). Monocyte recruitment during infection and inflammation. *Nature Reviews. Immunology*, *11*(11), 762–774. https://doi.org/10.1038/nri3070

Panico, S., Capolla, S., Bozzer, S., Toffoli, G., Dal Bo, M., & Macor, P. (2022). Biological Features of Nanoparticles: Protein Corona Formation and Interaction with the Immune System. *Pharmaceutics*, *14*(12), 2605-. https://doi.org/10.3390/pharmaceutics14122605

Patel, S. N., Lu, Z., Ayi, K., Serghides, L., Gowda, D. C., & Kain, K. C. (2007). Disruption of CD36 Impairs Cytokine Response to Plasmodium falciparum Glycosylphosphatidylinositol and Confers Susceptibility to Severe and Fatal Malaria In Vivo. *Journal of Immunology*, *178*(6), 3954–3961. https://doi.org/10.4049/jimmunol.178.6.3954

Pavlov, O. V., Niauri, D. A., Selutin, A. V., & Selkov, S. A. (2016). Coordinated expression of TNFα- and VEGF-mediated signaling components by placental macrophages in early and late pregnancy. *Placenta*, *42*, 28–36. https://doi.org/10.1016/j.placenta.2016.04.008

Pavlov, O. V., Selutin, A. V., Pavlova, O. M., & Selkov, S. A. (2020). Two patterns of cytokine production by placental macrophages. *Placenta*, *91*, 1–10. https://doi.org/10.1016/j.placenta.2020.01.005

Presence of microplastics and nanoplastics in food, with particular focus on seafood. (2016). *EFSA Journal*, *14*(6). https://doi.org/10.2903/j.efsa.2016.4501

Qiao, J., Chen, R., Wang, M., Bai, R., Cui, X., Liu, Y., Wu, C., & Chen, C. (2021). Perturbation of gut microbiota plays an important role in micro/nanoplastics-induced gut barrier dysfunction. *Nanoscale*, *13*(19), 8806–8816. https://doi.org/10.1039/d1nr00038a

Rackaityte, E., & Halkias, J. (2020). Mechanisms of Fetal T Cell Tolerance and Immune Regulation. *Frontiers in Immunology*, *11*. https://doi.org/10.3389/fimmu.2020.00588

Ragusa, A., Matta, M., Cristiano, L., Matassa, R., Battaglione, E., Svelato, A., De Luca, C., D'Avino, S., Gulotta, A., Rongioletti, M. C. A., Catalano, P., Santacroce, C., Notarstefano, V., Carnevali, O., Giorgini, E., Vizza, E., Familiari, G., & Nottola, S. A. (2022). Deeply in Plasticenta: Presence of Microplastics in the Intracellular Compartment of Human Placentas. *International Journal of Environmental Research and Public Health*, *19*(18). https://doi.org/10.3390/ijerph191811593

Ramsperger, A. F. R. M., Narayana, V. K. B., Gross, W., Mohanraj, J., Thelakkat, M., Greiner, A., Schmalz, H., Kress, H., & Laforsch, C. (2020). Environmental exposure enhances the internalization of microplastic particles into cells. *Science Advances*, *6*(50). https://doi.org/10.1126/sciadv.abd1211

Rees, A., Jenkins, B. J., Angelini, R., Davies, L. C., Cronin, J. G., Jones, N., & Thornton, C. A. (2024). Immunometabolic adaptation in monocytes underpins functional changes during pregnancy. *iScience*, *27*(5), 109779–109779. https://doi.org/10.1016/j.isci.2024.109779

Rees, A., Richards, O., Chambers, M., Jenkins, B. J., Cronin, J. G., & Thornton, C. A. (2022). Immunometabolic adaptation and immune plasticity in pregnancy and the bi-directional effects of obesity. *Clinical and Experimental Immunology*, *208*(2), 132–146. https://doi.org/10.1093/cei/uxac003

Robinson, D. P., & Klein, S. L. (2012). Pregnancy and pregnancy-associated hormones alter immune responses and disease pathogenesis. *Hormones and Behavior*, *62*(3), 263–271. https://doi.org/10.1016/j.yhbeh.2012.02.023

Roy, P. K., Hakkarainen, M., Varma, I. K., & Albertsson, A.-C. (2011). Degradable Polyethylene: Fantasy or Reality. *Environmental Science & Technology*, *45*(10), 4217–4227. https://doi.org/10.1021/es104042f

Saavedra, J., Stoll, S., & Slaveykova, V. I. (2019). Influence of nanoplastic surface charge on eco-corona formation, aggregation and toxicity to freshwater zooplankton. *Environmental Pollution*, *252*, 715–722. https://doi.org/10.1016/j.envpol.2019.05.135

Saidani, O., Umer, M., Alturki, N., Alshardan, A., Kiran, M., Alsubai, S., Kim, T. H., & Ashraf, I. (2024). White blood cells classification using multi-fold pre-processing and optimized CNN model. *Scientific Reports*, *14*(1). https://doi.org/10.1038/s41598-024-52880-0

Sammar, M., Siwetz, M., Meiri, H., Fleming, V., Altevogt, P., & Huppertz, B. (2017). Expression of CD24 and Siglec-10 in first trimester placenta: implications for immune tolerance at the fetal–maternal interface. *Histochemistry and Cell Biology*, *147*(5), 565–574. https://doi.org/10.1007/s00418-016-1531-7

Sampath, P., Moideen, K., Ranganathan, U. D., & Bethunaickan, R. (2018). Monocyte Subsets: Phenotypes and Function in Tuberculosis Infection. *Frontiers in Immunology*, *9*, 1726–1726. https://doi.org/10.3389/fimmu.2018.01726

Schliefsteiner, C., Ibesich, S., & Wadsack, C. (2020). Placental hofbauer cell polarization resists inflammatory cues in vitro. *International Journal of Molecular Sciences*, *21*(3). https://doi.org/10.3390/ijms21030736

Schmid-Schönbein, G. W., Shih, Y. Y., & Chien, S. (1980). Morphometry of Human Leukocytes. *Blood*, *56*(5), 866–875. https://doi.org/10.1182/blood.V56.5.866.866

Schwarzmaier, D., Foell, D., Weinhage, T., Varga, G., & Däbritz, J. (2013). Peripheral monocyte functions and activation in patients with quiescent Crohn's disease. *PloS One*, *8*(4), e62761–e62761. https://doi.org/10.1371/journal.pone.0062761

Sconocchia, G., Keyvanfar, K., El Ouriaghli, F., Grube, M., Rezvani, K., Fujiwara, H., McCoy, J. P., Hensel, N., & Barrett, A. J. (2005). Phenotype and function of a CD56+ peripheral blood monocyte. *Leukemia*, *19*(1), 69–76. https://doi.org/10.1038/sj.leu.2403550

Señarís, R., Garcia-Caballero, T., Casabiell, X., Gallego, R., Castro, R., Considine, R. V., Dieguez, C., & Casanueva, F. F. (1997). Synthesis of leptin in human placenta. *Endocrinology*, *138*(10), 4501–4504. https://doi.org/10.1210/endo.138.10.5573

Sharma, S., Rodrigues, P. R. S., Zaher, S., Davies, L. C., & Ghazal, P. (2022). Immune-metabolic adaptations in pregnancy: A potential stepping-stone to sepsis. *eBioMedicine, 86*. https://doi.org/10.1016/j.ebiom.2022.104337

She, S., Ren, L., Chen, P., Wang, M., Chen, D., Wang, Y., & Chen, H. (2022). Functional Roles of Chemokine Receptor CCR2 and Its Ligands in Liver Disease. *Frontiers in Immunology*, *13*, 812431–812431. https://doi.org/10.3389/fimmu.2022.812431

Simoni, M. K., Jurado, K. A., Abrahams, V. M., Fikrig, E., & Guller, S. (2017). Zika virus infection of Hofbauer cells. *American journal of reproductive immunology, 77*(2). https://doi.org/10.1111/aji.12613

Stojkovic, M., Ortuño Guzmán, F. M., Han, D., Stojkovic, P., Dopazo, J., & Stankovic, K. M. (2023). Polystyrene nanoplastics affect transcriptomic and epigenomic signatures of human fibroblasts and derived induced pluripotent stem cells: Implications for human health. *Environmental Pollution*, *320*. https://doi.org/10.1016/j.envpol.2022.120849

Summers, S., Henry, T., & Gutierrez, T. (2018). Agglomeration of nano- and microplastic particles in seawater by autochthonous and de novo-produced sources of exopolymeric substances. *Marine Pollution Bulletin*, *130*, 258–267. https://doi.org/10.1016/j.marpolbul.2018.03.039

Sun, L., Cornell, T. T., LeVine, A., Berlin, A. A., Hinkovska-Galcheva, V., Fleszar, A. J., Lukacs, N. W., & Shanley, T. P. (2013). Dual role of interleukin-10 in the regulation of respiratory syncitial virus (RSV)-induced lung inflammation. *Clinical and Experimental Immunology*, *172*(2), 263–279. https://doi.org/10.1111/cei.12059

Sun, Y., Ma, J., Li, D., Li, P., Zhou, X., Li, Y., He, Z., Qin, L., Liang, L., & Luo, X. (2019). Interleukin-10 inhibits interleukin-1β production and inflammasome activation of microglia in epileptic seizures. *Journal of Neuroinflammation*, *16*(1). https://doi.org/10.1186/s12974-019-1452-1

Sun, Y., Wu, S., Zhou, Q., & Li, X. (2021). Trophoblast-derived interleukin 9 mediates immune cell conversion and contributes to maternal-fetal tolerance. *Journal of Reproductive Immunology*, *148*. https://doi.org/10.1016/j.jri.2021.103379

Swieboda, D., Johnson, E. L., Beaver, J., Haddad, L., Enninga, E. A. L., Hathcock, M., Cordes, S., Jean, V., Lane, I., Skountzou, I., & Chakraborty, R. (2020). Baby's First Macrophage: Temporal Regulation of Hofbauer Cell Phenotype Influences Ligand-Mediated Innate Immune Responses across Gestation. *Journal of Immunology*, *204*(9), 2380–2391. https://doi.org/10.4049/jimmunol.1901185

Tacke, F., Alvarez, D., Kaplan, T. J., Jakubzick, C., Spanbroek, R., Llodra, J., Garin, A., Liu, J., Mack, M., Van Rooijen, N., Lira, S. A., Habenicht, A. J., & Randolph, G. J. (2007). Monocyte subsets differentially employ CCR2, CCR5, and CX3CR1 to accumulate within atherosclerotic plaques. *Journal of Clinical Investigation*, *117*(1), 185–194. https://doi.org/10.1172/JCI28549

Teng, M., Zhao, X., Wang, C., Wang, C., White, J. C., Zhao, W., Zhou, L., Duan, M., & Wu, F. (2022). Polystyrene Nanoplastics Toxicity to Zebrafish: Dysregulation of the Brain–Intestine–Microbiota Axis. *ACS Nano*, *16*(5), 8190–8204. https://doi.org/10.1021/acsnano.2c01872

Thaxton, J. E., & Sharma, S. (2010). Interleukin-10: a multi-faceted agent of pregnancy. *American Journal of Reproductive Immunology (1989)*, *63*(6), 482–491. https://doi.org/10.1111/j.1600-0897.2010.00810.x

Thomas, J. R., Appios, A., Zhao, X., Dutkiewicz, R., Donde, M., Lee, C. Y. C., Naidu, P., Lee, C., Cerveira, J., Liu, B., Ginhoux, F., Burton, G., Hamilton, R. S., Moffett, A., Sharkey, A., & McGovern, N. (2021). Phenotypic and functional characterization of first-trimester human placental macrophages, Hofbauer cells. *The Journal of experimental medicine*, *218*(1), e20200891. https://doi.org/10.1084/jem.20200891

Tian, L., Chen, Q., Jiang, W., Wang, L., Xie, H., Kalogerakis, N., Ma, Y., & Ji, R. (2019). A carbon-14 radiotracer-based study on the phototransformation of polystyrene nanoplastics in water: Versus in air. *Environmental Science: Nano*, *6*(9), 2907–2917. https://doi.org/10.1039/c9en00662a

Tsou, C. L., Peters, W., Si, Y., Slaymaker, S., Aslanian, A. M., Weisberg, S. P., Mack, M., & Charo, I. F. (2007). Critical roles for CCR2 and MCP-3 in monocyte mobilization from bone marrow and recruitment to inflammatory sites. *Journal of Clinical Investigation*, *117*(4), 902–909. https://doi.org/10.1172/JCI29919

Vanbervliet, B., Homey, B., Durand, I., Massacrier, C., Aït-Yahia, S., De Bouteiller, O., Vicari, A., & Caux, C. (2002). Sequential involvement of CCR2 and CCR6 ligands for immature dendritic cell recruitment: Possible role at inflamed epithelial surfaces. *European Journal of Immunology*, *32*(1), 231–242. https://doi.org/10.1002/1521-4141(200201)32:1<231::AID-IMMU231>3.0.CO;2-8

Wahl, A., Le Juge, C., Davranche, M., El Hadri, H., Grassl, B., Reynaud, S., & Gigault, J. (2021). Nanoplastic occurrence in a soil amended with plastic debris. *Chemosphere*, *262*. https://doi.org/10.1016/j.chemosphere.2020.127784

Wan, S., Wang, X., Chen, W., Wang, M., Zhao, J., Xu, Z., Wang, R., Mi, C., Zheng, Z., & Zhang, H. (2024). Exposure to high dose of polystyrene nanoplastics causes trophoblast cell apoptosis and induces miscarriage. *Particle and Fibre Toxicology*, *21*(1). https://doi.org/10.1186/s12989-024-00574-w

Wang, W., Sung, N., Gilman-Sachs, A., & Kwak-Kim, J. (2020). T Helper (Th) Cell Profiles in Pregnancy and Recurrent Pregnancy Losses: Th1/Th2/Th9/Th17/Th22/Tfh Cells. *Frontiers in Immunology*, *11*. https://doi.org/10.3389/fimmu.2020.02025

Wang, X., Jia, Z., Zhou, X., Su, L., Wang, M., Wang, T., & Zhang, H. (2023). Nanoplastic-induced vascular endothelial injury and coagulation dysfunction in mice. *Science of the Total Environment*, *865*. https://doi.org/10.1016/j.scitotenv.2022.161271

Wang, X., Zhao, Z., Wang, X., Hu, W., Chao luo, Chu, X., Qian, M., Wang, R., Yu, S., Wu, Q., Tang, J., & Zhao, X. (2023). Effects of polystyrene nanoplastic gestational exposure on mice. *Chemosphere*, *324*. https://doi.org/10.1016/j.chemosphere.2023.138255

Weingrill, R. B., Lee, M. J., Benny, P., Riel, J., Saiki, K., Garcia, J., Oliveira, L. F. A. de M., Fonseca, E. J. da S., Souza, S. T. de, D'Amato, F. de O. S., Silva, U. R., Dutra, M. L., Marques, A. L. X., Borbely, A. U., & Urschitz, J. (2023). Temporal trends in microplastic accumulation in placentas from pregnancies in Hawai'i. *Environment International*, *180*. https://doi.org/10.1016/j.envint.2023.108220

Woo, J. H., Seo, H. J., Lee, J. Y., Lee, I., Jeon, K., Kim, B., & Lee, K. (2023). Polypropylene nanoplastic exposure leads to lung inflammation through p38-mediated NF-κB pathway due to mitochondrial damage. *Particle and Fibre Toxicology*, *20*(1). https://doi.org/10.1186/s12989-022-00512-8

Xiao, M., Li, X., Zhang, X., Duan, X., Lin, H., Liu, S., & Sui, G. (2023). Assessment of cancer-related signaling pathways in responses to polystyrene nanoplastics via a kidney-testis microfluidic platform (KTP). *Science of the Total Environment*, *857*. https://doi.org/10.1016/j.scitotenv.2022.159306

Xiao, S., Wang, J., Digiacomo, L., Amici, A., De Lorenzi, V., Pugliese, L. A., Cardarelli, F., Cerrato, A., Laganà, A., Cui, L., Papi, M., Caracciolo, G., Marchini, C., & Pozzi, D. (2024). Protein corona alleviates adverse biological effects of nanoplastics in breast cancer cells. *Nanoscale*. https://doi.org/10.1039/d4nr01850h

Xing, Z., Han, J., Hao, X., Wang, J., Jiang, C., Hao, Y., Wang, H., Wu, X., Shen, L., Dong, X., Li, T., Li, G., Zhang, J., Hou, X., & Zeng, H. (2017). Immature monocytes contribute to cardiopulmonary bypass-induced acute lung injury by generating inflammatory descendants. *Thorax*, *72*(3), 245–255. https://doi.org/10.1136/thoraxjnl-2015-208023

Xiong, H., Carter, R. A., Leiner, I. M., Tang, Y. W., Chen, L., Kreiswirth, B. N., & Pamer, E. G. (2015). Distinct contributions of neutrophils and CCR2+ monocytes to pulmonary clearance of different Klebsiella pneumoniae strains. *Infection and Immunity*, *83*(9), 3418–3427. https://doi.org/10.1128/IAI.00678-15

Xue, J., Schmidt, S. V., Sander, J., Draffehn, A., Krebs, W., Quester, I., De Nardo, D., Gohel, T. D., Emde, M., Schmidleithner, L., Ganesan, H., Nino-Castro, A., Mallmann, M. R., Labzin, L., Theis, H., Kraut, M., Beyer, M., Latz, E., Freeman, T. C., Ulas, T., … Schultze, J. L. (2014). Transcriptome-based network analysis reveals a spectrum model of human macrophage activation. *Immunity*, *40*(2), 274–288. https://doi.org/10.1016/j.immuni.2014.01.006

Yang, Y., Wu, Q., & Wang, D. (2021). Dysregulation of G protein-coupled receptors in the intestine by nanoplastic exposure inCaenorhabditis elegans. *Environmental Science: Nano*, *8*(4), 1019–1028. https://doi.org/10.1039/d0en00991a

Zeldovich, V. B., Robbins, J. R., Kapidzic, M., Lauer, P., & Bakardjiev, A. I. (2011). Invasive extravillous trophoblasts restrict intracellular growth and spread of Listeria monocytogenes. *PLoS Pathogens*, *7*(3). https://doi.org/10.1371/journal.ppat.1002005

Zhang, T., Yang, S., Ge, Y., Wan, X., Zhu, Y., Li, J., Yin, L., Pu, Y., & Liang, G. (2022). Polystyrene Nanoplastics Induce Lung Injury via Activating Oxidative Stress: Molecular Insights from Bioinformatics Analysis. *Nanomaterials*, *12*(19). https://doi.org/10.3390/nano12193507

Zhu, F., Zhu, C., Wang, C., & Gu, C. (2019). Occurrence and Ecological Impacts of Microplastics in Soil Systems: A Review. *Bulletin of Environmental Contamination and Toxicology*, *102*(6), 741–749. https://doi.org/10.1007/s00128-019-02623-z

Zhu, H., Fan, X., Zou, H., Guo, R.-B., & Fu, S.-F. (2023). Effects of size and surface charge on the sedimentation of nanoplastics in freshwater. *Chemosphere*, *336*, 139194. https://doi.org/10.1016/j.chemosphere.2023.139194

Ziegler-Heitbrock, L., Ancuta, P., Crowe, S., Dalod, M., Grau, V., Hart, D. N., Leenen, P. J. M., Liu, Y.-J., MacPherson, G., Randolph, G. J., Scherberich, J., Schmitz, J., Shortman, K., Sozzani, S., Strobl, H., Zembala, M., Austyn, J. M., & Lutz, M. B. (2010). Nomenclature of monocytes and dendritic cells in blood. *Blood*, *116*(16), e74–e80. https://doi.org/10.1182/blood-2010-02-258558